

Journal of Water Resource and Protection

Editor-in-Chief : Jian Shen



Journal Editorial Board

ISSN: 1945-3094 (Print) ISSN: 1945-3108 (Online)

<http://www.scirp.org/journal/jwarp>

Editor-in-Chief

Prof. Jian Shen College of William and Mary, USA

Editorial Board (According to Alphabet)

Prof. J. Bandyopadhyay	Indian Institute of Management Calcutta, India
Dr. Antonio Dourado	University of Coimbra, Portugal
Prof. Peter Dillon	Fellow of the Royal Society of Canada(F.R.S.C), Canada
Dr. Qiuqing Geng	Swedish Institute of Agricultural and Environmental Engineering, Sweden
Dr. Jane Heyworth	University of Western Australia, Australia
Dr. C. Samuel Ima	University of Manitoba, Canada
Dr. Valentina Lady-gina	Russian Academy of Sciences, Russia
Dr. Dehong Li	Fudan University, China
Dr. Chih-Heng Liu	Feng Chia University, Taiwan, China
Dr. Sitong Liu	Dalian University of Technology, China
Dr. Xiaotong Lu	Nanjing University, China
Dr. Donghua Pan	Beijing Normal University, China
Dr. Dhundi Raj Pathak	Osaka Sangyo University, Japan
Dr. Van Staden Rudi	Griffith University, Australia
Dr. Dipankar Saha	Central Ground Water Board, India
Prof. Matthias Templ	Methodology Department of Statistics, Austria
Dr. Dehui Wang	Guangzhou Institute of Geochemistry, China
Dr. Yuan Zhao	College of William and Mary, USA
Dr. Lifeng Zhang	Center for Advanced Water Technology, Singapore
Dr. Chunli Zheng	Dalian University of Technology, China
Prof. Zhiyu Zhong	Changjiang Water Resources Commission, China
Dr. Yuan Zhang	Chinese Research Academy of Environmental Science, China

Editorial Assistants

Pan LIU Wuhan University, China
Fenfang QU Email: jwarp@scirp.org

Guest Reviewers (According to Alphabet)

T. A. Arowolo	Mehmet Erdem	Christian Jungnickel	Ulas Tezel
J. M. M. Avalos	Chunsheng Fang	Yiquan Le	Mustafa Tuzen
E. Álvarez Ayuso	Uday Chand Ghosh	Woojin Lee	Wenying Xu
Abdelkrim Azzouz	Huaming Guo	Benjamin Michen	Guangxu Yan
Haq Nawaz Bhatti	Jan Hoinkis	Adrian Oehmen	Jianfeng Yang
Ederio D. Bidoia	Xiuyi Hua	F. Pliakas	Wenzheng Yu
S. Chegrouche	Minsheng Huang	Donald O. Rosenberry	Jianxian Zeng
Salah Chegrouche	Pavel Janoš	Baoyou Shi	Lingyan Zhu
Morten L. Christensen	Juliang Jin	J. Sirajudeen	Zhiwei Zhu
Adil Denizli	Branimir Jovancicevic	Mustafa Soylak	Joseph T. Zume
		K. Suzuki	Qiting Zuo

TABLE OF CONTENTS

Volume 1 Number 2

August 2009

Long-Term Study of Lake Evaporation and Evaluation of Seven Estimation Methods: Results from Dickie Lake, South-Central Ontario, Canada

H. X. YAO.....59

Dechlorination of Trichloroethylene in Groundwater by Nanoscale Bimetallic Fe/Pd Particles

T. L. LI, S. J. LI, Y. C. LI, Z. H. JIN.....78

Electrokinetic Phenomena of Modified Polytetrafluoroethylene Membranes in the Oily Sewage from Oil Field

A. G. LIN, Y. H. YAO, G. LIU, G. Z. ZHANG, X. F. LIN.....84

Plantago Ovata Efficiency in Elimination of Water Turbidity

G. N. BIDHENDI, T. SHAHRIARI, S. SHAHRIARI.....90

Remove of Phenolic Compounds in Water by Low-Temperature Plasma: A Review of Current Research

J. F. ZHANG, J. R. CHEN, X. Y. LI.....99

Water Quality Analysis of the Songhua River Basin Using Multivariate Techniques

Y. LI, L. Y. XU, S. LI.....110

Modeling and Control of pH in Pulp and Paper Wastewater Treatment Process

J. Y. KANG, M. X. WANG, Z. J. XIAO.....122

Health Risk Assessment on Rural Drinking Water Safety—A Case Study in Rain City District of Ya'an City of Sichuan Province

F. Q. NI, G. D. LIU, H. Z. REN, S. C. YANG, J. YE, X. Y. LU, M. YANG.....128

Uncertainty Analysis of Interpolation Methods in Rainfall Spatial Distribution—A Case of Small Catchment in Lyon

T. TAO, B. CHOCAT, S. Q. LIU, K. L. XIN.....136

Screening and Domestication of High Effective Microorganism Used in Oil Containing Wastewater Remediation

X. Y. XU, X. CHEN, Y. D. FAN.....145

Journal of Water Resource and Protection (JWARP)

Journal Information

SUBSCRIPTIONS

The *Journal of Water Resource and Protection* (Online at Scientific Research Publishing, www.SciRP.org) is published monthly by Scientific Research Publishing, Inc., USA.

E-mail: jwarp@scirp.org

Subscription rates: Volume 1 2009

Print: \$50 per copy.

Electronic: free, available on www.SciRP.org.

To subscribe, please contact Journals Subscriptions Department, E-mail: jwarp@scirp.org

Sample copies: If you are interested in subscribing, you may obtain a free sample copy by contacting Scientific Research Publishing, Inc at the above address.

SERVICES

Advertisements

Advertisement Sales Department, E-mail: jwarp@scirp.org

Reprints (minimum quantity 100 copies)

Reprints Co-ordinator, Scientific Research Publishing, Inc., USA.

E-mail: jwarp@scirp.org

COPYRIGHT

Copyright©2009 Scientific Research Publishing, Inc.

All Rights Reserved. No part of this publication may be reproduced, stored in a retrieval system, or transmitted, in any form or by any means, electronic, mechanical, photocopying, recording, scanning or otherwise, except as described below, without the permission in writing of the Publisher.

Copying of articles is not permitted except for personal and internal use, to the extent permitted by national copyright law, or under the terms of a license issued by the national Reproduction Rights Organization.

Requests for permission for other kinds of copying, such as copying for general distribution, for advertising or promotional purposes, for creating new collective works or for resale, and other enquiries should be addressed to the Publisher.

Statements and opinions expressed in the articles and communications are those of the individual contributors and not the statements and opinion of Scientific Research Publishing, Inc. We assumes no responsibility or liability for any damage or injury to persons or property arising out of the use of any materials, instructions, methods or ideas contained herein. We expressly disclaim any implied warranties of merchantability or fitness for a particular purpose. If expert assistance is required, the services of a competent professional person should be sought.

PRODUCTION INFORMATION

For manuscripts that have been accepted for publication, please contact:

E-mail: jwarp@scirp.org

Long-Term Study of Lake Evaporation and Evaluation of Seven Estimation Methods: Results from Dickie Lake, South-Central Ontario, Canada

Huaxia YAO

Dorset Environmental Science Centre, Ontario Ministry of Environment, Dorset, Ontario, P0A 1E0, Canada

E-mail: huaxia.yao@ontario.ca

Received March 31, 2009; revised April 20, 2009; accepted May 4, 2009

Abstract

Establishing satisfactory calculation methods of lake evaporation has been crucial for research and management of water resources and ecosystems. A 30 year dataset from Dickie Lake, south-central Ontario, Canada added to the limited long-term studies on lake evaporation. Evaporation during ice-free season was calculated separately using seven evaporation methods, based on field meteorology, hydrology and lake water temperature data. Actual evaporation determined during a portion of a year was estimated using a lake energy budget model, and the estimation was used as reference evaporation for evaluation of the seven methods. The deviation of method-induced evaporation from the reference evaporation was compared among the seven methods, and a performance rank was proposed based on the root mean squared deviation and coefficient of efficiency. As for the whole ice-free season (roughly May to November), the water balance was the best method, followed by Makkink, DeBruin-Kejiman, Penman, Priestley-Taylor, Hamon, and Jensen-Haise methods. As for shorter duration (a week to a month), the DeBruin-Kejiman was the best method, followed by Penman, Priestley-Taylor, Makkink, Hamon, Jensen-Haise, and water balance method. Annual and seasonal changes of energy budget terms and the compensation function of lake heat storage in evaporation flux were also analyzed.

Keywords: Long-Term Study, Lake Evaporation, Water Balance, Energy Budget, Lake Temperature, Stream Discharge

1. Introduction

Natural lakes and artificial reservoirs provide a valuable water resource. The quantity and quality of lake water resource are important for agriculture, fisheries, recreation, domestic and industrial water supply, aquatic ecosystem, and hydropower [1–2]. Lake water availability is regulated by the water balance and energy budget processes which in turn are closely tied to climate variations, land use change or other human influences [3–5]. For example, a common indicator of water availability – lake water level – is influenced by four major processes or factors: 1) precipitation on the lake and its drainage watersheds; 2) surface and subsurface runoff generated from the watersheds; 3) runoff leaving the lake; and 4) direct

evaporation loss from the lake surface. Therefore, it is crucial to understand the lake evaporation process, establish satisfactory calculation methods, and identify the effects of lake evaporation on lake level and water resources.

Long-term observations and field data are important for understanding lake evaporation, creating estimation methods, and evaluating effects of evaporation change (caused by climate change or land use change) on water resources. However, it is challenging or difficult to directly measure lake evaporation for a long time, because it involves significant financial investment in instruments, field maintenance, and field work on a lake. Usually lake evaporation is estimated or calculated by a formula and using regular meteorological and hydrological data. Lake evap-

poration is affected not only by climatic variables, but also by lake characteristics such as depth, surface area, and water clarity and temperature. Lake water itself influences the energy budget and lake evaporation through the changes in water temperature and water mixing (turn over). Accurate accounting of energy budget processes requires observations of temperature profiles of lake water. As a result, these field difficulties have severely restricted the number of long-term evaporation studies.

Methods, equations or models for determining lake evaporation may be categorized into four categories: energy budget, aerodynamic transfer (or mass transfer), combination of aerodynamic transfer and energy budget, and empirical method. Most literature studies using one or more of these methods have utilized short-term field monitoring and datasets. In this paper “long-term” studies mean those that conduct and utilize monitoring data of multiple years to more than 5 years. Lengers *et al.* [6] completed a comprehensive study of lake evaporation and effects of climate variation by using 10 year data from a small lake in Wisconsin USA. In the article by Lengers *et al.*, some long-term studies were summarized. Apart from these summarized examples, there are other long-term studies that have been conducted: a lake in Northwest Territories of Canada for six years [7], the small Lake Kinneret in Israel for five years [8], the large Lake Okeechobee (1732 km^2) in Florida USA for five years [9], a small reservoir (8.8 km^2) in Minas Gerais State, Brazil for

three years [10], the large man-made Lake Mead (506 km^2) in Las Vegas, Nevada USA for three years [11], the large Bear Lake in Idaho and Utah, USA for two years [12], the Cottonwood Lake Area in North Dakota USA for 5 years [13], the Mirror Lake in New Hampshire USA for 6 years [14], the Perch Lake in eastern Ontario Canada for 11 years [15], several lakes in Minnesota USA for 11 years [16], and several more examples using two-year data [17–19]. Scheider *et al.* [20–21] and Hutchinson *et al.* [22] have reported on lake evaporation study of 15 years (1976–1992) for lakes in Muskoka area of Ontario, Canada.

The study examples mentioned above are listed in Table 1, illustrating the limited number of long-term studies. There are only 14 examples of studies in Table 1 where five or more years of data are used. The Lake Ziway study with the longest data record of 30 years made many simplifications in its calculations of monthly and annual average evaporation and did not provide details of the evaporation process. Therefore, additional studies of lake evaporation using long-term data are needed to describe the evaporation process and its variability; and to confirm and compare the applicability of available estimation methods. A detailed analysis of 30 year (1978–2007) field data for Dickie Lake (the lake is located in the same Muskoka-Haliburton area as monitored and reported by Scheider *et al.* and Hutchinson *et al.*) is presented in this paper.

Table 1. Study examples of long-term lake evaporation.

Authors	Study site	Country	Years of data	Methods used
Vallet-Coulomb	Lake Ziway	Ethiopia	30	Three methods
Hutchinson <i>et al.</i>	Muskoka Area	Canada	15	Energy budget
Rasmussen <i>et al.</i>	Cedar Lake etc.	USA	11	Seven methods
Robertson <i>et al.</i>	Perch Lake	Canada	11	Energy budget
Lengers <i>et al.</i>	Sparkling Lake	USA	10	Energy budget
Robertson <i>et al.</i>	Perch Lake	Canada	10	Energy budget
Winter <i>et al.</i>	Mirror Lake	USA	6	Energy budget
Rosenberry <i>et al.</i>	Mirror Lake	USA	6	15 methods
Gibson <i>et al.</i>	Yellowknife	Canada	6	Two methods
Rosenberry <i>et al.</i>	Cottonwood Lake	USA	5	13 methods
Winter <i>et al.</i>	Williams Lake	USA	5	11 methods
Sturrock <i>et al.</i>	Williams Lake	USA	5	Energy budget
Assouline	Lake Kinneret	Israel	5	Two methods
Abtew	Lake Okeechobee	USA	5	Seven methods
Myrup <i>et al.</i>	Lake Tahoe	USA	3	Two methods
Sacks <i>et al.</i>	Two lakes	USA	3	Energy budget
Dos Reis <i>et al.</i>	Lake Serra Azul	Brazil	3	Two methods
USGS	Lake Mead	USA	3	Energy budget
Amayreh	Bear Lake	USA	2	Two methods
Hamblin <i>et al.</i>	Lake Malawi	Mozambique	2	Three methods
Keskin <i>et al.</i>	Lake Egirdir	Turkey	2	Six methods
Linacre	Copenhagen	Australia	2	Three methods

Apart from the need for long-term data, methods for evaporation estimation should be discussed and assessed, because more than 30 methods or equations have been proposed and most of them perform differently for different geographical areas. Winter *et al.* [23] compared 11 well-used methods with the energy budget method by using high-quality data for five years from Williams Lake, and proposed a ranking based on best to least performance. Their ranking is: Penman, DeBruin-Kejiman, Makkink, Priestley-Taylor, Hamon, Jensen-Haise, mass transfer, DeBruin, Papadakis, Stephens-Stewart, and Brutsaert-Stricker. Rosenberry *et al.* [13,14] compared as more as 15 methods with energy-budget method using 6-year data and proposed their ranking. Rasmussen *et al.* [16] compared seven methods for use in lake temperature modeling. The evaluation of seven methods by Abtew [9] suggested that simple models (such as the modified Turc model only using solar radiation and maximum air temperature) could perform better than Penman-combination or Priestley-Taylor model requiring many more parameters. The four methods—Priestley-Taylor, DeBruin-Kejiman, Papadakis and Penman were compared with energy budget by Mosner and Aulenbach [24] using single-year data, and the Priestley-Taylor was found to be the best of the four methods. Xu and Singh [25] tested eight radiation-based evaporation models in order to estimate future lake levels. Singh and Xu [26] evaluated 13 mass-transfer equations against pan evaporation data. Delclaux *et al.* [27] compared five monthly evaporation methods and the best results of lake evaporation were obtained by the Abtew model and Makkink model. Comparisons of estimation methods were also made by Keskin and Terzi [18] and Sadek *et al.* [28]. All these comparisons provided somehow different conclusions depending on sites and data used.

As indicated by Winter *et al.* [23], earlier comparisons of evaporation methods did not use extensive or long term data. Also comparisons have been focused more on large lakes in arid and semiarid climates than on small lakes in humid and sub-humid climates. The lakes in cold or boreal ecozones (such as those located on the Canadian Shield) have received even less attention. The evaluation of methods needs to be made for a longer period of time, a wider scope of lake sizes and more climatic settings. In our study, seven commonly used methods are compared with each other and assessed by using long-term data from Dickie Lake on the Canadian Shield where such comparison has rarely been made. Only one case of method comparison was reported for Canadian Shield: Singh and Xu [26].

Another issue in evaporation studies is the standard or reference that was used to verify estimation methods. Actual lake evaporation can be measured by an instrument such as the eddy covariance system, but long-term data from the system has not been reported. A common

measure of lake evaporation is by using an evaporation pan, with a limitation: the pan coefficient (multiplying the coefficient with the pan evaporation data to get lake evaporation) depends on season, location and the specific pan in use [9]. In case a reliable and direct measure of long-term evaporation did not exist, many reported comparison studies chose to evaluate methods by comparing evaporation results with that of an energy budget method, as the latter was considered the best method to estimate lake evaporation [6,13,14,23,24]. In our study of Dickie Lake, there was no data from pan evaporation or eddy covariance instrument, the energy-budget results were used to be the reference for evaluating performance of other estimation methods.

Therefore, our study has three goals: 1) provide an evaporation study using long-term 30-year datasets obtained for a small lake located in the Canadian Shield region; 2) estimate evaporation of ice-free season for 30 years using seven methods, and discuss their applicability to cold ecoregions; and 3) compare deviations of method-calculated evaporation to the energy-budget-estimated evaporation, and identify the better methods for estimating lake evaporation for the region.

2. Site and Data Description

The Muskoka-Haliburton study region as shown in Figure 1 is located in south-central Ontario, Canada, to the east of Lake Huron, one of the five Great Lakes in North America. Environmental monitoring programs including hydrological and meteorological observations were started and managed by the Dorset Environmental Science Centre, Ontario Ministry of the Environment in 1976, and have been continuous till present. The program includes nine lakes and their contributing watersheds, as representatives of inland lakes on the Canadian Shield landscape, which typically consists of exposed bedrock and numerous lakes. The lakes and watersheds in the Muskoka-Haliburton study area drain into Muskoka River or Gull River which contributes to Muskoka Lake and finally into Georgian Bay of Lake Huron. The region is relatively undeveloped by humans, with the exception of small towns or villages like Huntsville, Bracebridge or Dorset, and some scattered cottages alongside shorelines or in forested areas.

The study lake, Dickie Lake, is one of the nine lakes (Figure 1, Number 6), and is located between Bracebridge and Dorset, about 20 km from both. The lake, streams and drainage watersheds, and monitoring gages are shown in Figure 2. There are five main streams going into the lake, and their watersheds are numbered as 5, 6, 8, 10 and 11 in Figure 2. These stream watersheds occupy a large portion of the total drainage area. There is a weir (gauge) at the end of each stream to monitor water levels at that particular point and the levels are converted to stream dis-

charges with calibrated level-discharge relationships. A small portion of the drainage area, which is close to the lake's shoreline and does not have obvious streams, has not been monitored by gauges. The outflow on the south-west side of the lake is also monitored. The lake's water level is observed at a location off the inlet of watershed 6. The areas of the five main watersheds are 0.30, 0.22, 0.67, 0.79, and 0.76 km² respectively, giving a gauged drainage area of 2.74 km². The ungauged drainage area is 1.32 km² whereas the total drainage area is 4.06 km². The lake itself has an area of 0.94 km². The lake's outlet point controls a total area of 5.0 km².

The geology of Dickie Lake drainage area is composed of three surficial geology types [21]: shallow surficial deposits (less than 1 m in depth) covering 78 % of the area, deep surficial deposits (greater than 1 m in depth) covering 3 %, and organic soils covering 19 %. Therefore, the soil is thin and poorly developed, making surface runoff the dominant runoff generation while groundwater runoff from bedrock is minimal. Forest cover is almost continuous in the watershed although it contains some areas of exposed bedrock. The percentages of wooded land and exposed bedrock among the whole watershed

are 83 % and 17 % respectively. Small logging operations and dwellings around the lake and watershed exist, but their influence on the hydrological cycle is minimal. Consumptive use of lake and stream water is also minimal.

The climate of the study area is cold and humid in fall and winter, with less precipitation in summer than in fall or winter, and usually has significant snow/ice melting in spring. As presented by the data records, annual mean air temperature is 4.9 °C, and average annual precipitation is 1010 mm.

The data collection and processing was completed using a meteorology station located at Heney Lake approximately 1.0 km away from Dickie Lake (Figure 1). The data used for calculations include daily precipitation, daily mean temperature, relative humidity, wind speed, and daily global radiation. This station provides a majority of data used for the Dickie Lake study. When a data point was missing or unreliable at the Heney station, three other nearby stations located close to Chub Lake, Plastic Lake and Harp Lake were used to give a proper data value. The processed data are available for 30 years: 1978–2007.

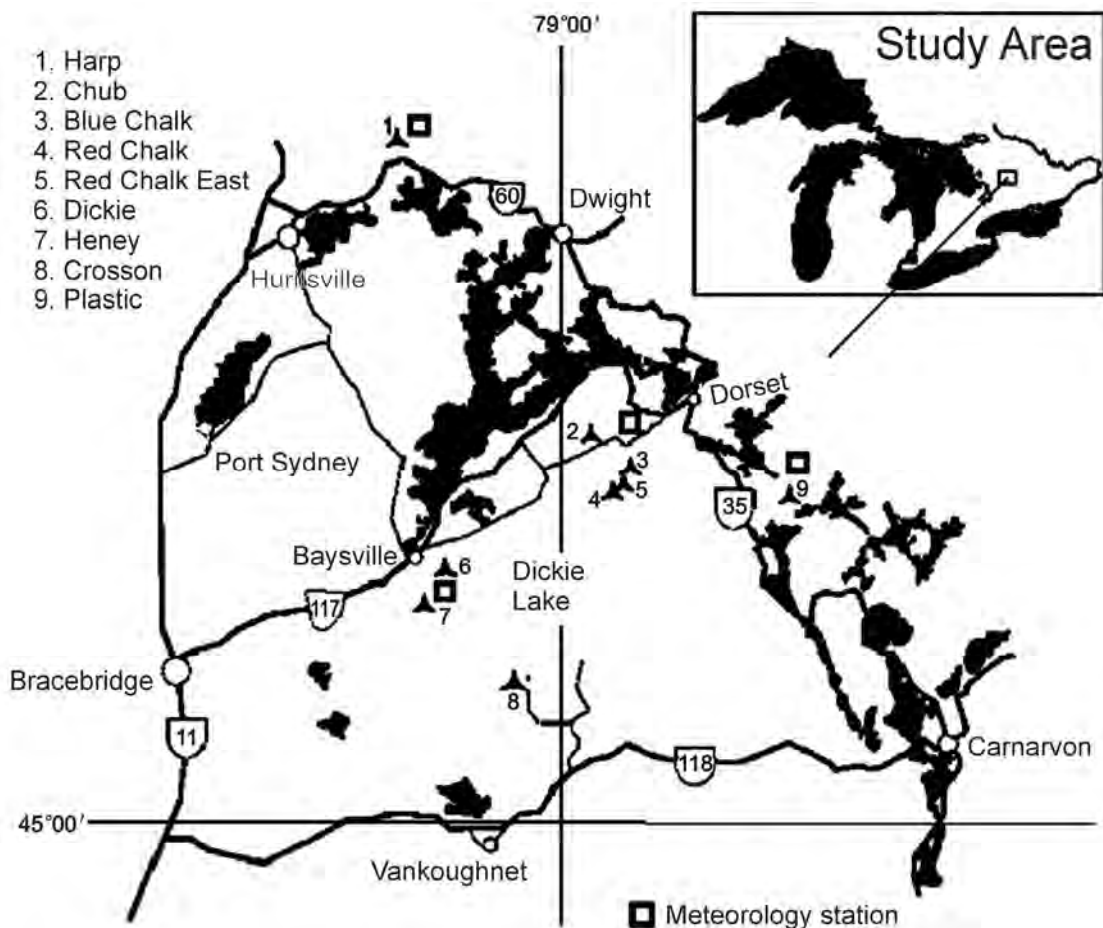


Figure 1. Locations of study area and study lake.

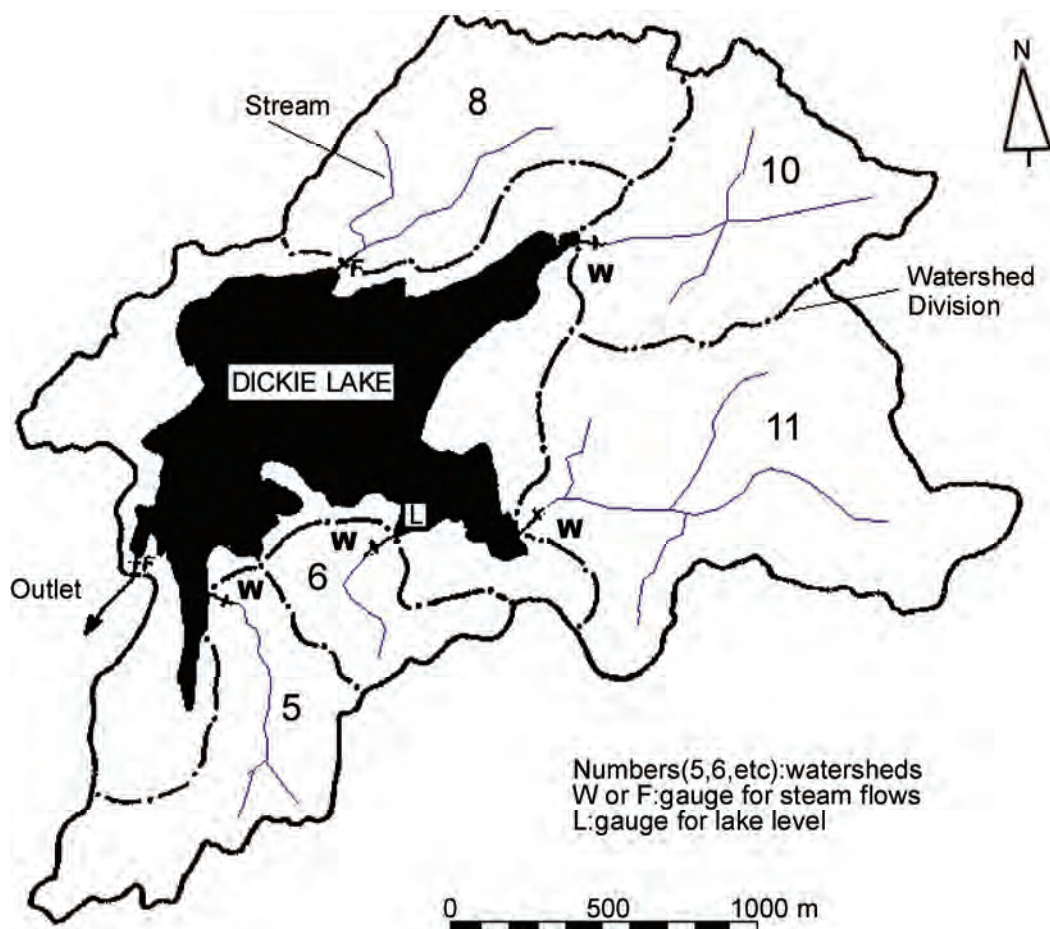


Figure 2. Dickie Lake and its watersheds (W and F mean stream gauge type: weir and flume).

Stream water level data are obtained from field recording charts which are used to provide hourly and daily discharges for five watershed streams. Daily mean discharges are available for 30 years: 1978–2007. They are used for evaporation estimation via lake water balance calculations.

Lake temperature profiles (water temperature at 1 m intervals from lake surface to lake bottom) were conducted at one and central point of the lake, on varying dates throughout a year, mostly during the ice-free season. A period between two observation dates consists of 6 to 45 days, two weeks on average. The water depth measured at the deepest and central part of the lake varies between 9 and 12 meters, therefore, the number of vertical profile zones changes slightly in the year, with one zone being one meter thick. Available data covers a period of 30 years (1978–2007).

Lake levels were monitored once every two or three weeks on average, during ice-free season only, for 23 years: 1980 to 2002. They are used to calculate water balance.

For clarification, the three timing concepts used in the study are explained. Lake temperature profile observation

begins in early May but not fix on a specific date, ends in mid November. The time length between any two observation dates is called a “period”. A period has a range of 6 – 45 days depending on actual field work, and is used for evaporation calculations. The lake level observation begins in May and ends in November (differs between years, and differs from the lake profile observation dates). The time length between two observation dates is called an “interval”. A period and an interval may cover some same days, but do not necessarily coincide completely with each other, as water temperature and lake level may not be observed on a same date. An interval has a range of 2 – 34 days, and is used for water balance calculations. The length of whole ice-free time appointed in the study, or the total cumulative time over all intervals in a year, is called a “span”. It starts from the earliest day of lake level observations that falls within the periods and ends at the last day of level observations falling into the periods. The span for water balance is 68 – 190 days long depending on the year.

The concept “period” is important for calculating the evaporation using any lake-heat-storage-based method, because only the first day and last day of the period have

observations of the lake's temperature profile which is needed to know lake heat storage. For those methods using lake temperature data, total evaporation in periods have to be calculated before a daily evaporation rate averaged over the period can be known or the daily rates are approximately allocated (see a later allocation explanation). For other methods not using lake temperature data, daily evaporation can be calculated first, and the periods are not necessarily required. However, for consistency, the periods are used for all methods in this study.

Listed in Table 2 is the number of periods of each year, number of consecutive days covered by the periods, number of intervals, and span length in a year. For example, there are 21 periods in 1980 which cover 180 consecutive days (from Julian day 126 to 305), and 17 intervals which cover 141 days (the span from Julian day 162

to 302). There are no intervals assigned for years 1978 and 1979 as the lake level monitoring was started in 1980, and no intervals for years 2003–2007 as recorded level data in these years were found unreliable.

3. Methods

3.1. Reference Evaporation Derived by Energy Budget

The energy budget is often used for lake evaporation calculations. For a lake and for a given time period previously defined, its energy budget is written as

$$\lambda E = R_{net} + H_{sed} + A_{net} - H - S \quad (1)$$

Table 2. Calculation periods and intervals.

Year	Periods	Days in periods	Intervals	span
1978	22	169		
1979	23	179		
1980	21	180	17	141
1981	21	171	21	162
1982	13	189	24	176
1983	13	189	26	183
1984	12	196	24	183
1985	11	171	24	161
1986	8	176	73	174
1987	6	164	44	161
1988	6	175	24	169
1989	7	189	26	183
1990	8	183	26	183
1991	7	197	27	190
1992	6	161	15	148
1993	5	180	12	169
1994	5	174	9	114
1995	5	168	9	139
1996	5	121	5	101
1997	5	177	13	153
1998	11	180	10	68
1999	13	184	12	149
2000	13	176	14	164
2001	12	166	15	160
2002	11	185	21	152
2003	11	149		
2004	11	163		
2005	11	190		
2006	12	190		
2007	12	198		
Total	326	5290	490	

where all energy terms are in unit of Joule. λE is latent energy used by evaporation of lake water during the period, λ is the latent heat of vaporization ($2.46 \times 10^6 \text{ J kg}^{-1}$), E is the evaporation (mm) within the period, R_{net} is net radiation, H_{sed} is heat released by lake sediments and is negligible for most cases, A_{net} is net heat advected into the lake from precipitation, inflows and outflows, and is also negligible, H is sensible heat transfer from lake surface to atmosphere, and S is the change of heat stored in the lake (due to temperature changes) during the period. The negligibility of the net heat advection A_{net} could be supported by the study results of Lengers *et al.* [6] for Sparkling Lake (0.64 km^2 , similarly small as Dickie Lake's area 0.94 km^2). They found that this advection term only had a mean value of 0.1 W m^{-2} in 10 summers, very small compared to other energy budget components (107 W m^{-2} of R_{net} , or 89 W m^{-2} of λE). Although a lacking of stream water temperature data at our site does not warrant a rigorous calculation of the advection term, it is believed negligible.

The sensible heat term can be expressed as $H=B \cdot \lambda E$, where B is the mean Bowen ratio for the period. Removing the two negligible terms, Equation (1) is rewritten as

$$E = \frac{R_{net} - S}{\lambda(1+B)} \quad (2)$$

The net radiation is an accumulation of daily net radiation in the period:

$$S = S_2 - S_1 = \frac{\rho_w c_w}{a_{s2}} \sum_{j=1}^{m_2} T_2(j) \cdot a_2(j) \cdot z_2(j) - \frac{\rho_w c_w}{a_{s1}} \sum_{j=1}^{m_1} T_1(j) \cdot a_1(j) \cdot z_1(j) \quad (4)$$

where S_2 and S_1 are heat storage on the last and first day respectively, $\rho_w=1000 \text{ kg m}^{-3}$ is water density, $c_w=4186 \text{ J kg}^{-1} \text{ }^\circ\text{C}^{-1}$ is specific heat of water, a_{s2} and $a_2(j)$ are the lake surface area and water area (m^2) of any zone j ($j=1, 2, \dots, m_2$ starting from the lake surface zone) on the last day, $T_2(j)$ and $z_2(j)$ are the temperature and thickness of zone j on the last day. Similarly, a_{s1} , $a_1(j)$, $T_1(j)$, $z_1(j)$ are the surface area, water area, water temperature and zone thickness respectively on the first day. Water area a (m^2) at a height h (m) from lake bottom is estimated by an empirical relation derived from observed lake morphometry data [29] as follows.

$$a = -389 \cdot h^3 + 10245 \cdot h^2 + 11592 \cdot h - 3340 \quad (5)$$

As in Equation (6), the period-mean Bowen ratio B is calculated from daily Bowen ratios which is derived from air and lake surface temperatures [30].

$$B = \frac{\gamma}{n} \sum_{i=1}^n \frac{T_s(i) - T_a(i)}{e_{ss}(i) - e_{sa}(i)} \quad (6)$$

$$R_{net} = \sum_{i=1}^n [(1 - \alpha_{sw})r_{swd}(i) + (1 - \alpha_{lw})r_{lwd}(i) - r_{luw}(i)] \quad (3)$$

where i is the order of any day in the period ($i=1, 2, \dots, n$ days), $r_{swd}(i)$ is daily downward shortwave radiation which is observed at the meteorological station, $\alpha_{sw}=0.07$ is the shortwave albedo of water (value taken from Lengers *et al.* [6]), $r_{lwd}(i)$ is daily downward longwave radiation, $\alpha_{lw}=0.03$ is the longwave albedo, and $r_{luw}(i)$ is daily upward longwave radiation. Longwave radiations are calculated by $r_{lwd}(i)=\varepsilon_a \sigma T_a^4$, $r_{luw}(i)=\varepsilon_s \sigma T_s^4$, where $\varepsilon_a=0.91$ and $\varepsilon_s=0.97$ are emissivity of the atmosphere and surface water respectively, T_a and T_s are daily air temperature and surface water temperature (in unit of $^\circ\text{K}$). The daily air temperature is provided by routine monitoring, while surface water temperature is observed only on the first and last day of a period (roughly 14–21 days long). The daily water temperature within a period is obtained by interpolation between the two days' temperature values.

The heat storage change S in Equation (2) is calculated by using vertical lake zones and lake temperature profiles. Temperature profiles are observed at the central lake where it has the deepest water. The water body is divided into vertical zones from lake surface to lake bottom, and the number of zones may differ a little among periods. The heat stored in the lake on the last and first day of the period is calculated, and their difference is the change in heat storage,

where γ is psychrometric constant ($67 \text{ Pa } ^\circ\text{C}^{-1}$), n is the number of days in a period, i is any day within a period, $T_s(i)$ and $T_a(i)$ are daily mean temperature ($^\circ\text{C}$) of lake surface and air above the lake respectively, $e_{ss}(i)$ and $e_{sa}(i)$ are saturated vapour pressure (Pa) at the lake surface and air temperatures. The saturated vapour pressure is calculated with the Arden Buck Formula [31]:

$$e_{sa} = 611.21 \cdot \exp \left[\frac{(18.678 - T_a / 234.5)T_a}{257.14 + T_a} \right] \quad (7)$$

Daily evaporation is not obtained by using Equation (2) as the field collection of lake temperature profiles is not conducted every day in a period. After the total evaporation E is calculated as above, daily evaporation is allocated from the total amount based on a distribution pattern. Hamon method is the easiest way to estimate daily evaporation and uses only air temperature. Therefore, a time series of daily evaporation is created by using the Hamon method (described later), their summation gives a total amount, and the ratio of daily evaporation to total evaporation is determined. By applying the same ratios to

the total amount value obtained from the energy budget method, daily evaporation for the energy budget method are obtained. A further discussion on the allocation caveat will be provided in the Discussion section.

3.2. Evaporation Methods

Seven methods are selected for calculation of lake evaporation at Dickie Lake and are later compared to each other. They are Hamon (HM), Penman (PM), Priestley-Taylor (PT), DeBruin-Kejiman (DK), Jensen-Haise (JH), Makink (MK) and water balance (WB). These methods are commonly used and once compared in literature, but they have not been compared or evaluated for lakes on the cold Canadian Shield, using dataset as long as 30 years. Water balance method has not been compared with other methods in the published reports. Calculations are conducted for the defined periods of each year, and two values are estimated – the total evaporation amount in a period, and daily evaporation rates for the period. Depending on individual methods, the total evaporation is given first, then daily rates are calculated from the total value; or the daily evaporation rate is calculated first, then the total value is derived from daily rates. Comparisons of the seven methods are made on basis of interval and span, not on daily basis. However, daily evaporation rate is required to provide the evaporation amount within an interval, as the dates in an interval are different from the dates in a period.

$$E = \frac{\Delta}{\Delta + \gamma} \cdot \frac{R_{net} - S}{\lambda} + \frac{\gamma}{\Delta + \gamma} \cdot 0.0026 \cdot (1 + 0.54\bar{u}) \cdot (1 - \bar{q})\bar{e}_{sa} \cdot n \quad (10)$$

where R_{net} and S are the net radiation (Joule) and lake heat storage change in the period, \bar{u} is the mean daily wind speed ($m s^{-1}$) for the period, \bar{q} is the mean daily relative humidity (≤ 1.0), \bar{e}_{sa} is the mean daily saturated vapour pressure (Pa), Δ is the mean slope of the saturated vapour pressure – temperature curve at the air temperature, and n is number of days in the period. The two terms related to the slope Δ and psychrometric constant γ are expressed as empirical relations of air temperature [34]:

$$\frac{\Delta}{\Delta + \gamma} = 0.439 + 0.01124T_a \quad \frac{\gamma}{\Delta + \gamma} = 0.5495 - 0.01119T_a \quad (11)$$

Total evaporation is obtained first as the lake heat storage change in a period (S) is included in Equation (10). The total evaporation E is allocated to each day of the period as done for the case of energy budget.

3.2.3. Priestley-Taylor Method

Evaporation is estimated based on radiation and heat storage only, as done by Winter *et al.* [23].

3.2.1. Hamon Method

It is often used to estimate lake evaporation or watershed potential evaporation because of its simplicity [32]. For a given lake, daily evaporation e (mm) is calculated from daily temperature T_a ($^{\circ}C$) as follows.

$$e = 0.63 \cdot D^2 \cdot 10^{\frac{7.5T_a}{T_a + 273}} \quad (8)$$

where D is the ratio of maximum sunshine duration (hour to 12 hours, and is determined by latitude of the lake and the date:

$$D = \frac{1}{90} \arccos\{-\tan(\varphi) \cdot \tan[23.45^{\circ} \sin(\frac{J-80}{365} \cdot 360^{\circ})]\} \quad (9)$$

where φ is the latitude (45.13° for Dickie Lake), J is the Julian day of any date of interest.

Total evaporation E in a period is the sum of daily evaporation of all included days.

3.2.2. Penman Method

A format of Penman equation, once recommended by Food and Agriculture Organization [33], is used and slightly modified to calculate lake evaporation. The modification is an addition of the lake heat storage change rather than taking only the net radiation. The evaporation in a period is written as

$$E = 1.26 \cdot \frac{\Delta}{\Delta + \gamma} \cdot \frac{R_{net} - S}{\lambda} \quad (12)$$

where the variable $\Delta/(\Delta + \gamma)$ is estimated in Equation (11).

3.2.4. DeBruin-Kejiman Method

The DeBruin-Kejiman equation is written as [23,35]

$$E = \frac{\Delta}{0.95\Delta + 0.63\gamma} \cdot \frac{R_{net} - S}{\lambda} \quad (13)$$

where the slope of saturated vapour pressure curve Δ could be estimated by using Equation (11), and net radiation and lake heat storage change have been estimated in the energy budget calculations.

3.2.5. Jensen-Haise Method

Daily evaporation is first calculated by the following Equation [23].

$$e = [0.014(1.8T_a + 32) - 0.5] \cdot \frac{r_{swd}}{\lambda} \quad (14)$$

where T_a is daily temperature ($^{\circ}\text{C}$), r_{swd} is daily shortwave radiation as used in Equation (3). The total evaporation in a period is the sum of the daily rates.

3.2.6. Makkink Method

Daily evaporation is calculated as [23]

$$e = 0.61 \frac{\Delta}{\Delta + \gamma} \frac{r_{swd}}{\lambda} - 0.012 \quad (15)$$

And then the total evaporation is obtained.

3.2.7. Water Balance Method

As shown in Figure 2, the lake's inflows from five major streams are measured, the inflows from ungauged watersheds can be prorated from measured flows, and the lake outflow, lake level and precipitation are also known. Therefore, the lake evaporation during a time span (or interval) can be estimated by using a water balance equation for the lake.

Water balance analysis is made for a time in ice-free season (early May – mid November) as long as the lake level data are available. For a span in a year, the water balance is expressed as

$$E_{WB} = P + R - O - \Delta L \quad (16)$$

where E_{WB} is the total evaporation (mm) during the span, P is the precipitation volume (mm) during the span, R is the runoff (mm) from all watersheds (gauged and ungauged), O is the outflow volume at the lake outlet, and ΔL is the level change over the span.

The span length of a year varies with years, because the starting date and ending date may differ between years. Water balance estimation must begin and end at a day when the lake level is known. After an estimation is completed for a year (May to November usually), a new estimation for the next year is made. Regarding the inflow from ungauged watershed area, a proration method was applied to the study area [20,22] to derive discharge from ungauged area based on the assumption: the areal runoff is equal among the lake's watersheds. An evaluation of errors originated by the proration was made by Devito and Dillon [36] using two lakes other than Dickie Lake in the same region, and the errors were within 10% of the annual runoff measured. Therefore, we use the same method to get an estimation of the ungauged runoff.

Groundwater inflow and outflow, or groundwater net flow to the lake, are not included in Equation (16) as they are assumed negligible. This assumption was applied to the study area before [20,22,36], and was used in other regions [37]. The characteristic shallow surficial till and largely impermeable bedrock in the Canadian Shield region support the assumption, as it is supported by the small ratio 0.07 of groundwater inflow against surface water inflow to Lake Michigan [38], and by a satisfactory analysis of water balance in 30 years for Dickie Lake

without including groundwater flow [Yao *et al.*, Data Report in editing, Ontario Ministry of Environment].

A similar equation as Equation (16) is applied to any interval within a span, and the evaporation amount of the interval is obtained.

3.3. Comparison and Evaluation of Seven Methods

The difference of method-calculated evaporations from the energy-budget E_{WB} values is used as an accuracy index of an evaporation method. Comparing the differences of seven methods will provide a quantitative evaluation of their performance and accuracy. The root mean square deviation (RMSD) is a frequently-used measure of the differences between values predicted by an estimator and the values observed from the thing being estimated. Another indication of how well the estimator follows/predicts the variations in the measured values could be given by a coefficient of efficiency (CE) as proposed and applied by Nash and Sutcliffe [39]. This CE index is expressed as

$$CE = 1 - \frac{\sum (E_{est} - E_{ref})^2}{\sum (E_{ref} - E_{mean})^2} \quad (17)$$

where E_{est} and E_{ref} are the estimated and reference (or measured) evaporation for a span (or interval) respectively, and E_{mean} is the mean of reference evaporation. A larger CE number indicates a more accurate estimator.

Both indexes RMSD and CE are used in our study to evaluate and compare the accuracy and performance of the seven evaporation methods, and a performance rank is then proposed. The estimated evaporation is plotted against the reference evaporation for examining each method's bias and errors. The comparison is conducted separately for the span (longer time) and interval (shorter time) because a method might perform quite differently between the two time scales.

4. Results

Results of energy budget calculation for 30 years (1978–2007) and the resulted reference evaporation used for comparison are presented first. They are followed by the results of evaporation estimated with the seven methods. Then method comparison results are presented.

4.1. Energy Budget

Span-mean values of energy budget variables (net radiation, sensible heat flux, evaporative heat flux, and lake heat storage rate) and meteorological variables are illustrated in Figure 3 to show their inter-annual changes. Figure 3(a) shows the meteorological variables, and Figure 3(b) shows the energy budget fluxes, with the source

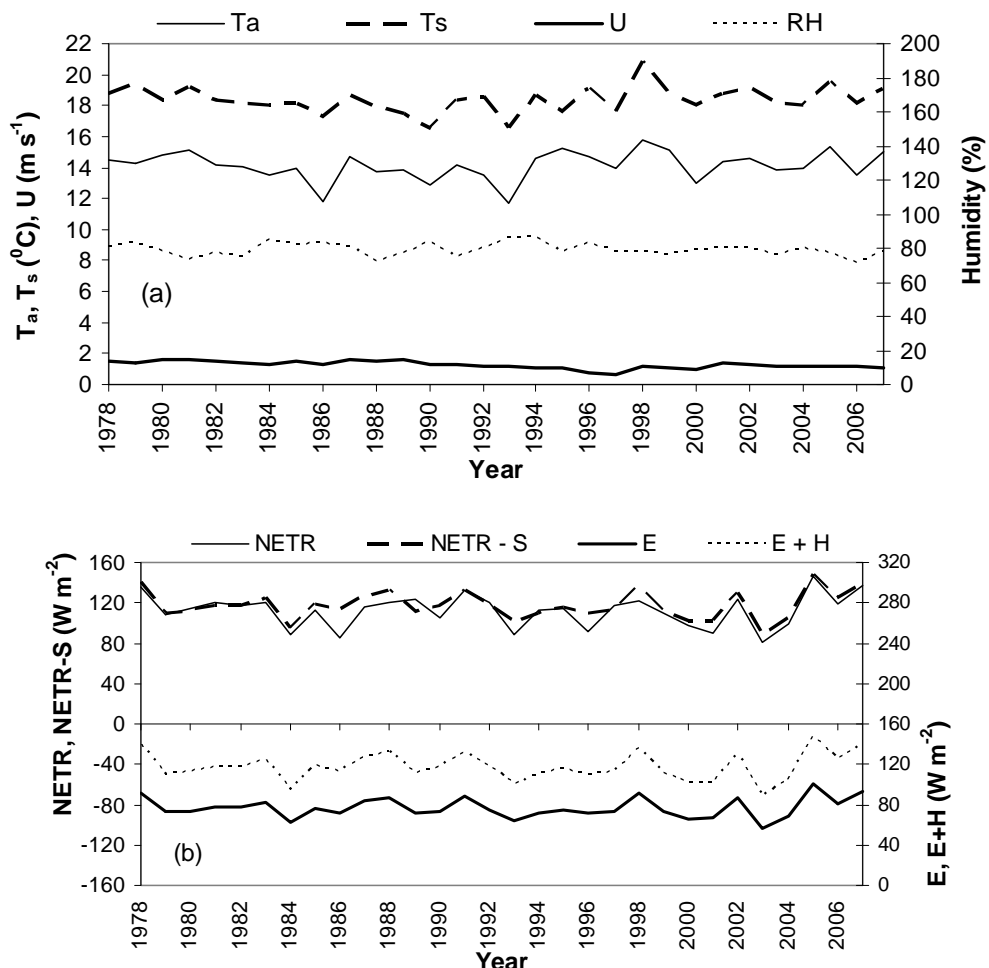


Figure 3. Span averages of (a) meteorological variables, and (b) energy budget variables.

items in upper section and consumptive items in lower section. Air temperature and lake surface temperature change in an identical way, as is usually expected. Net radiation flux changes coincidentally with temperature. Very little correspondence is seen between humidity (or wind speed) and temperature (or net radiation). Furthermore, lake heat storage rate possesses a tiny portion in source energy (net radiation - heat storage). For a majority of 30 years, the lake heat storage contributes very little to the energy source on annual basis. For this reason, the consumptive term (E or $E+H$) has a strong correspondence to net radiation flux: climbing or dropping in the same years.

Daily mean values of meteorological and energy budget variables (the 30-year mean for any day between the Julian day 121 and 319) are illustrated in Figure 4 to show seasonal changes. Air temperature has some fluctuations while demonstrating a clear curving. Corresponding to air temperature, the lake surface temperature has a similar changing curve, but smoother. To their contrast, relative humidity does not have clear seasonal

change although it increases slightly, nor does wind speed have clear changes.

The seasonal patterns of energy terms demonstrate two phenomena. 1) The energy source (net radiation minus lake heat storage change, NETR-S) determines how much energy could be consumed by sensible and evaporative fluxes, therefore the source term NETR-S and consumptive term $E+H$ have the same changing pattern – climbing in the summer to their peaks in mid July (around day 200) and dropping in the late summer and fall. 2) There is a time lag between net radiation NETR and consumption $E+H$, because of the function of lake heat storage. Unlike $E+H$, net radiation is high in May and June, and then decreases quickly in July and August till November. By dividing the curves at the Julian day 200 (July 20), lake water uses net radiation to increase its temperature or increase heat storage over the first section of the curve, the usable energy source for evaporation and sensible heat conduction is less than the net radiation, and therefore, the high radiation rate does not produce a high

$E+H$ rate in May and June. In July the lake is not absorbing net radiation and the high radiation finally creates the highest evaporation rate. Contrarily, lake water reduces its temperature over the second section of the curve, and releases its stored heat to compensate for the decreasing radiation. The usable energy source is more than the net radiation. $E+H$ does not decrease as quickly as the net radiation because of the lake heat compensation. Especially in late October and November, energy provided by lake water overrides the net radiation to maintain a small evaporation flux.

The total reference evaporation in a span of a year, as calculated with the energy budget equations, fluctuates irregularly because of its natural changes with meteorological inputs and the difference in span length (number

of days in a span differs, see Table 2). The reference evaporation in a period among the 30 years (totally 326 periods) has large fluctuations too, because a period can be in the hot summer or cold fall, and the period length can be quite different. Therefore, these total reference evaporation rates are not plotted in a figure. But they will be the basis for methods comparison. In order to illustrate the inter-annual variations in evaporation rates, all daily evaporation rates within a span of a year (121–198 days depending on the year, see Table 2) is averaged to obtain the annual average rate, and the average rates over 30 years are shown in Figure 5. The rate varies between 2.0 – 3.5 mm/d, with lower rates in 1979–1986 and 1999–2004, and higher rates in 1987–1992 and 2005–2007. Not a clear increase or decrease trend is found.

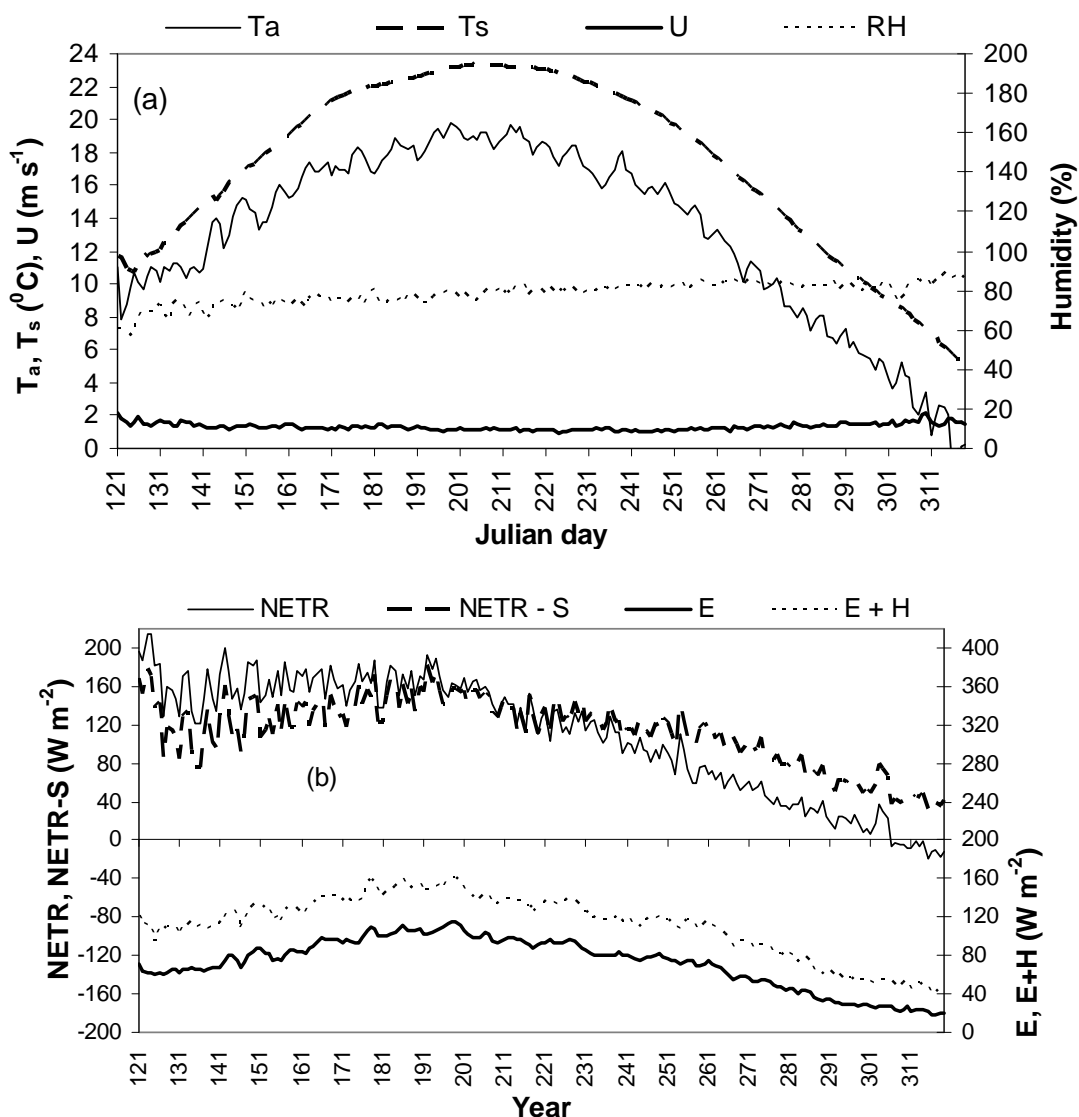


Figure 4. Seasonal changes and patterns of (a) meteorological variable, and (b) energy budget variables, the mean values of daily variables over 30 years.

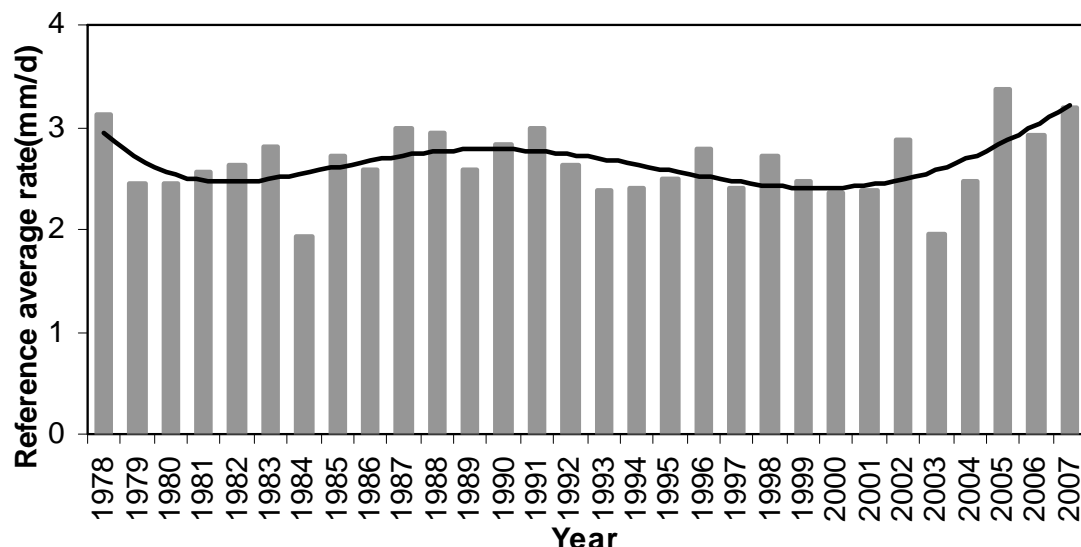
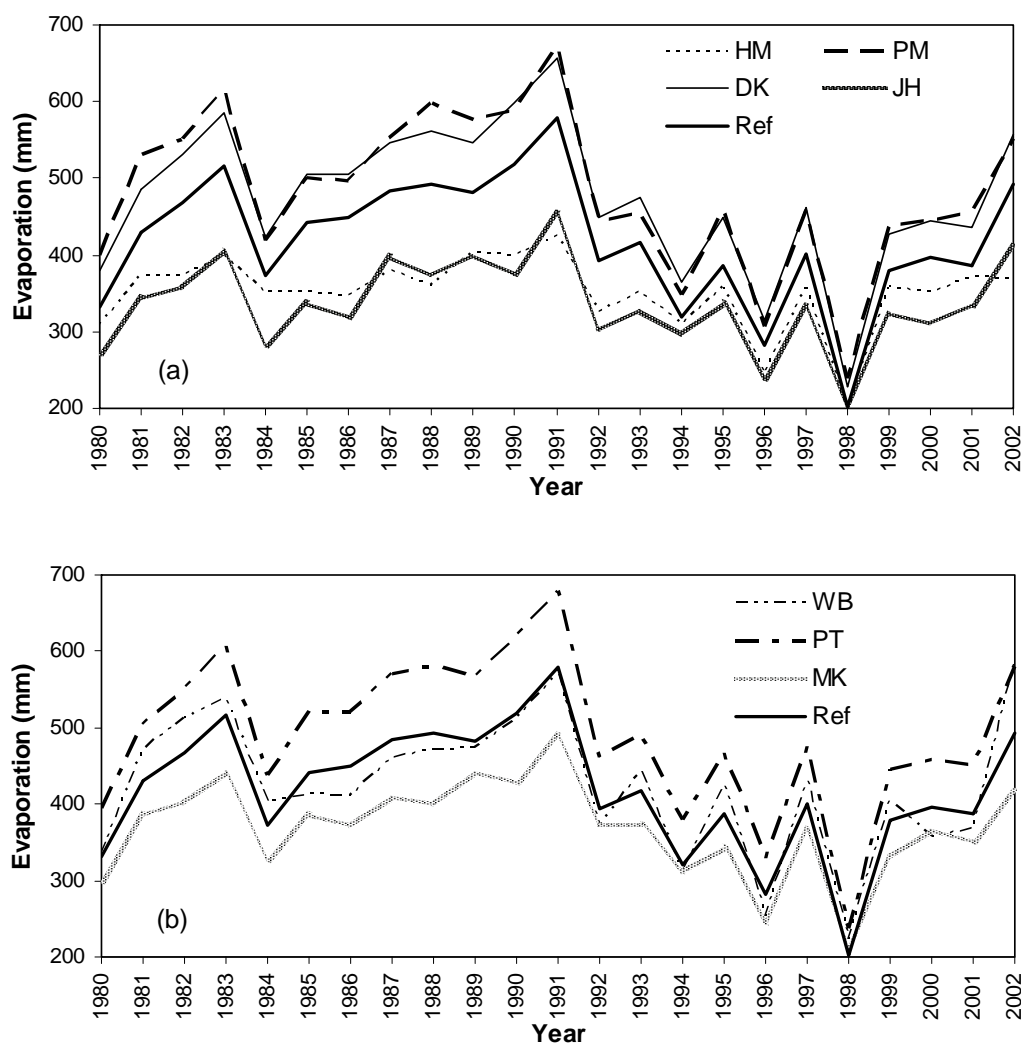


Figure 5. Annual reference evaporation rate averaged over all the days in the span of a year (the bar showing averaged evaporation rate in mm/d, the solid line showing an inter-annual variation pattern of the rates).



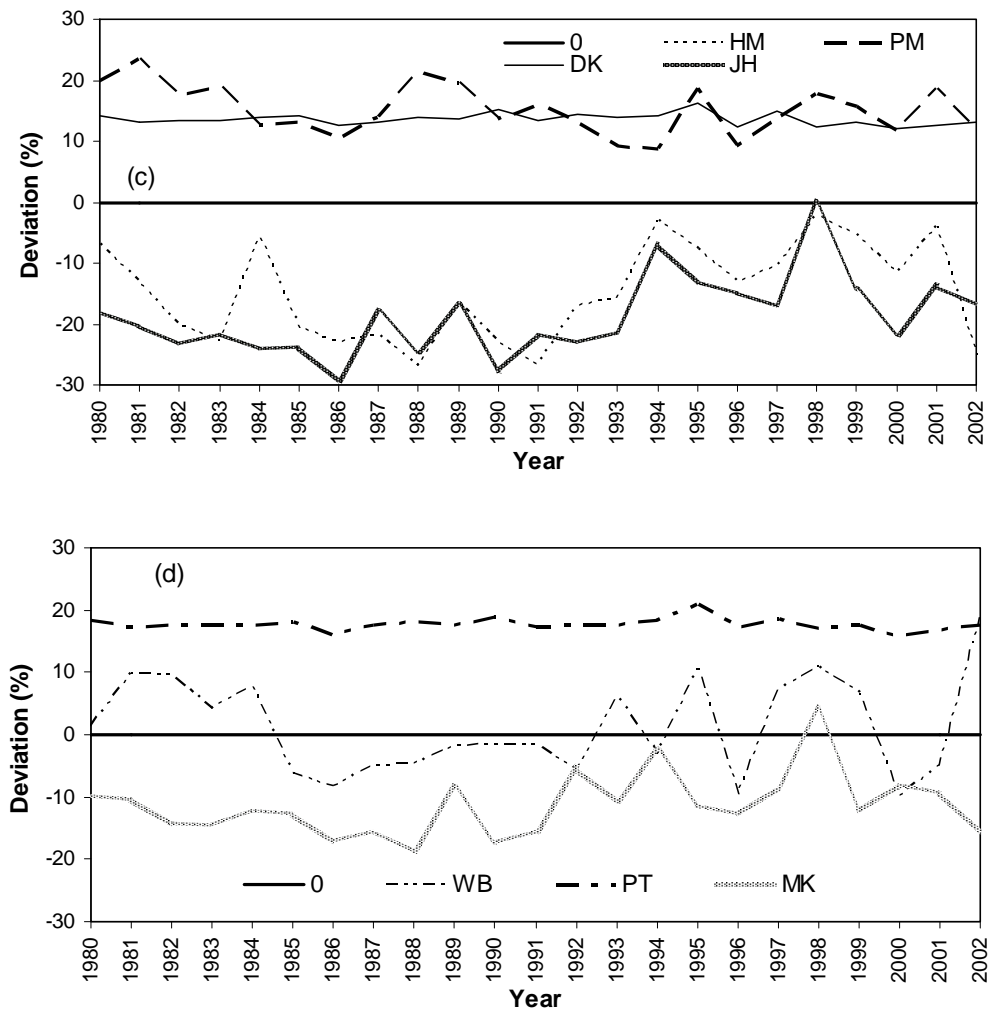


Figure 6. Comparison of method-estimated evaporation with reference evaporation for each of the 30 years: (a) span evaporation (mm) by four methods (HM, PM, DK, JH), (b) span evaporation (mm) by remaining three methods (PT, MK, WB), (c) percent deviation of estimated evaporation from the reference (with HM, PM, DK, JH), and (d) percent deviation of estimated evaporation from the reference (with PT, MK, WB).

Table 3. RMSD and CE values of estimated vs. reference evaporation, and ranked performance of seven evaporation methods when used to span length. The rank of six methods as appeared in Winter *et al.* study and Rosenberry *et al.* study are also listed for comparison.

Method	RMSD (mm)	CE	Rank	Rank by Winter	Rank by Rosenberry
WB	32.8	0.84	1	N/A	N/A
MK	56.5	0.54	2	4	5
DK	58.3	0.51	3	3	3
PM	68.1	0.33	4	2	4
PT	75.6	0.17	5	5	2
HM	80.6	0.06	6	6	6
JH	89.2	-0.15	7	7	7

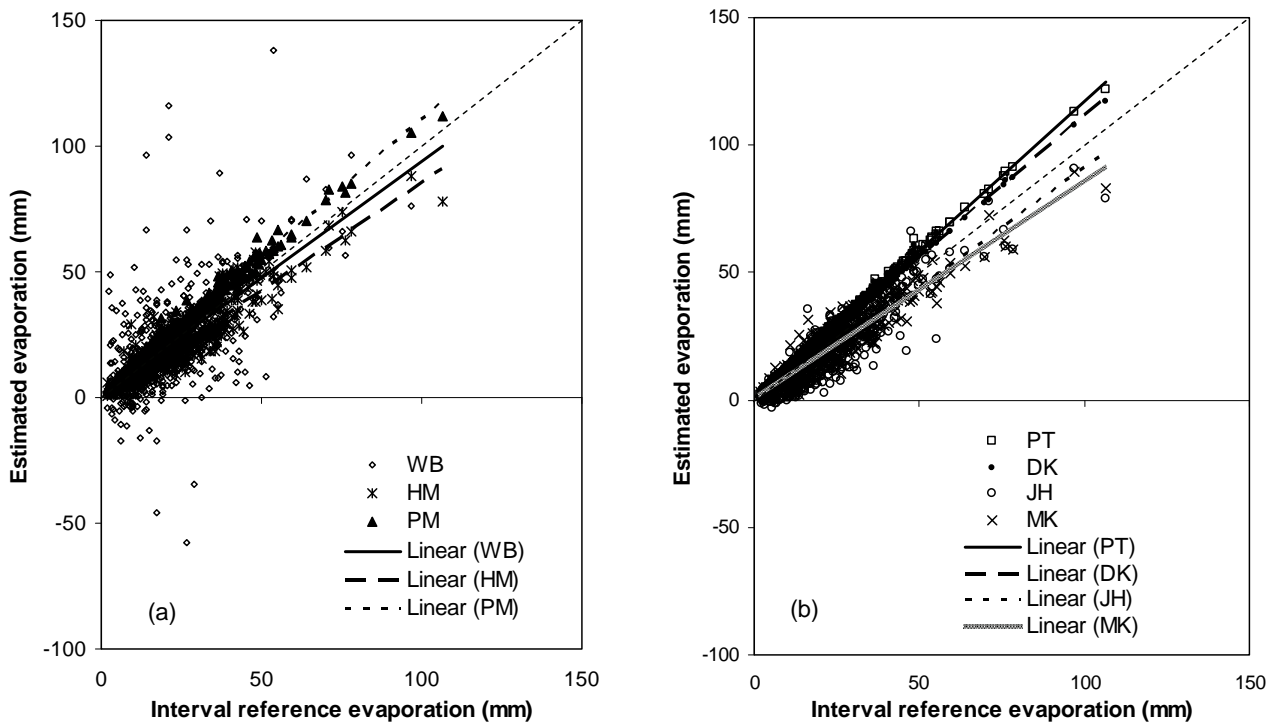


Figure 7. Comparison of interval evaporation against the reference: (a) evaporation from WB, HM and PM and their linear trends, (b) evaporation from PT, DK, JH and MK and their trends.

Table 4. RMSD and CE values and ranked performance of seven methods when used to interval evaporation.

Method	RMSD (mm)	CE	Rank
DK	3.5	0.94	1
PM	4.1	0.92	2
PT	4.7	0.89	3
MK	5.6	0.85	4
HM	6.4	0.80	5
JH	7.3	0.74	6
WB	18.6	-0.66	7

4.2. Evaporation from Seven Methods and Method Comparison

Among the seven methods, six provide evaporation estimations for 30 years (1978–2007): Hamon (HM), Penman (PM), Priestley-Taylor (PT), DeBruin-Kejiman (DK), Jensen-Haise (JH) and Makkink (MK), as they rely on meteorological data. The water balance (WB) provides estimations for 23 years (1980–2002) because the lake level observation data is available only for these years. Therefore, the results from these 23 years are presented and used for comparison. Estimated evaporation in an-

nual spans are shown in Figure 6. The results are divided into two groups in the figure to provide a better distinguishing, as all results plotted on one figure would make the lines difficult to be distinguished. One group includes four methods: HM, PM, DK and JH, the other group includes three methods: PT, MK and WB. Results of evaporation obtained from the seven methods and the reference evaporation from energy budget are shown in Figure 6(a) and (b). Evaporations from WB are mostly close to reference evaporation, results of Penman, Priestley-Taylor, DeBruin-Kejiman and Makkink methods are away from the reference, whereas results of

Hamon and Jensen-Haise are even farther from the reference.

Another feature that is seen from Figure 6(a) and (b) is the inter-annual change. Except for the Hamon method, evaporations of the other six methods have almost identical changing patterns: very low in 1984 and 1998, very high in 1983, 1991 and 2002. The major reason for this similarity is that they use a controlling meteorological factor – solar radiation which has had the inter-annual change. The Hamon uses only air temperature which does not show such a change style.

The percent deviations (or errors) of method-estimated evaporation from the reference evaporation are shown in Figure 6(c) and (d). The WB deviations are scattered around the zero level (zero error level), with both positive and negative errors, being the best evenly scattered over the 23 years. The PM or PT or DK deviations are scattered above the zero level (over estimated) for all 23 years. The overestimation of Penman and Priestley-Taylor methods are often reported [9]. The HM, JH and MK deviations are scattered below the zero level (under estimated) for all years except for 1998.

Values of root mean squared deviation (RMSD) between estimated and reference span evaporation, and values of coefficient of efficiency (CE) are listed in Table 3. A lower RMSD value or a higher CE value indicates a lower error between the estimated and observed evaporation, i.e. a better performance in evaporation calculation. Therefore, a performance rank from best to least is determined by the RMSD and CE values, and the rank is: WB, MK, DK, PM, PT, HM, and JH.

Method comparison results with regards to span evaporation might differ from a comparison using interval evaporation. The estimated evaporations for 490 intervals in the 23 years are illustrated in Figure 7 against their corresponding reference evaporations, with three methods in Figure 7(a) and other four methods in Figure 7(b). A linear trend line is shown for each method's result, and the slope 1:1 center line is also drawn. Surprisingly, the results from WB scattered greatly around the center line, indicating the worst result (opposite to being the best result with the span comparison), although its trend is mostly close to the center line. Method PM, PT and DK tend to overestimate evaporations, while method HM, JH and MK tend to underestimate evaporations.

Similarly to span comparison, the RMSD and CE values of estimated interval evaporation vs. the reference are summarized in Table 4. The rank is: DK, PM, PT, MK, HM, JH and WB. The performance and ranking of seven methods, when applied to estimate evaporation in shorter time duration, are different from the performance when applied to estimate evaporation in longer duration.

Why the water balance calculations do not give reliable evaporations for intervals? When the time duration becomes shorter, the magnitude of evaporation item be-

comes smaller in the water balance items (compared to precipitation, runoff, outflow, lake level change), and influence of data mistakes or observation uncertainties become more obvious. For instance, if the evaporation is in a magnitude of 30 mm for an interval of 10 days, then any single mistake in lake level, precipitation or discharge could reach to 5 mm, and the mistake could cause a 17% influence on evaporation through water balance accounting. Combined influence of multiple mistakes could cause severer error in evaporation result. But for an evaporation of 500 mm in a span of 7 months, the influence of the same mistake would be 1%.

Collectively assessing Table 3 and Table 4, it is noted that the method HM and JH perform comparatively worse in both cases of span and interval, and should be avoided if other methods are applicable. The DK, MK, PM and PT perform either the best or better than other methods in both cases, and therefore should be well applied to lake evaporation calculation. The water balance WB can be satisfactorily used to long duration (annual, open water season), but should not be used to short duration (weeks, month).

5. Discussion

There may be concerns about the collection location of meteorological data or the distance of the weather station to the lake. Our data are from a station located approximately 1.0 km away from Dickie Lake, not from a raft facility on the lake. This concern was addressed by the study results of Winter *et al.* [23]. They used 11 evaporation methods including six we used here, and they compared the differences caused by using raft-based, land-based (near the lake) and remote-site-based (60 km away) data. Their results indicated that the usage of raft- and land-based data did not result in marked differences in evaporation rates for those six methods. Therefore, the location of our meteorology station on land instead of on lake is not a concern, although raft-based data would have been desirable.

As indicated before, the energy-budget equations only calculated a total evaporation amount within a period because of limited number of lake temperature profiles, and the daily evaporation rate in the period was allocated by using daily rates estimated from the Hamon formula. These allocated daily evaporations used as reference rates could contain potential errors associated with the allocation, since Hamon formula only utilized air temperature and could have large bias from true evaporation rate. Two rational are suggested to argue for the daily allocation. Method comparison in the study was made on the basis of annual span evaporation or interval evaporation, not daily rates. The high accuracy of energy-budget results for periods and spans have been ensured by the method itself. Secondly, although the Hamon evaporation amount for a

period might be less accurate than that of energy budget, the distribution pattern of daily rates within the period is usually similar between the two methods. The similar distribution is used to allocate daily rates for energy budget method. Resulted daily rates would not be exactly the same as the values that would be calculated on daily basis if there were available water temperature data, however, the resulted rates should be quite close to those values.

The performance rank of the six methods (not including WB) recommended by Winter *et al.* [23] and the rank of same six methods recommended by Rosenberry *et al.* [14] are also listed in Table 3. It would be understandable that the three ranks may be different because the lakes are in different locations, and the datasets used are different. However, the three ranks are similar to some extent. DeBruin-Kejiman and Penman are among the better methods, with DK being the 3rd position among all three ranks; Hamon and Jensen-Haise are among those showing poorer results, positioned at 6th and 7th among all ranks. If comparing two ranks, the difference between our rank and Winter rank is that Makkink, DeBruin-Kejiman and Penman are positioned at 2, 3 and 4 in our rank, against 4, 3 and 2 in Winter rank. The difference between our rank and Rosenberry rank is that Makkink and Priestley-Taylor are positioned at 2 and 5 in our rank, against 5 and 2 in Rosenberry rank. In other words, it is more possible and reliable to use an evaporation method from the energy-aerodynamics combination group, such as Penman, DeBruin-Kejiman and Priestely-Taylor. A method from the two-parameter (solar radiation and temperature) group, such as Makkink, may provide a satisfactory estimation of lake evaporation. But a method from the temperature-only group, such as Hamon, provides poorer estimations.

An effort is tried to interpret physical or logic reasons to why the methods perform in a way as shown in Table 3, why some methods perform better than other ones. First of all the accuracy of the reference method – energy budget would not be doubted, as it is based on strictly-defined theories and has been proved by many researchers. It provides reliable evaporation reference provided that the input data are correctly collected. The best performer – water balance method (Equation (16)) has the ability to provide good evaporation estimations, if the in and out items are well measured. The runoff coming from 2/3 watershed area of Dickie Lake has been well monitored, precipitation and outflow are well monitored too, and lake level is measured too. This data information ensures that estimated evaporation in spans is reasonable and reliable. The second-ranked Makkink method (Equation (15)) has a simple empirical format and uses only air temperature and short-wave radiation as input. These two factors are the most important among many meteorological factors. Its equation has a fairly correct description of

the two key factors, and the equation applies well to the lake in the Canadian Shield as it did to its original datasets. Although it gives fairly good evaporation estimates, it has a drawback of underestimation. Probably a minor adjustment to the equation (i.e. change the constant 0.61) can improve this drawback.

The third-ranked DeBruin-Kejiman method is an empirical equation similar to Makkink, considers more affecting factors (temperature, short- and long-wave radiations, lake heat storage) than MK does. Its performance is accepted just because it can be applied to the studied lake without equation adaption. Actually the overestimation problem as seen from Figure 6 could be improved by adjusting the equation. The fourth-ranked Penman method (Equation (10)) has been widely used to estimate lake evaporation or watershed potential evapotranspiration, having taken consideration of all affecting factors. There might be two reasons leading to its overestimation problem: the function in relation to the wind speed and the period-averaging treatments in wind speed and air humidity. The fifth-ranked Priestley-Taylor method (Equation (12)) is an empirical equation similar to DK. Its not-good performance means that probably it needs adjustment to be well applied to the study area, for example changing its constant 1.26. One common concern for the three methods (DK, PM, PT) which all overestimate evaporation is noted but has not been identified: they all include a net radiation in their equations. If the net radiation were not correctly measured or calculated, a systematic overestimation would have occurred.

The sixth-ranked Hamon method (Equation (8)) does not give good estimates simply because it only considers air temperature as the controlling factor. Unless the meteorological data is severely restricted, this method is not recommended for lake evaporation. The seventh-ranked Jensen-Haise method (Equation (14)) includes very site-dependent parameters, and may be not applicable to our study lake without proper adjustment. The evaporation is badly underestimated.

The data length of 30 years would remind that a timely trend analysis may be worthwhile. All meteorological and energy budget variables were checked to find potential trends or periodic cycles in the 30 years, but none has been found to have a significant trend at Dickie Lake. Linacre [40] proposed that lake-evaporation rate is generally decreasing at around 0.1 mm/d per decade around the world, chiefly on account of reduced solar radiation. The estimated rates by energy budget method for Dickie Lake do not show such a reduction. The averaged daily rate in ice-free season for three decades (1981–1990, 1991–2000, 2001–2007, with the third decade being 7 years only) is 2.66, 2.57 and 2.74 mm/d respectively, the rate decreases by 0.09 mm/d from the first to second decade, but increases 0.17 mm/d from the second to third decade.

Apart from the traditional methods such as the energy budget and seven methods used here that need meteorological data, a newer way to estimate lake evaporation is by using isotope technology. Saxena [41] estimated evaporation from a central Swedish lake by measuring oxygen-18 content in lake water, stream inflows and outflow, and precipitation. The results of isotope method were further compared with results of bulk-aerodynamic and Bowen ratio methods [42]. Except for some situations such as high-precipitation events, high-outflow periods or rapid lake-volume change periods, the evaporation estimated from the three methods agreed. A similar experimental study was conducted by He *et al.* (personal correspondence with one of the authors, 2009) for Dickie Lake by measuring oxygen-18, and their results gave a total evaporation 660 mm for year 2003 (January 1 to December 31). For comparison, a total evaporation for the same year was calculated using the Makkink method (it needed air temperature and radiation data, not needing lake temperature), and the calculated evaporation was 451 mm. This reveals a significant difference between isotope-estimated evaporation and Makkink-estimated evaporation.

6. Conclusions

The 30 year dataset from Dickie Lake provided a valuable opportunity to conduct a long-term study on lake evaporation. Evaporations in longer spans and shorter intervals during ice-free season were calculated separately using seven evaporation methods, based on field meteorology, hydrology and lake water temperature data. A reference value of the evaporation was provided by a lake water energy budget, and was used to evaluate the performance of the seven methods. The deviations of method-induced evaporation from reference evaporation were compared among the seven methods, and a performance rank was proposed based on the comparison. For purpose of evaporation in long time duration such as a span or a year, the best-to-least methods were ranked as: water balance, Makkink, DeBruin-Kejiman, Penman, Priestley-Taylor, Hamon, and Jensen-Haise. For purpose of evaporation in short time such as an interval or a month, the best-to-least methods were ranked as: DK, PM, PT, MK, HM, JH and WB. Overall, four methods (MK, DK, PM and PT) work better than other three methods.

Details of energy budget, correspondences between energy terms and meteorological variables, annual or seasonal changes of these terms and variables, and the compensation function of lake heat storage in evaporation flux were also analyzed and illustrated. Within the ice-free duration of a year, lake water absorbed a portion of net radiation in early and mid summer, and released the absorbed energy in the fall to compensate for evaporation.

Strong correspondence existed between net radiation and consumptive heat flux (latent and sensible heat) but with a time lag, or between temperature and the heat flux. From year to year, the lake heat storage did not play a notable role in energy budgeting, and lake evaporation or consumptive heat flux was controlled by the net radiation. Our study results have shown a similar energy budget pattern as other studies in similar climatic regions, and identified a performance rank for the evaporation calculation methods to be used for lakes in Canadian Shield.

7. Acknowledgements

The author would like to thank Robert Girard for his assistance in lake morphometry and profile data, and thank Joe Findeis and Ron Ingram for their assistance in meteorology data. Thank Peter Dillon, Lance Aspden and Christiane Guay for their discussion and comment. Numerous former governmental staff and university partners have contributed to the data collection and management.

8. References

- [1] G. Krantzberg, "The Great Lakes, a 35th year anniversary: Time to look forward," *Electronic Green Journal*, Vol. 26, pp. 1–4, 2008.
- [2] N. D. Yan, A. M. Paterson, K. M. Somers, and W. A. Scheider, "An introduction to the Dorset special issue: transforming understanding of factors that regulate aquatic ecosystems on the southern Canadian Shield," *Canadian Journal of Fisheries and Aquatic Sciences*, Vol. 65, pp. 781–785, 2008.
- [3] J. J. Gibson and W. D. Edwards, "Regional water balance trends and evaporation-transpiration portioning from a stable isotope survey of lakes in northern Canada," *Global Biogeochemical Cycles*, Vol. 16, No. 10, pp. 1–14, 2002.
- [4] Minnesota DNR Waters, "Lake-ground water interaction study at White Bear Lake, Minnesota," Minnesota Department of Natural Resources Report, Minnesota, USA, 1998.
- [5] G. Weyhenmeyer, "Rates of change in physical and chemical lake variables – are they comparable between large and small lakes?" *Hydrobiologia*, Vol. 599, pp. 105–110, 2008.
- [6] J. D. Lenters, T. K. Kratz, and C. J. Bowser, "Effects of climate variability on lake evaporation: Results from a long-term energy budget study of Sparkling Lake, northern Wisconsin (USA)," *Journal of Hydrology*, Vol. 308, pp. 168–195, 2005.
- [7] J. J. Gibson, R. Reid, and C. Spence, "A six-year isotopic record of lake evaporation at a mine site in the Canadian subarctic: Results and validation," *Hydrological Processes*, Vol. 12, pp. 1779–1792, 1998.
- [8] Y. Mahrer and S. Assouline, "Evaporation from Lake

- Kinneret, 2. Estimation of the horizontal variability using a two-dimensional numerical mesoscale model," *Water Resources Research*, Vol. 29, pp. 911–916, 1993.
- [9] W. Abtew, "Evaporation estimation for Lake Okeechobee in South Florida," *Journal of Irrigation and Drainage Engineering*, Vol. 127, pp. 140–147, 2001.
- [10] R. J. Dos Reis and N. L. Dias, "Multi-season lake evaporation: energy-budget estimates and CRLE model assessment with limited meteorological observations," *Journal of Hydrology*, Vol. 208, pp. 135–147, 1998.
- [11] U.S. Geological Survey, "Estimating Evaporation from Lake Mead," USGS Scientific Investigations Report, No. 2006-5252, Arizona, USA, 2006.
- [12] J. A. Amayreh, "Lake evaporation: a model study," in *Dissertation Abstracts International* 57-03, Section B, Utah State University, pp. 1938, 1995.
- [13] D. O. Rosenberry, D. I. Stannard, T. C. Winter, and M. L. Martinez, "Comparison of 13 equations for determining evapotranspiration from a prairie wetland, Cottonwood Lake Area, North Dakota, USA," *Wetlands*, Vol. 24, pp. 483–497, 2004.
- [14] D. O. Rosenberry, T. C. Winter, D. C. Buso, and G. E. Likens, "Comparison of 15 evaporation methods applied to a small mountain lake in the northeastern USA," *Journal of Hydrology*, Vol. 340, pp. 149–166, 2007.
- [15] E. Robertson and P. J. Barry, "The water and energy balances of Perch Lake (1969–1980)," *Atmosphere-Ocean*, Vol. 23, pp. 238–253, 1985.
- [16] A. H. Rasmussen, M. Hondzo, and H. G. Stefan, "A test of several evaporation equations for water temperature simulations in lakes," *Water Resources Bulletin*, Vol. 31, pp. 1023–1028, 1995.
- [17] P. F. Hamblin, H. A. Bootsma, and R. E. Hecky, "Surface meteorological observations over Lake Malawi/Nyasa," *Journal of Great Lakes Research*, Vol. 29, pp. 19–23, 2003.
- [18] M. E. Keskin and O. Terzi, "Evaporation estimation models for Lake Egirdir, Turkey," *Hydrological Processes*, Vol. 20, pp. 2381–2391, 2006.
- [19] E. T. Linacre, "Data-sparse estimation of lake evaporation, using a simplified Penman equation," *Agricultural and Forest Meteorology*, Vol. 64, pp. 237–256, 1993.
- [20] W. A. Scheider, R. A. Reid, B. A. Locke, and L. D. Scott, "Studies of lakes and watersheds in Muskoka-Haliburton, Ontario: Methodology (1976–1982)," Data Report DR 83/1 of Ontario Ministry of the Environment, Dorset, Ontario, Canada, 1983.
- [21] W. A. Scheider, C. M. Cox, and L. D. Scott, "Hydrological data for lakes and watersheds in Muskoka-Haliburton study area (1976–1980)," Data Report DR 83/6 of Ontario Ministry of the Environment, Dorset, Ontario, Canada, 1983.
- [22] B. A. Hutchinson, L. D. Scott, M. N. Futter, and A. Morgan, "Hydrology data for lakes and catchments in Muskoka/Haliburton (1980–1992)," Data Report DR 93/2 of Ontario Ministry of the Environment, Dorset, Ontario, Canada, 1994.
- [23] T. C. Winter, D. O. Rosenberry, and A. M. Sturrock, "Evaluation of 11 equations for determining evaporation from a small lake in the north central United States," *Water Resources Research*, Vol. 31, pp. 983–993, 1995.
- [24] M. S. Mosner and B. T. Aulenbach, "Comparison of methods used to estimate lake evaporation for a water budget of Lake Seminole, southwestern Georgia and northwestern Florida," in *Proceedings of the 2003 Georgia Water Resources Conference*, Athens, Georgia, USA, 2003.
- [25] C.-Y. Xu and V. P. Singh, "Evaluation and generalization of radiation-based methods for calculating evaporation," *Hydrological Processes*, Vol. 14, pp. 339–349, 2000.
- [26] V. P. Singh and C.-Y. Xu, "Evaluation and generalization of 13 mass-transfer equations for determining free water evaporation," *Hydrological Processes*, Vol. 11, pp. 311–323, 1997.
- [27] F. Delclaux, A. Coudrain, and T. Condom, "Evaporation estimation on Lake Titicaca: a synthesis review and modelling," *Hydrological Processes*, Vol. 21, pp. 1664–1677, 2007.
- [28] M. F. Sadek, M. M. Shahin, and C. L. Stigter, "Evaporation from the reservoir of the High Aswan Dam, Egypt: A new comparison of relevant methods with limited data," *Theoretical and Applied Climatology*, Vol. 56, pp. 57–66, 1997.
- [29] R. A. Reid, R. Girard, and A. C. Nicolls, "Morphometry and catchment areas for the calibrated watersheds," Data Report DR 87/4 of Ontario Ministry of the Environment, Dorset, Ontario, Canada, 1987.
- [30] V. T. Chow, D. R. Maidment, and L. W. Mays, "Applied hydrology," McGraw-Hill Book Company, New York, 1988.
- [31] A. L. Buck, "New equations for computing vapour pressure and enhancement factor," *Journal of Applied Meteorology*, Vol. 20, pp. 1527–1532, 1981.
- [32] H. Yao and I. F. Creed, "Determining spatially-distributed annual water balances for ungauged locations on Shikoku Island, Japan: a comparison of two interpolators," *Hydrological Sciences Journal*, Vol. 50, pp. 245–263, 2005.
- [33] J. Doorenbus and W. O. Pruitt, "Guidelines for predicting crop water requirements," *Irrigation and Drainage Paper No. 24*, Food and Agriculture Organization of the United Nations, Rome, Italy, 1977.
- [34] H. Yao, A. Terakawa, and S. Chen, "Rice water use and response to potential climate changes: calculation and application to Jianghan, China," in *Proceedings of the International Conference on Water Resources and Environment Research*, Kyoto, Japan, Vol. 2, pp. 611–618, 1996.
- [35] H. A. R. DeBruin and J. Q. Kejiman, "The Priestley-Taylor evaporation model applied to a large, shallow lake in the Netherlands," *Journal of Applied Meteorology*, Vol. 18, pp. 898–903, 1979.
- [36] K. J. Devito and P. Dillon, "Errors in estimating stream

- discharge in small headwater catchments: influence on interpretation of catchment yields and input – output budget estimates,” Technical Report 1993 of Ontario Ministry of the Environment, Dorset, Ontario, Canada, 1993.
- [37] S. W. Hostetler and P. J. Bartlein, “Simulation of lake evaporation with application to modeling lake level variations of Harney-Malheur Lake, Oregon,” Water Resources Research, Vol. 26, pp. 2603–2612, 1990.
- [38] N. G. Grannemann, R. J. Hunt, J. R. Nicholas, T. E. Reilly, and T. C. Winter, “The importance of ground water in the Great Lakes region,” Water-Resources Investigation Report 00-4008, U. S. Geological Survey, Lansing, Michigan, 2000.
- [39] J. E. Nash and J. V. Sutcliffe, “River flow forecasting through conceptual models: Part I – a discussion of principles,” Journal of Hydrology, Vol. 10, pp. 282–290, 1970.
- [40] E. T. Linacre, “Evaporation trends,” Theoretical and Applied Climatology, Vol. 79, pp. 11–21, 2004.
- [41] R. K. Saxena, “Estimation of lake evaporation from a shallow lake in central Sweden by oxygen-18,” Hydrological Processes, Vol. 10, pp. 1273–1281, 1998.
- [42] R. K. Saxena, C. Jaedicke, and L. C. Lundin, “Comparison mass-balance, bulk aerodynamic and bowen ratio methods,” Physics and Chemistry of the Earth, Part B: Hydrology, Oceans and Atmosphere, Vol. 24, pp. 851–859, 1999.

Dechlorination of Trichloroethylene in Groundwater by Nanoscale Bimetallic Fe/Pd Particles

Tielong LI^{1,2}, Shujing LI¹, Yongchao LI¹, Zhaohui JIN¹

¹College of Environmental Science and Engineering, Nankai University, Tianjin, China

²Tianjin Key Laboratory of Environmental Remediation and Pollution Control/Ministry of Education Key Laboratory of Environmental Processes and Criteria, Nankai University, Tianjin, China

E-mail: litielong@nankai.edu.cn

Received November 29, 2008; revised January 13, 2009; accepted February 14, 2009

Abstract

Palladium/iron bimetallic nanoparticles were synthesized using microemulsion method in the water-in-oil (W/O) microemulsion system, which was made up of *iso*-octane, cetyltrimethyl-ammonium bromide (CTAB), butanol and water and characterized by measuring the conductivity of the solution. Transmission electron microscope (TEM) and energy dispersive X-ray microanalysis (EDX) analysis showed that the average diameter of synthesized palladium/iron bimetallic nanoparticles was less than 80 nm, which was much smaller than the particles produced by the solution method. The palladium/iron bimetallic nanoscale particles produced in the laboratory showed better performance on dechlorinating TCE than the other materials. The nanoscale Fe/Pd particles exhibited high reactivity. When Pd content is 0.5%, the best TCE dechlorination efficiency is achieved within 30min. And Fe/Pd nanoparticles show persistent reaction activity in some sense.

Keywords: Trichloroethylene, Microemulsion, Nanoscale Pd/Fe Particles

1. Introduction

Chlorinated hydrocarbons are dense non-aqueous phase liquids (DNAPLs), which are utilized by a number of industries as solvents in large quantities on a regular basis. Given this high frequency of use, handling, and transportation, along with past disposal and storage practices, DNAPL compounds presently represent a significant threat to soil and groundwater resources. Trichloroethylene (TCE), has been widely detected in areas adjacent to dry cleaners, automobile manufacturers or shops, asphalt processing plants, and military bases, listed as a priority pollutant by the US EPA, is one of the most commonly detected chlorinated organic compounds in surface water, groundwater and soil. Cleanup of soils and groundwater contaminated by chlorinated hydrocarbons such as TCE and PCBs has been a challenging task for decades.

Remediation of DNAPL-contaminated sites is especially critical because DNAPLs in the subsurface represent a long-term source for groundwater contamination.

Aquifers contaminated with DNAPLs are extremely difficult to remediate with standard pump-and-treat methods. Since DNAPLs are extremely difficult and costly to remove, a cost-effective, reliable technology is needed to treat DNAPL contaminants.

Various technologies have been explored for dechlorination of TCE, including bioremediation [1], thermal treatment [2], and permeable reactive barriers [3]. Among many technologies tested so far, abiotic dechlorination using zerovalent iron, Fe^0 , particles appears to be one of the most promising technologies [4,5]. The most common metal being utilized for this purpose is iron due to its dehalogenation efficiency, cost, and benign environmental impact. However, due to the limited reactivity, the TCE reduction rate of granular iron particles has been found very slow, with half-lives in the order of days or longer [6,7]. As a result, toxic intermediate byproducts such as vinyl chloride (VC) are often detected [8,9]. In order to further enhance the dechlorination reaction rates and minimize byproduct formation, bi-metal systems of palladized iron (Fe complex) were

developed and used [10–12]. Various strategies have been explored to enhance the dechlorination rates using Fe⁰-based particles. Because dechlorination of chlorinated compounds by Fe⁰-based particles is a surface-mediated process, increasing the surface area of iron will increase the dechlorination rate. Therefore, reducing particle size can greatly enhance the degradation rate. Coating iron particles with a second catalytic metal such as Pd, Pt, Ag, or Ni can also accelerate the dechlorination process and thereby prevent formation of toxic byproducts [13–15]. Zhang et al. reported that reducing Pd-coated iron particle size from millimeters to nanometers (10–100 nm) increased TCE degradation rate by 10–100 times. Typically, Fe⁰-based nanoparticles were prepared by reducing Fe (II) or Fe(III) in aqueous solution using a strong reducing agent (e.g., sodium borohydride, NaBH₄). However, due to the extremely high reactivity, the initially formed nanoparticles tend to either react rapidly with surrounding media (e.g., dissolved oxygen (DO) or water) or agglomerate rapidly, resulting in the formation of much larger (in the micrometer to millimeter scale) particles or flocs and rapid loss in reactivity [16]. To overcome these drawbacks, a microemulsion [17,18] with the cetyltrimethyl-ammonium bromide (CTAB) as the surfactant was used in the preparation of the Fe/Pd nanoparticles and the chemical reactivity for degradation of TCE in water was studied in the experiment of dechlorination in this study. And the nanoparticles were characterized by using the transmission electron microscope (TEM) and energy dispersive X-ray microanalysis (EDX). The water-in-oil (W/O) microemulsion system was made up of iso-octane, CTAB, butanol and water, and was characterized by measuring the conductivity of the solution. The average diameter of synthesized palladium/iron bimetallic nanoparticles using the microemulsion method was less than 80 nm, which was much smaller than the particles produced by the solution method. And then the primary objective of this work was to 1) prepare the nanoparticles in the CTAB microemulsion under inert conditions; and 2) characterize the resultant nanoparticles with respect to their physical stability and chemical reactivity for degradation of TCE in water. And the performance of the nanoparticles produced in the laboratory was studied by dechlorinating TCE. The degradation rate of TCE by the nano palladium/iron bimetallic particles produced in the laboratory was quantified and compared with nano iron particles.

2. Experiments

The experiments were divided into five parts. And laboratory grade chemicals were used in this experimental study.

2.1. Conductivity

The conductivity was measured using a microprocessor conductometer (DDS-307, ShangHai Precision and Scientific Instrument Corporation). The conductivity was measured to an accuracy of $\pm 0.5\%$ of full scale reading within each range.

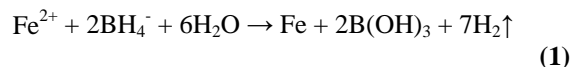
2.2. Titration

In order to construct the phase diagram of water/CTAB +n-butanol/iso-octane system, the titration method was used. Based on the literature review and preliminary tests, the mass ratio of co-surfactant-to-surfactant was fixed, and a predetermined amount of hydrocarbon iso-octane was added to the surfactant mixture. Water was then titrated into the octane–surfactant mixture (octane/(octane+surfactant) weight ratio of (S)) and changes were observed by visual inspection and conductivity measurement and the information was used in developing a phase diagram.

2.3. Production of Fe/Pd Nanoparticles

The preparation of iron nanoparticles was achieved by mixing rapidly the same volumes of two W/O microemulsion solutions, with FeSO₄ solubilized in one solution and NaBH₄ as the reducing agent in the other solution. Then firstly, two water/CTAB/isoctane microemulsions (A and B), differing only in the type of aqueous phase, were prepared. The CTAB was selected as surfactant, with n-butanol as the co-surfactant and iso-octane as the oil phase. A solution of 0.2 M FeSO₄ was added to the above mixture. The compositions of the microemulsion system used are summarized in Table 1. The weight ratio of iso-octane to surfactant was 3. After completely stirring, a transparent yellow solution microemulsion A was obtained. With the same method microemulsion B was prepared, whereas the aqueous phase of microemulsion B was 1.3 mol/L KBH₄ solution.

And then microemulsions A and B were quickly mixed at the protection of argon in a conical flask for preparation of nanoiron. The reduction reaction made the solution turbid with gas production and with a black color solid dispersed in the solution. The reduction reaction could be expressed as

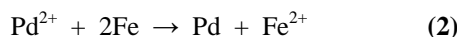


After the gas evolution, the mixtures were stirred for another 20 min with vigorous stirring (3000r/min). And then loading of Pd to the Fe⁰ particles was accomplished by adding known quantities of PdCl₂ into the microemulsion-Fe⁰ solution and allowing for reaction for 30 min under vacuum. The amount of Pd added in this study

Table 1. Compositions of microemulsions system.

Surfactant	Co-Surfactant	Oil	Aqueous
ME	CTAB	butanol	<i>iso</i> -octane
			FeSO ₄
Weight (%)	11	10	31
			48

was 0.5% (w/w) of Fe. Palladium was deposited on the iron surface through the following redox reaction 2,



At the end of the reaction, the microemulsion system with the well-dispersed iron nanoparticles was transferred into a sealed vessel filled with argon by a double-tipped needle. The resulting black-gray solids were settled by magnet, and the supernatant was decanted. Then the solids were washed with deionized water and finally with a mixture of anhydrous ethanol and acetone (volume ratio is 1:1) for six times, respectively. Finally, the resultant black-gray solids were dried under argon atmosphere, and then stored in another sealed vessel filled with argon.

2.4. Characterization of Particles

The particles obtained using the microemulsion were characterized using the Philips EM400ST transmission electron microscope (TEM) and energy dispersive X-ray microanalysis (EDX).

2.5. Dechlorination of TCE

Pd content can affect TCE dechlorination efficiency strongly. In order to select the optimal Fe/Pd ratio, experiments were designed to investigate the effect of Pd content on TCE dechlorination efficiency of nanoscale Pd/Fe within 30min. In this study, Pd/Fe ratios were 0.2%, 0.5%, 1%, 2% respectively. For comparison, Fe and Fe/Pd nanoparticles were also prepared following similar procedures but use the liquid reduction method. Experiments were conducted to investigate the reduction of TCE using the two synthesized iron particles. Dechlorination of 15 mg/L TCE solution with the 1.5 g/L iron-to-solution loading was investigated. TCE solutions (173 mL) were mixed with the iron particles in separate bottles with Teflon coated caps. The mix was stirred using a platform shaker operated at 200 rpm. The concentration of TCE was analyzed using a HP 6890 GC equipped with an electron capture detector (ECD).

Experiments were also designed to evaluate Fe/Pd nanoparticles' persistent activity. Batch experiments were conducted in 175 ml serum bottles. In each batch

bottle, 45 μ L TCE stock solution was repeatedly spiked into 173ml deionized water which was deoxygenated with Argon. Initial TCE concentration is 56g/L. The solution contained 0.2768g of Fe/Pd nanoparticles.

3. Results and Discussion

3.1. Phase Behavior of Water/Mixed-Surfactants/Isooctane Microemulsion System

In order to construct the phase diagram of water/mixed-surfactants/*iso*-octane microemulsion system, the titration method was used. The optimum weight ratio mentioned above was used to prepare the mixed-surfactants/n-butanol mixture (EM). A predetermined amount of hydrocarbon *iso*-octane was added to the surfactant mixture. Water was then titrated into the *iso*-octane/surfactant mixture and changes were observed by visual inspection and conductivity measurement and the information was used to develop a phase diagram. The phase behavior of the water/mixed-surfactants/*iso*-octane system is represented in Figure 1. As can be seen in Figure 1, an ideal W/O region has been observed where n-butanol: mixed-surfactants=1:2 (weight ratio), which will be used as the microemulsion system to produce nanoscale particles.

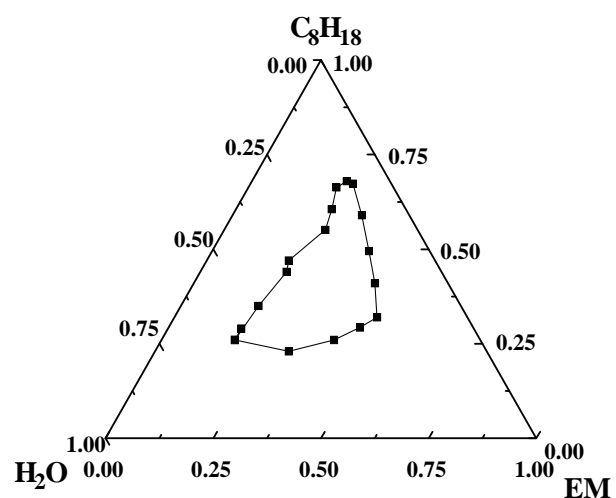


Figure 1. Microemulsion phase diagram of CTAB/Butanol/*Octane/H₂O* system.

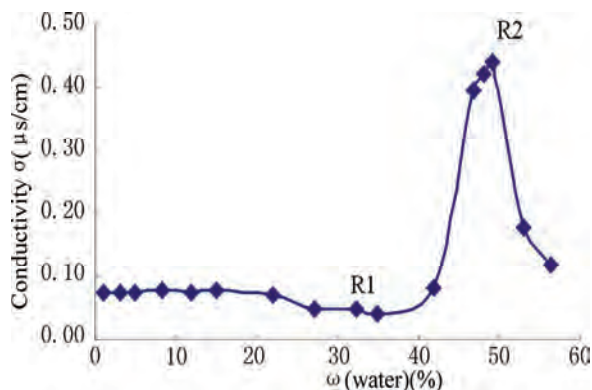


Figure 2. Variation of conductivity with amount of water in microemulsion.

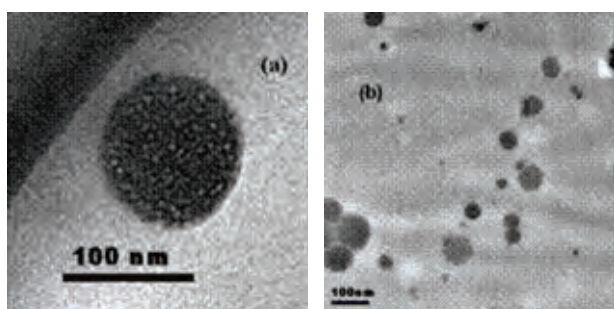


Figure 3. Characterizing the nanoscale Fe/Pd particles produced by microemulsion method; (a), (b) transmission electron micrograph (TEM) of the particles.

3.2. Conductivity

The variation of conductivity with different water con-

tent (W0) is shown in Figure 2. Two turning points (R1, R2) are found in Figure 2. Almost no change was observed in the initial conductivity of the iso-octane/surfactant mixture before R1. This is attributed to the formation of surfactant-bonded water in the system. But after R1 the conductivity increased sharply upon addition of the water into the iso-octane/surfactant mixture since it formed water-in-oil (W/O) microemulsion. In this region, water was present in micelle form and the water droplet size and number increased with an increased amount of water. When the droplet size increased, it was easy to exchange charges between the droplets and hence the conductivity increased. The conductivity reached a maximum when the water content was 50 % (wt%, R2). This can be explained by the saturation of droplets and the percolation of charges through the droplet clusters with minimum resistance. When more water was added to the system after R2, it leads to phase separation and the conductivity was lowered. The optically clear W/O microemulsion system which was formed between R1 and R2 can be used as microreactors for preparation of nanoscale materials.

3.3. Characterization of Synthesized Nanoscale Particles

A small amount of microemulsion containing the palladium/iron bimetallic particles were withdrawn from the reaction vessel, and then preserved in a small sealed glass tube. For the TEM and EDX investigations, a small drop of microemulsion containing iron nanoparticles was deposited on a copper grid.

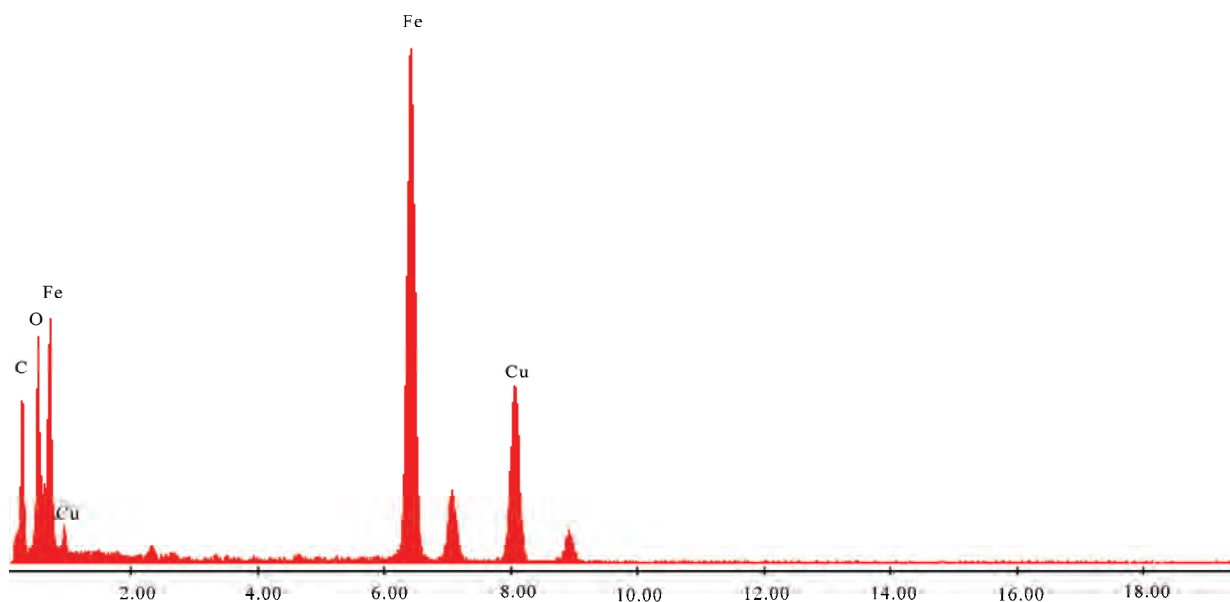


Figure 4. Energy dispersive X-ray microanalysis (EDX) of products.

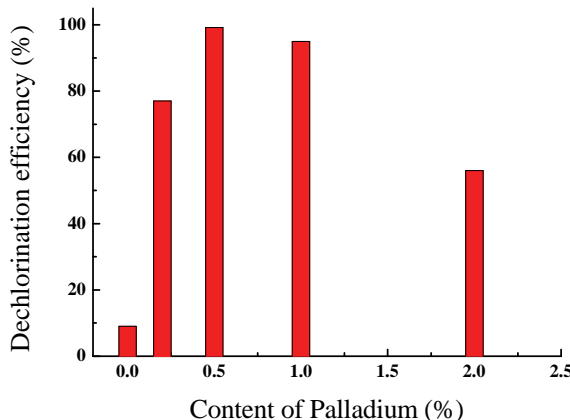


Figure 5. Effect of Pd content on TCE dechlorination efficiency of nanoscale Pd/Fe(Reaction conditions: catalyst added 1.6 g/L, T=25°C, pH= 6.98, TCE concentration=14.8 mg/L, stirring at 250rpm, reaction for 30min).

Morphology of the particles is shown in Figure 3(a), (b). From the TEM images, the particles were nearly spherical in shape and uniform in size with the average particle size less than 80 nm. The EDX for the sample is shown in Figure 4. It also shows that the product consisted of Fe and Pd, and no other notable peaks were observed.

3.4. Dechlorination of TCE

As shown in Figure 5, it is apparent that Pd content affects TCE dechlorination efficiency of nanoscale Pd/Fe. By comparison, Fe nanoparticles with Pd showed significant dechlorination. When Pd content was 0.5%, the best TCE dechlorination efficiency was achieved. But, Lower TCE was observed along with Pd content increasing. When Pd content was 2%, TCE dechlorination efficiency was merely 60%. Dechlorination efficiency decreasing was probably attributable to Pd films coating on the surface of Fe nanoparticles closely, that prevented Fe oxidation.

Figure 6 shows that degradation of TCE can be greatly enhanced when a small fraction (0.5% of Fe) of Pd was coated on the Fe particles. At the rather modest Fe dose of 1.5 g/L, even the NPI particles prepared by liquid method were able to eliminate 61% of TCE in the batch reactor within 0.5 h. When the particles were prepared by microemulsion, 98% of TCE was destroyed within 0.5 h. In contrast, a TCE degradation of only 8% was observed when the nanoscale Fe particles were prepared by microemulsion.

It can conclude that dechlorination efficiency of trichloroethylene with Fe/Pd nanoparticles is above 99% in 30min from Figure 7. It is also expected that the nanoparticles can remain reactive for extended period of time in the subsurface environment.

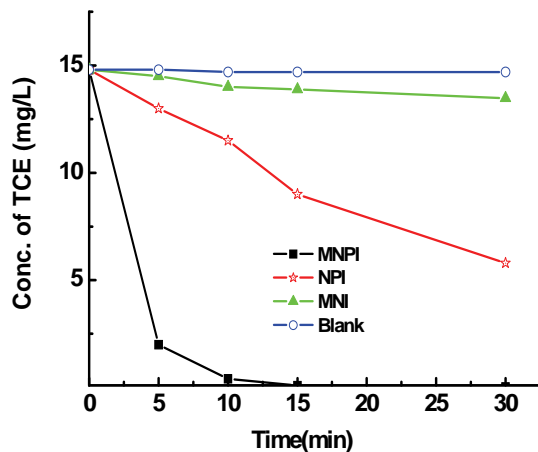


Figure 6. Dechlorination of TCE using nanoscale iron particles (MNI), nanoscale Fe/Pd particles (MNPI) prepared in microemulsion method, and nanoscale Fe/Pd particles prepared in liquid method (NPI). Fe dose was 1.5 g/L in all cases. Pd-to-iron ratio was 0.5/100 (w/w).

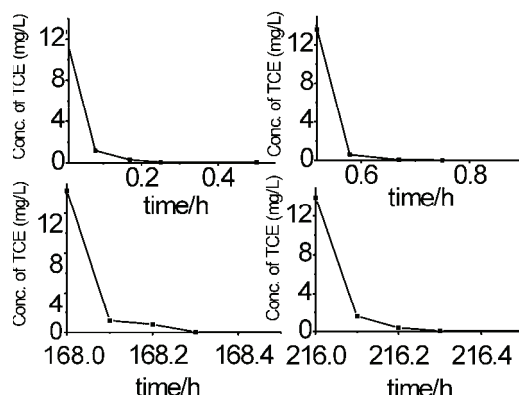


Figure 7. TCE concentration change with time in a multiple spiking experiment (reaction conditions: Fe/Pd added 1.6 g/L, T=25°C, pH=6.98, TCE concentration=14.8 mg/L, stirring at 250rpm).

4. Conclusions

Based on the experimental study, the following conclusions are advanced:

Iron and Fe/Pd nanoparticles were successfully produced by the solution method and the microemulsion method. For the microemulsion method, the particles were uniform in size and were less than 80 nm, and appear to be clearly discrete and well-dispersed.

It showed in our results that the Fe/Pd nanoparticles synthesized in our lab have the potential of remediation of TCE. The reduction rate of TCE by the microemulsion Fe/Pd product was the highest compared with the solution product and to the iron prepared by microemulsion. Particle size is an important factor in determining the degradation rate of TCE.

The nanoscale Fe/Pd particles exhibited high reactivity. When Pd content is 0.5%, the best TCE dechlorination efficiency is achieved. And Fe/Pd nanoparticles show persistent reaction activity in some sense.

5. Acknowledgments

This work was supported by Doctoral Fund for Young Scholar of Ministry of Education of China (No. 20070055053).

6. References

- [1] J. Munakata Marr, P. L. McCarty, and M. S. Shields, "Enhancement of trichloroethylene degradation in aquifer microcosms bioaugmented with wild type and genetically altered Burkholderia (*Pseudomonas*) cepacia G4 and PR1," *Environmental Science and Technology*, Vol. 30, No. 6, pp. 2045–2052, 1996.
- [2] A. K. Friis, H. J. Albrechtsen, and G. Heron, "Redox processes and release of organic matter after thermal treatment of a TCE-Contaminated aquifer," *Environmental Science and Technology*, Vol. 39, No. 15, pp. 5787–5795, 2005.
- [3] H. Shen and J. T. Wilson, "Trichloroethylene removal from groundwater in flow-through columns simulating a permeable reactive barrier constructed with plant mulch," *Environmental Science and Technology*, Vol. 41, No. 11, pp. 4077–4083, 2007.
- [4] L. J. Matheson and P. G. Tratnyek, "Reductive dehalogenation of chlorinated methanes by iron metal," *Environmental Science and Technology*, Vol. 28, No. 12, pp. 2045–2053, 1994.
- [5] C. B. Wang and W. X. Zhang, "Synthesizing nanoscale iron particles for rapid and complete dechlorination of TCE and PCBs," *Environmental Science and Technology*, Vol. 31, No. 7, pp. 2154–2156, 1997.
- [6] T. L. Johnson, M. M. Scherer, and P. G. Tratnyek, "Kinetics of halogenated organic compound degradation by iron metal," *Environmental Science and Technology*, Vol. 30, No. 8, pp. 2634–2640, 1996.
- [7] G. D. Sayles, G. You, M. Wang, and M. J. Kupferle, "DDT, DDD, and DDE dechlorination by zerovalent iron," *Environmental Science and Technology*, Vol. 31, No. 12, pp. 3448–3454, 1997.
- [8] W. A. Arnold and A. L. Roberts, "Pathways and kinetics of chlorinated ethylene and chlorinated acetylene reaction with Fe(0) particles," *Environmental Science and Technology*, Vol. 34, No. 9, pp. 1794–1805, 2000.
- [9] W. S. Orth and R. W. Gillham, "Dechlorination of trichloroethene in aqueous solution using Fe⁰," *Environmental Science and Technology*, Vol. 30, No. 1, pp. 66–71, 1996.
- [10] T. Li and J. Farrell, "Reductive dechlorination of trichloroethene and carbon tetrachloride using iron and palladized-iron cathodes," *Environmental Science and Technology*, Vol. 34, No. 1, pp. 173–179, 2000.
- [11] P. Zhang, X. Tao, Z. Li, and R. S. Bowman, "Enhanced perchloroethylene reduction in column systems using surfactant-modified zeolite/zero-valent iron pellets," *Environmental Science and Technology*, Vol. 36, No. 16, pp. 3597–3603, 2002.
- [12] G. V. Lowry and M. Reinhard, "Pd-catalyzed TCE dechlorination in groundwater: solute effects, biological control, and oxidative catalyst regeneration," *Environmental Science and Technology*, Vol. 34, No. 15, pp. 3217–3223, 2000.
- [13] W. X. Zhang, C. B. Wang, and H. L. Lien, "Treatment of chlorinated organic contaminants with nanoscale bimetallic particles," *Catalogue Today*, Vol. 40, No. 4, pp. 387–395, 1998.
- [14] Y. Xu and W. X. Zhang, "Subcolloidal Fe/Ag particles for reductive dehalogenation of chlorinated benzenes," *Industrial And Engineering Chemistry Research*, Vol. 39, No. 7, pp. 2238–2244, 2000.
- [15] B. Schrick, J. L. Blough, A. D. Jones, and T. E. Mallouk, "Hydrodechlorination of trichloroethylene to hydrocarbons using bimetallic nickel-iron nanoparticles," *Chemistry of Materials*, Vol. 14, No. 12, pp. 5140–5147, 2002.
- [16] F. He and D. Y. Zhao, "Preparation and characterization of a new class of starch-stabilized bimetallic nanoparticles for degradation of chlorinated hydrocarbons in water," *Environmental Science and Technology*, Vol. 39, No. 9, pp. 3314–3320, 2005.
- [17] F. Li, C. Vipulanandan, and K. K. Mohanty, "Microemulsion and solution approaches to nanoparticle iron production of degradation of trichloroethylene," *Colloids Surface*, Vol. 223, No. 1–3, pp. 103–112, 2003.
- [18] A. J. Zarur and J. Y. Ying, "Reverse microemulsion synthesis of nanostructured complex oxides for catalytic combustion," *Nature*, Vol. 403, No. 6, pp. 65–68, 2000.

Electrokinetic Phenomena of Modified Polytetrafluoroethylene Membranes in the Oily Sewage from Oil Field

Aiguo LIN¹, Yihua YAO², Gang LIU¹, Guozhong ZHANG¹, Xiufeng LIN³

¹*China University of Petroleum, Dongying, Shandong, China*

²*Shenli Oilfield Luming Company, Dongying, Shandong, China*

³*University of Regina, Saskatchewan, Canada*

E-mail: shlc_zxk@yahoo.com.cn

Received December 12, 2008; revised March 30, 2009; accepted April 3, 2009

Abstract

Experimental investigations of electrokinetic phenomena of modified polytetrafluoroethylene membranes in the oily sewage from oil field were performed by using the streaming potential method. The zeta potentials of the membranes in the oily waste water are estimated on the basis of Helmholtz—Smoluchowski equation. The experiment and calculation results show that the membranes are charged negatively, whose zeta potentials maintain at around -20mV. And the aperture of membranes, the temperature and the filtration flux have little influence on the streaming potentials and the zeta potentials of the membranes. Also the suspended particulates in the oily sewage are charged negatively. The membranes have strong ability to withhold the suspended substance and powerful antipollution competence because of the role of the charges on the membranes.

Keywords: Oily Sewage, Membrane, Electrokinetic Phenomena, Streaming Potential, Zeta Potential

1. Introduction

At present, flood development is used primarily in most oilfields all over China. As the water contents of main productive zones have entered the middle or high stage, oily sewage treatment problems in nearly every oilfield are getting more and more rigorous. In order to meet the requests of sewage discharge in remote producing field and produced water reinjection in low permeable sub-layer oilfields, the water quality must be handled more deeply based on the routine sewage disposal technology. Membrane separation technology is one of the most important developing tendency in deep treatment [1,2]. The researches on electrokinetic phenomena of membranes have attracted extensive attention in membrane science, interface science and other academic circles [3–6]. When electrolyte solution leaking porous membrane vertically(or tangentially) with definite differential pressure, potential difference will appear accordingly between two

sides of the membrane, and valid electric charges on the membrane surface are usually originated from the ion absorption in solution or the liberation of some functional group on membrane micro bore surface. The existence of membrane surface charges influences the ion distribution nearby the contact interface between the membrane and the solution, and results in the formation of so-called ion diffuse electric double layer in neighboring membrane surface [7,8]. Electrokinetic phenomena will appear when the solution and the membrane surface move relatively as a result of pressure difference and other outside forces. However, the reports on electrokinetic phenomena of membranes in oily sewage disposal are few. Experimental investigations on electrokinetic phenomena of modified polytetrafluoroethylene membranes (The polytetrafluoroethylene membranes undergo chemical modification, hot-rolling and surface radiation treatment, which make the reprimanding oil abilities and water affinities of the membrane enhanced

remarkably and the antipollution abilities also improved) in handling the oily waste water of oilfields are mainly performed in the paper.

2. Experimentation

2.1. Experimental Apparatuses and Equipments

Membrane fine filtration equipments. (Figure 1) under the pressure offered by centrifugal pump, oily sewage from the stuff fluid tank leak out membrane subassembly to the permeated fluid storage tank. This flow chart is divided into dead end filtration and mixed current filtration based on the way by which the stuff fluid leak the membrane (The experiments here used mixed current filtration). The membranes used in the tests are modified polytetrafluoroethylene membranes which are supplied by First Petroleum Technology Ltd., whose bore diameters are separately 0.45 and 0.8 μm . In the tests, the pressure differences between both sides of membrane subassembly are measured with EJA110A differential pressure transmitter (used at low pressure) and AM1151 capacitive differential pressure transmitter (used at high pressure), the measuring ranges of which are separately 0~40KPa and 0~300KPa, the accuracy figures 0.1% and 0.5%, and the output electric currents are both 4~20mA. Electric signal outputted from differential pressure transmitter are inputted to the computer by HK-PCI812 data acquisition board whose system syn-

thesis error is not more than 0.2%. The flow measurement of membrane assembly used glass rotameter, the main technical descriptions of which are: the measurement range 60~600L/h, the accuracy figure 1.5%. There are agitator made by self and temperature control equipment in stuff fluid tank in order to maintain the homogenization of the stuff fluid and control its temperature. To keep the sample temperature as it is collected, THD-0515W low temperature thermostatic bath was used to maintain the temperature of sample bottle, and the main technical descriptions of the bath are the measurement range -5~100°C, the waveness ± 0.05 °C.

HP 34401A digital multimeter is used to measure potential differences between both sides of membrane assembly as oily sewage leaking. WTW high accuracy inoLab 740, made in Xiamen Longlide Environment Technique exploitation Co. Ltd., is used to measure electrical conductivities of oily waste water in different temperatures. The dynamic viscosities of the sewage are tested by the concentric cylinder rotary rheometer MCR301, of which the main technical descriptions are: the minimal torque 0.1 μNm , the maximum torque 200 mNm . Zetasizer3000 Zeta potential measuring instrument, made by Malvern corporation in England, could detect the electrokinetic potentials of the test solution, and the test temperatures are able to be adjusted within 10~70°C. The paper test Zeta potentials of suspended particles in oily sewage before and after treatment with this equipment.

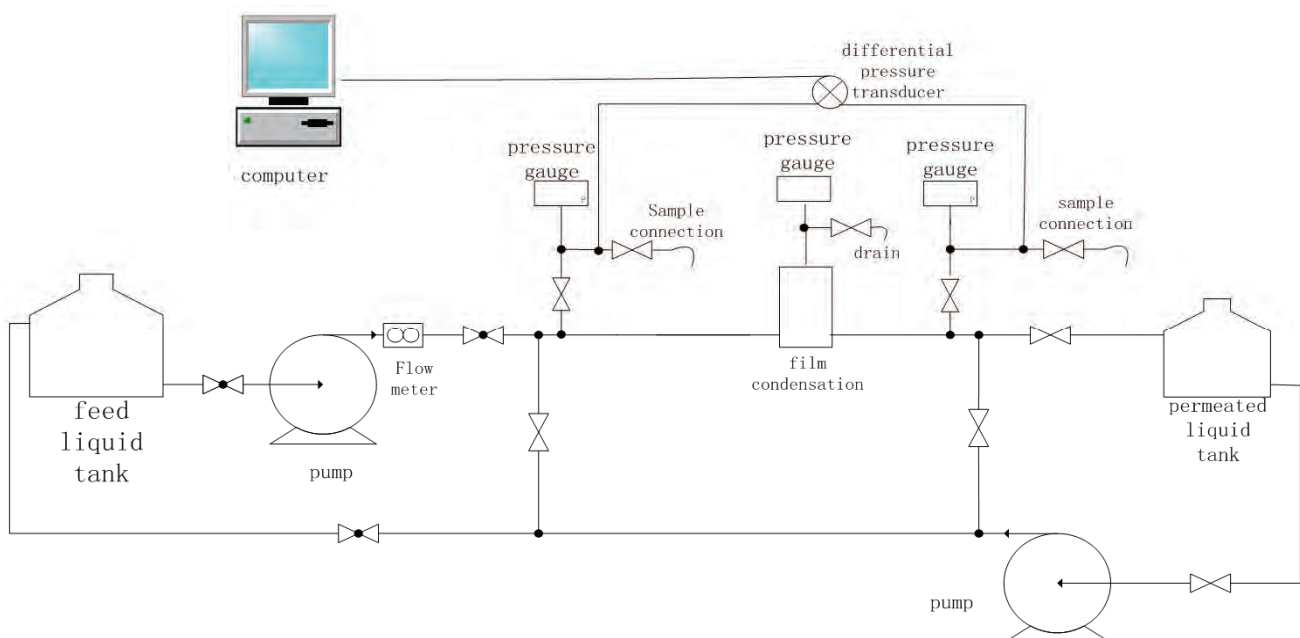


Figure 1. Membrane filtration experimental apparatus of oily sewage.

2.2. Test Water Samples

The oily sewages handled in this paper are all from a sewage plant of Shengli Oilfield. In the water, suspended solid content is $10 \sim 50\text{mg/L}$, total mineralization 48497.1mg/L , oil content $20 \sim 100\text{mg/L}$ (measured with 721 light meter), the median diameter of suspended particles around $4 \mu\text{m}$ (measured with COULTER fully automatic particle size analyzer COULTER MULTISIZER II).

3. Experiment Results and Analysis

3.1. Experiment Basis

According to the surface and colloid science [7], potential differences between both sides of capillary pore net or porous bung made by powder compacting will appear when fluid leaking by force of compression. Millipore filter can be considered made up from lots of punctuates, and potential differences will also arise during filtering. The streaming potential is then the gradient of potential differences changing with pressure differences when electrostatic current through the membranes is zero, i.e., when solution leaking porous membrane vertically at specified pressure difference ΔP , there will be a potential difference ΔE between both sides of membrane accordingly, and the streaming potential can be described as:

$$\nu = d(\Delta E) / d(\Delta P) \quad (1)$$

The streaming potentials of membranes can be obtained by tested directly, in which, just connect a voltmeter between the two ends [9]. The streaming potentials can only describe the membrane charged properties qualitatively, but not the quantitative magnitude which can be indicated with Zeta potentials of the membrane surface. The double electrode layer theory considers that there is a “glide surface”, on which the solution and surface move relatively, at some distance away from the surface within the membrane surface ion diffuse electric double layer, and the potential difference between “glide surface” and main part of the solution is called Zeta potential. Zeta potential of the membrane surface is an important parameter which determines electrokinetic phenomena of membranes, and depends on membrane material and solution system intently [10]. The micro bore surface Zeta potential (ζ) [3] of modified polytetrafluoroethylene membranes can be estimated by outstanding Helmholtz-Smoluchowski equation using membrane streaming potential which has been obtained:

$$\nu = \frac{d(\Delta E)}{d(\Delta P)} = \frac{\varepsilon_0 \varepsilon_r \zeta}{\mu k} \Rightarrow \zeta = \frac{\nu \mu k}{\varepsilon_0 \varepsilon_r} \quad (2)$$

In which, ν is the streaming potential, whose unit is V/Pa ; k the electric conductivity of solution, unit S/m ($1\text{S} = 1\text{c} \cdot \text{s}^{-1} \cdot \text{V}^{-1}$); μ the viscosity, unit $\text{Pa} \cdot \text{s}$, ε_r and ε_0 are separately relative dielectric constant and vacuum dielectric constant, whose units are F/m ($1\text{F} = 1\text{c} \cdot \text{V}^{-1}$).

Helmholtz-Smoluchowski equation is suit for the case when the pipe diameter or capillary tube diameter is far larger than the thickness of double electrode layer. The thicknesses of double electrode layer of membrane borehole wall are nanometer degree, while the bore diameters of modified polytetrafluoroethylene membranes used in the experiments are meter degree, in which the latter are far larger than the former, so the equation is fit for the estimate of the membrane surface Zeta potentials here.

3.2. Membrane Surface Zeta Potentials

As the membrane bore diameters, filtering temperatures, filtering flow rates and other elements have obvious effects on filtering effect, and those elements also probably influence the membrane surface Zeta potentials, filtering tests with membranes of different bore diameters were performed under different temperatures and specified flow rates. The potential differences of oily waste water between both sides of the modified PTFE filter membrane are measured with HP 34401A digital multimeter at correspondent operating conditions. The streaming potential ν of the membrane at different operating conditions could be calculated according to Formula (1) with the potential difference ΔE and the pressure difference ΔP obtained from experiments. Some results are shown in Table 1.

The table shows that, although there are differences among the membrane bore diameters and operating conditions, the changes of membrane streaming potentials are not obvious: of the 9 tests, the average maximal value is -5.01 mV/KPa , the maximal value -5.3 mV/KPa , the minimum value -4.9 mV/KPa and the standard deviation 0.13642 mV/KPa . In fact, the absolute value of membrane streaming potentials is probably affected by the electrolyte concentration of solution, types and valence states of basic ion and negative ion and other elements [6]. It is found that the oily waste water investigated here contains Na^+ with a concentration of 15951.58mg/L and Mg^{2+} of only 261.91 mg/L through water quality analysis, so the effect of Na^+ is dominating, and as its concentration is far larger than the critical concentration given in reference [6], the components of the waste water would not change suddenly. Thus the slight alternation of ion concentration caused by sample collection and other reasons would not influence the value of membrane

Table 1. Membrane streaming potentials at different operating conditions.

Sequence number	Bore diameter of membrane (μm)	Temperature ($^{\circ}\text{C}$)	Given flow rate (L/h)	ν (mV/Kpa)
1	0.8	30	600	-4.9
2	0.8	50	400	-5.1
3	0.8	70	250	-5.0
4	0.45	30	400	-4.9
5	0.45	50	250	-4.9
6	0.45	70	600	-5.0
7	0.45	30	250	-5.3
8	0.45	50	600	-4.9
9	0.45	70	400	-5.1

Table 2. Conductance ratios and dynamic viscosity of oily waste water under different temperatures.

Temperature of water sample ($^{\circ}\text{C}$)	30	50	70
Conductance ratio (S/m)	2.5	3.5	4.9
dynamic viscosity (mPa·s)	0.944	0.689	0.544

Note: the conductance ratios shown in the table were measured by inoLab 740, of which the measuring range is LR001 and the accuracy degree is $0.001 \mu\text{s}/\text{cm}$.

Table 3. Dynamic viscosities factors μ of oily waste water under different temperatures.

Temperature of water sample ($^{\circ}\text{C}$)	30	50	70
Dynamic viscosity (mPa·s)	0.944	0.689	0.544

According to the data above, Zeta potentials of modified polytetrafluoroethylene membranes can be calculated through Formula (2). Table 4 shows Zeta potentials of the membrane surface under different experiment conditions.

streaming potentials, which is accordant to the experiment results shown in Table 1.

It has been told before that the membrane streaming potentials can not indicate the magnitude of membrane surface electrical properties quantitatively. In order to estimate the membrane surface Zeta potentials and quantitatively describe the electrical properties, Helmholtz-Smoluchowski equation is needed. The correlating parameters in the equation are defined as shown in Table 2 and Table 3 by experiments.

It is thus evident that the Zeta potentials of modified polytetrafluoroethylene membrane surface are between $-18.67 - -21.94\text{mV}$, of which the average value is -20.06mV and the standard deviation 1.3078 . In other words, during the oil sewage treatment using modified polytetrafluoroethylene membrane, the membrane sur-

face charged negatively and the influences on membrane surface Zeta potentials caused by membrane bore diameters and operating conditions are not obvious. The Zeta potentials of membrane surface are maintained around -20mV .

Table 4. Zeta potential on the modified PTFE membrane under different conditions.

No.	Zeta/mV	No.	Zeta/mV
1	-18.67	6	-21.52
2	-19.85	7	-20.19
3	-21.52	8	-19.07
4	-18.67	9	-21.94
5	-19.07		

Table 5. Zeta potential of suspended particles under different temperatures.

Sequence number	Temperature (°C)	Zeta potential (mV)
1	30	-14.2
2	40	-1.8
3	50	-4.4
4	60	-8.2
5	70	-12.3

3.3. Zeta Potentials of the Suspended Particles in Oily Waste Water

In order to profoundly study the electrokinetic phenomena of modified polytetrafluoroethylene membranes, the charging properties of suspended particles should be known. As the electrical properties of general colloidal particles are not expressed with the value of electric charges but the Zeta potential ζ , the paper measured Zeta potentials of suspended particles under various temperatures by Zetasizer3000 Zeta potential test set, and the results are shown in Table 5.

Obviously, the Zeta potentials are all negative and of the same electrical properties as the surface Zeta potentials. Zeta potential changes apparently as temperature changes, but not show regular patterns of increasing or decreasing monotonously, which is probably relevant with the vergent suspended particles and the fact that sampling sewage could not be absolute uniform.

Seen from the separation behavior, conventional membrane separation filtration is based on a physical sieving rule, that is, the membrane allows the components with smaller bore diameters to go through but entraps those with larger or similar bore diameters. Obviously, with the decrease of the particle diameters, the membrane bore diameters should decreases correspondently, which is bound to cause such problems as decreasing flux and increasing operating costs. However, besides physical sieving, the charging membrane has Donnan effect. According to the Donnan balance model, when the solution leak through membrane with charging group, the concentration of counter ions(those ions taking opposite charges to that fixed in the membrane) in the membrane is larger than that in the solution body, while the behavior of ions with same charges is just opposite. Donnan potential difference is thus formed and prevents the ions with same charges in the solution body from diffusing to the membrane. In order to maintain electrically neutral, the membrane also entraps counter ions. So such charging membrane has particular adsorptive separation properties. Additionally, charging groups generate in the membrane, which strengthens the hydrophilicity and increases the perme-

ability of the membrane. Meanwhile, the antipollution competence of the membrane is improved markedly because of the charge effect that charges with the same electric nature reject each other.

Thus the modified polytetrafluoroethylene membranes have strong ability withholding the suspended substance and powerful antipollution competence as a result of the role of the charges on the membranes when used to handle oily waste water, which prolong the backwashing cycle and service life of the filter element. The content about the effectiveness of the modified polytetrafluoroethylene membranes processing oily sewage will be elaborated in other papers.

4. Conclusions

When dealing with oily waste water, the streaming potentials of the modified polytetrafluoroethylene membranes maintain around -5mV/KPa while the membrane surface Zeta potentials around -20mV, which are slightly dependent on such operating conditions as membrane bore diameters, flow rates, etc. The Zeta potentials of the suspended particles in the sewage being processed are also negative.

The membranes have strong ability withholding the suspended substance and powerful antipollution competence because of the role of the charges on the membranes.

5. References

- [1] A. G. Lin, P. Y. Liu, G. Liu, and G. Z. Zhang, "Progresses of membrane separation technique in oil-bearing water treatment in oil fields," *Industrial Water Treatment*, Vol. 26, No. 1, pp. 5–8, 2006.
- [2] Q. X. Zou and Z. Y. Lu, "Survey of oil-field waste water treatment," *Industrial Water Treatment*, Vol. 21, No. 8, pp. 1–3, 2001.
- [3] W. R. Bowen and X. W. Cao, "Electrokinetic effects in membrane pores and the determination of zeta-potential," *Journal of Membrane Science*, Vol. 140, pp. 267–273. 1998.
- [4] A. Szymczyk and P. Fievet, "Characterization of surface properties of ceramic membranes by streaming and membrane potentials," *Journal of Membrane Science*, Vol. 146, pp. 277, 1998.
- [5] J. M. M. Peeters, "Characterization of nanofiltration membranes by streaming potential measurements," *Colloids and Surface A: Physicochemical and Engineering Aspects*, Vol. 150, No. 1–3, pp. 247–259, 1999.
- [6] J. Wang and X. L. Wang, "Electrokinetic phenomena of poly olefin microporous membranes in the electrolyte solutions studied by using the streaming potential method," *Journal of Chemical Engineering of Chinese Universities*, Vol. 17, No. 4, pp. 372–376, 2003.
- [7] Z. Shen and G. T. Wang, "Surface and colloid science [M]," Chemical Industry Press, 1997.
- [8] S. Sdukhin and B. V. Derjaguin, "Surface and colloid science [M]," London: Wiley - Interscience Publication, 1974.

- [9] M. F. Zhu, C. Y. Gong, and J. Y. Su, "Experimental method of the streaming potential of charge modified microporous membrane," Chinese Medical Equipment Journal, Vol. 1, pp. 1–4, 1996.
- [10] M. Nystrom and M. Lindstrom, "Streaming potential as a tool in the characterization of ultrafiltration membranes," Colloid Surface, Vol. 36, pp. 297, 1989.

Plantago Ovata Efficiency in Elimination of Water Turbidity

Gholamreza Nabi BIDHENDI¹, Toktam SHAHRIARI¹, Sh SHAHRIARI²

¹*Faculty of Environment, University of Tehran, Tehran, Iran*

²*Department of Architecture, University of Payamnoor, Tehran, Iran*

E-mail: ghhendi@ut.ac.ir, Shahriari1353@yahoo.com

Received January 23, 2009; revised May 19, 2009; accepted May 21, 2009

Abstract

Coagulation and flocculation are the most important processes in water treatment plants. Nowadays, in Iran, coagulants which have the most usage in water treatment are Aluminum Sulphate (Alum) and Ferric Chloride. Using synthetic coagulants are not economical and useful for health in developing countries. The aim of this research is to survey and compare the Ferric Chloride coagulant function and this coagulant accompany with Plantago ovata coagulant aid under variable pH for eliminating of water turbidity.

This study was performed in lab scale for water containing artificial turbidity of clay. The experiments were done in three turbidity ranges 100, 50, 20 NTU and two ranges of pH 7 and 8. The amount of Ferric Chloride in all experiments were 10 ppm and P.ovata extarct in optimum concentration for turbidity of 100, 50, 20 NTU was 0.2 ppm, 0.1 ppm and 0.04 ppm respectively. The optimum pH was 7. Using P.ovata coagulant aid in turbidity 100, 50, 20 NTU can eliminate 94.1, 94.5, 88.15 percent of above turbidities, while using Ferric Chloride coagulant alone in optimum pH can eliminate 90.3, 85.16, 80.2 percent of the turbidities mentioned above. Results show that P.ovata extract is less efficient in high turbidities when used as a coagulant aid. Plantago ovata, as a coagulant aid, showed positive influence on turbidity removal from water. In addition, optimized pH showed important role in reducing turbidity.

Keywords: Water Treatment, Coagulation and Flocculation, Jar Test, Turbidity, Plantago Ovata, Ferric Chloride

1. Introduction

About million peoples of the world suffering lack of sanitary drinking water. Every year, more than 6 million peoples (about 2 million children) are dieing, because of polluted drinking water, and developing countries expend a lot for importing chemical materials like Poly Aluminum Chloride and Alum [1]. Surface water has got different kinds of suspended materials which cause turbidity and color [2,3]. Coagulation and flocculation are physic and chemical processes in which small particles causing turbidity and color change into giant particles and finally their elimination will be performed by different physical methods such as sedimentation, and filtration [4]. Coagulants were used many years ago and Egyptians used Alum 2000 year B.C. [5]. Usually, metallic salts such as Alum, Ferric Sulphate, Ferro Sulphate,

Ferric Chloride, Anion, cation and non ionic organic polymers are among coagulant materials [6]. Several researches have been done on the function of coagulant materials and appointing the best pH [7]. Nowadays by using usual salts of Iron and aluminum a new group of coagulants named inorganic polymers have been produced and used in many countries of the world especially China, Japan, Russia and Western European countries [8,9]. Among them Poly Aluminium Chloride (PACl) the most usual is vastly used [8]. Inorganic metallic salts make unstable the particles by pressing double electrical layers around colloid particles, while polymers perform instability functions by absorption in colloid particle surface and making bridge among polymer particles [10]. Using metal coagulants and Al and Fe(III) salts started in U.S. since 1880. Application of active silica (a kind of anionic polymer) as coagulant aid was presented in 1930.

Then synthetic poly electrolytes entered the market and presented interesting abilities in elimination turbidity since 1960 [11]. Many of the developing countries are using natural poly electrolytes like Chitosan [12–14].

Historical records of using different parts of plants such as, root, stem and seed for making clear water is related to Sanskrit book which says more than 4000 years ago Indians used seeds of Nirmali tree for making clear water from turbid water of the rivers. In many countries of the world using artificial polymers as coagulant and coagulant aid have been forbidden because of bad effects on human health [12,13,15,16]. This research studies the application of *P.ovata* as a coagulant aid. In addition, because of lack of comprehensive studies concerning elimination of turbidity with *P.ovata* as a coagulant aid and also in accompany with coagulant Ferric Chloride.

Plantago ovata is a native Iranian plant. It is a small, one year old plant without or with very short stem covered with soft fiber, from Plantaginaceae family and its height is 7 to 30 centimeters [17–21]. *P.ovata* seeds contain Mosilaj, protein, fixed oil, cellulose and starch [17]. *P.ovata* seeds contain 30 percent [22] or 10 percent [23] musilaj which produces D-galacturonic acid under hydrolyze [17,22,24].

2. Materials and Methods

In this study, while preparing artificial water turbidity, the effect of adding coagulant aid in optimum pH to improve turbidity elimination was studied, and necessary comparisons were made practically. It is not possible to store enough water containing natural turbidity in the laboratory because of instability. Therefore, in this study, water containing three turbidities: high turbidity of 100 NTU, medium 50 NTU and low 20 NTU were added to the tap water by clay which was sieved with mesh 60 for making artificial turbidity. Ferric Chloride ($\text{FeCl}_3 \cdot 6\text{H}_2\text{O}$) made in Merck KGaA as coagulant and extract of *P.ovata* as coagulant aid were used. Sulphuric acid (1N) was used in this study to regulate pH value. The experiments were performed in the water and waste water lab of the faculty of environment, University of Tehran.

Experimental conditions of all experiments are as follows:

1) Experiments were performed in $25 \pm 2^\circ\text{C}$ because temperature is one of the most effective parameters on density, viscosity and amount of coagulants in keeping conditions.

2) The volume of applied water was 500 cc for all three applied turbidities.

3) Chemical oxygen demand (COD) was determined by Spectrophotometer DR/2000HACH.

4) TOC of samples for examining TOC before and after using coagulant aid *P.ovata* was measured by Spe-

ctrophotometer HACH- LANGE DR/5000 uv/vis.

5) pH of the samples was measured by digital pH meter Metrohm Model 691.

6) Turbidity was determined by turbidity meter gage HANNA.

7) Digital scale METTLER AE200 was used for weighing.

All the experiments were performed by using jar experiment method. Jar unit PHIPPS & BIRD STIRRER MODEL 7790-402 was used.

2.1. Preparation of *P.ovata* Extract

At first, the seeds of plants were soaked in water for 24 hours. The obtained gelatine was filtered and dried at $105 \pm 5^\circ\text{C}$ in oven. The obtained powder was used for the experiments. Plants contain mosilaj, protein, cellulose and starch [17,22,24].

2.2. Method of Experiment

In this study, at first 5 samples of 500 ml water which its pH and turbidity has already been measured and contained the turbidity of 100, 50 or 20 NTU, was poured in special jar vessels, one time with known amount of coagulant Ferric Chloride and another time with coagulant Ferric Chloride with in accompany coagulant aid *P.ovata*.

The samples were shaken for one minute with 100 cycles per minute, then 25 minutes with 30 cycles per minute to make Floc. During this time, formation of Flocs were observed, then Flocs were allowed to settle for 30 minutes and after that jars were sampled for analyzing and measuring turbidity and pH. The residual turbidity was compared with initial turbidity. In addition, pH variations were examined. This method was repeated for four times, Sulphuric acid (1N) was used to study the influence of pH on efficiency of coagulant aid *P.ovata*. Then pH variation as well as final turbidity of the samples was compared with the initial values.

3. Discussion and Conclusions

In this research, the role of *P.ovata* in elimination of water turbidity was studied, using coagulation and flocculation processes. *P.ovata* coagulant aid was used to reduce Ferric chloride consumption and optimum value and optimum pH were determined. One of the most important parameters was the amount of produced sludge which examined in each stage. Obtained results concerning use of Ferric Chloride alone and with coagulant aid in variable pH, were shown in Figures 1 to 10.

Figures 1, 3 and 5 show results for pH, 7 and for consumption Ferric Chloride alone and with coagulant aid *P.ovata*. Figures 2, 4 and 6 for pH, 8 is produced.

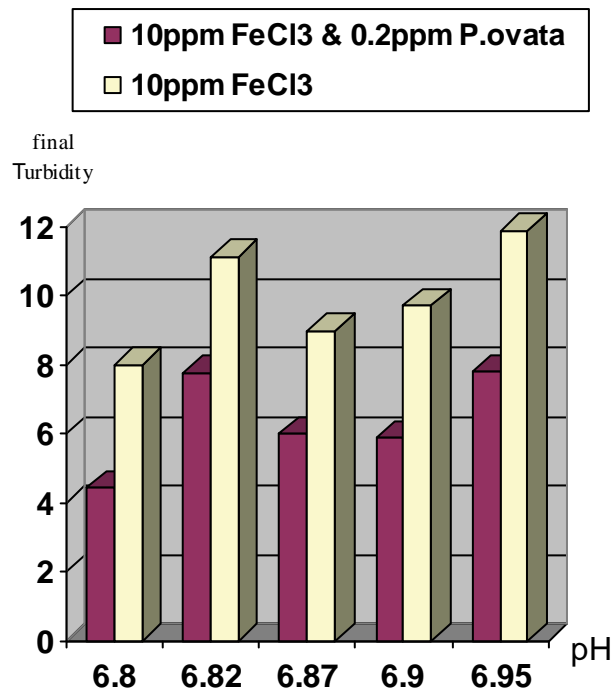


Figure 1. Comparison of final turbidities at initial pH 7 and 100(NTU) turbidity in two stages. Stage1: Ferric Chloride coagulant and Stage2: Ferric Chloride coagulant in accompany with P.ovata coagulant aid.

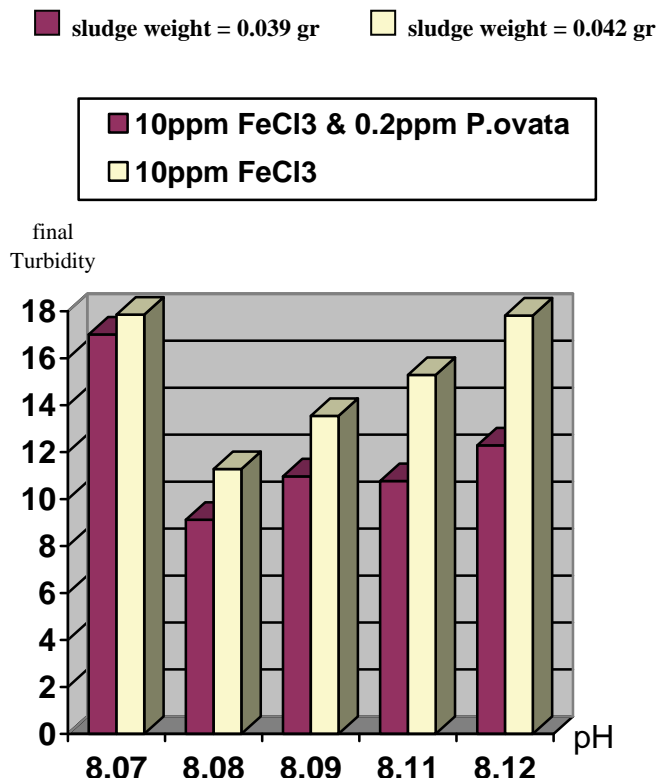


Figure 2. Comparison of final turbidities at initial pH 8 and 100(NTU) turbidity in two stages. Stage1: Ferric Chloride coagulant and Stage2: Ferric Chloride coagulant in accompany with P.ovata coagulant aid.

■ sludge weight = 0.039 gr □ sludge weight = 0.042 gr

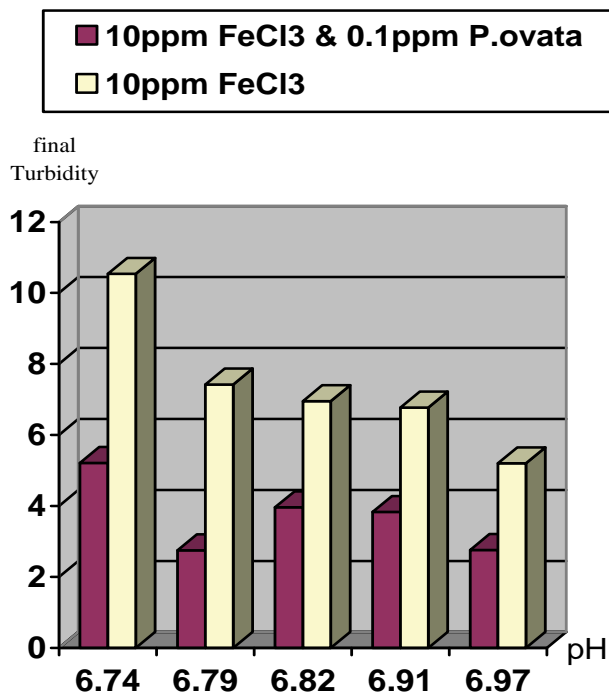


Figure 3. Comparison of final turbidities at initial pH 7 and 50(NTU) turbidity in two stages. Stage1: Ferric Chloride coagulant and Stage2: Ferric Chloride coagulant in accompany with P.ovata coagulant aid.

■ sludge weight = 0.028 gr □ sludge weight = 0.026 gr

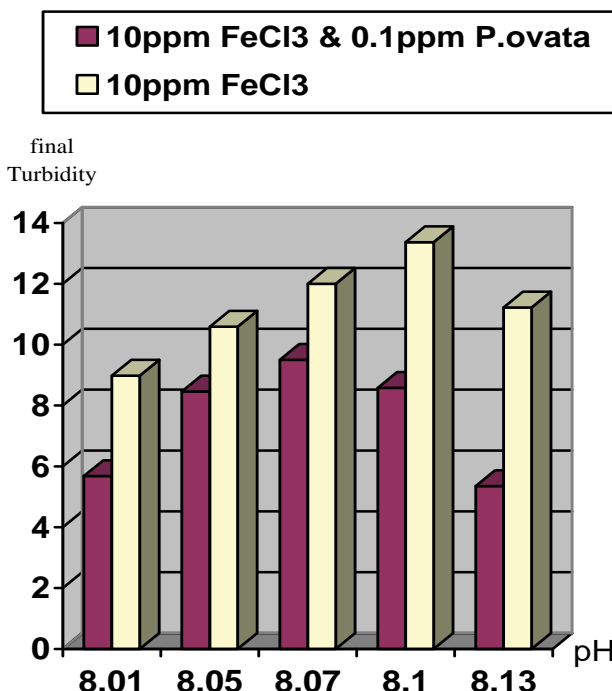


Figure 4. Comparison of final turbidities at initial pH 8 and 50(NTU) turbidity in two stages. Stage1: Ferric Chloride coagulant and Stage2: Ferric Chloride coagulant in accompany with P.ovata coagulant aid.

■ sludge weight = 0.032 gr □ sludge weight = 0.028 gr

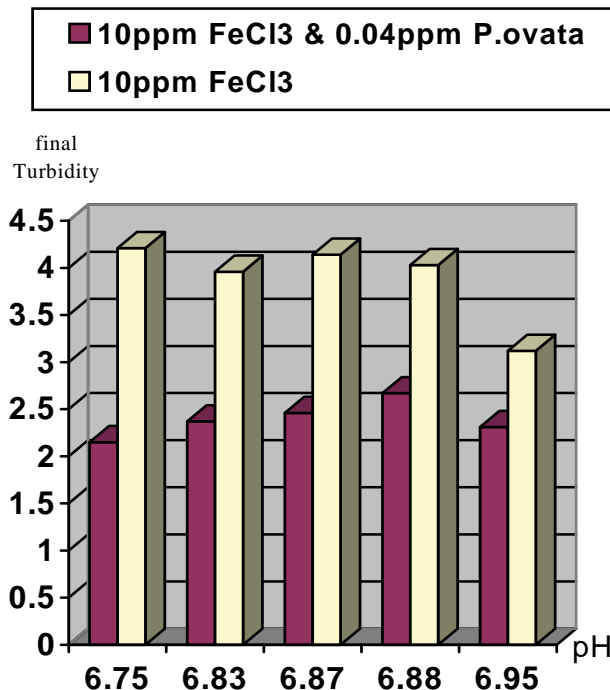


Figure 5. Comparison of final turbidities at initial pH 7 and 20 (NTU) turbidity in two stages. Stage1: Ferric Chloride coagulant and Stage2: Ferric Chloride coagulant in accompany with P.ovata coagulant aid.

■ sludge weight = 0.010 gr □ sludge weight = 0.010 gr

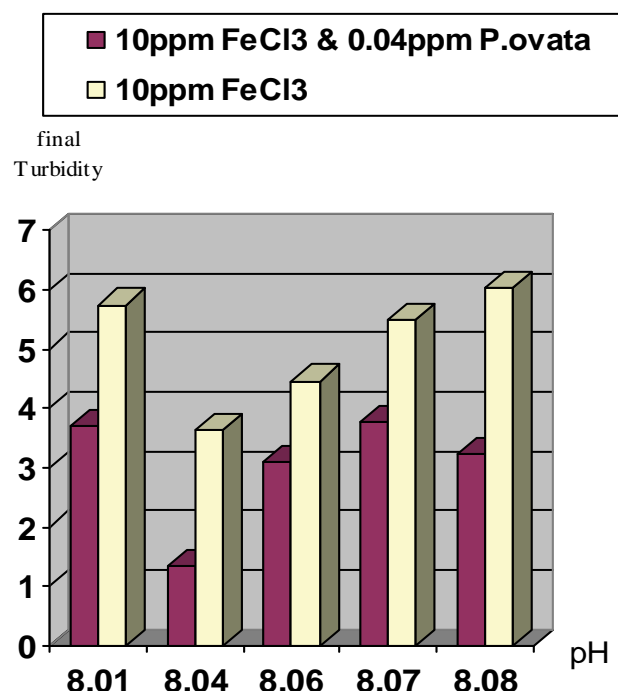


Figure 6. Comparison of final turbidities at initial pH 8 and 20 (NTU) turbidity in two stages. Stage1: Ferric Chloride coagulant and Stage2: Ferric Chloride coagulant in accompany with P.ovata coagulant aid.

■ sludge weight = 0.012 gr □ sludge weight = 0.014 gr

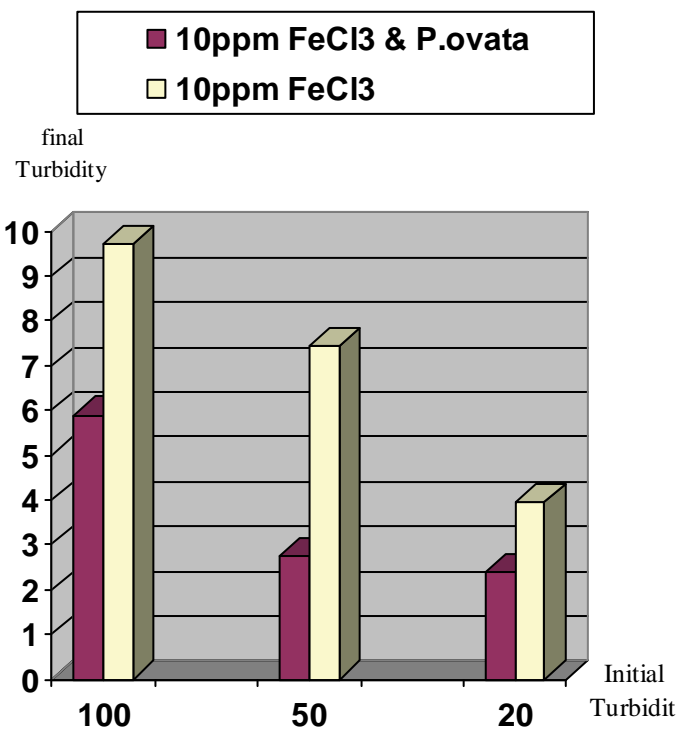


Figure 7. Comparison of final turbidities for the applied turbidities: high, moderate and low in two stages. Stage1: Ferric Chloride coagulant and Stage2: Ferric Chloride coagulant in accompany with P.ovata coagulant aid, pH 7.

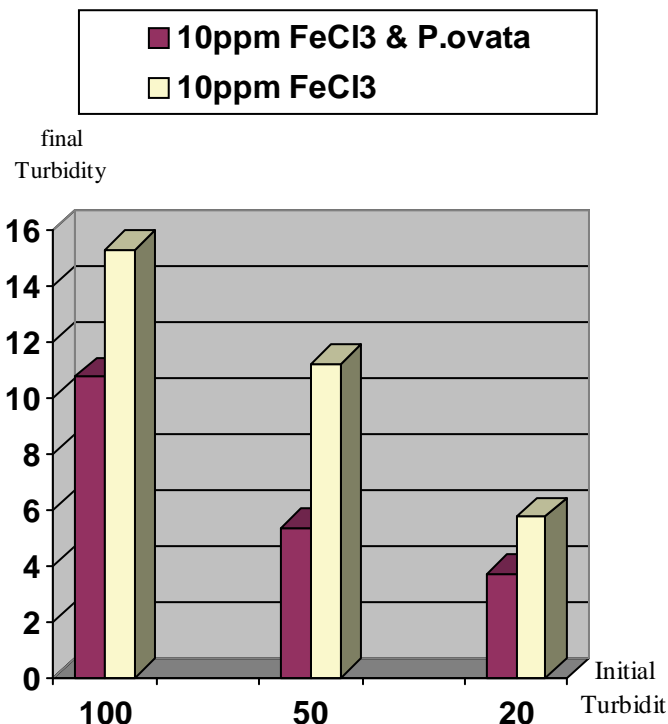


Figure 8. Comparison of final turbidities for the applied turbidities: high, moderate and low in two stages. Stage1: Ferric Chloride coagulant and Stage2: Ferric Chloride coagulant in accompany with P.ovata coagulant aid, pH 8.

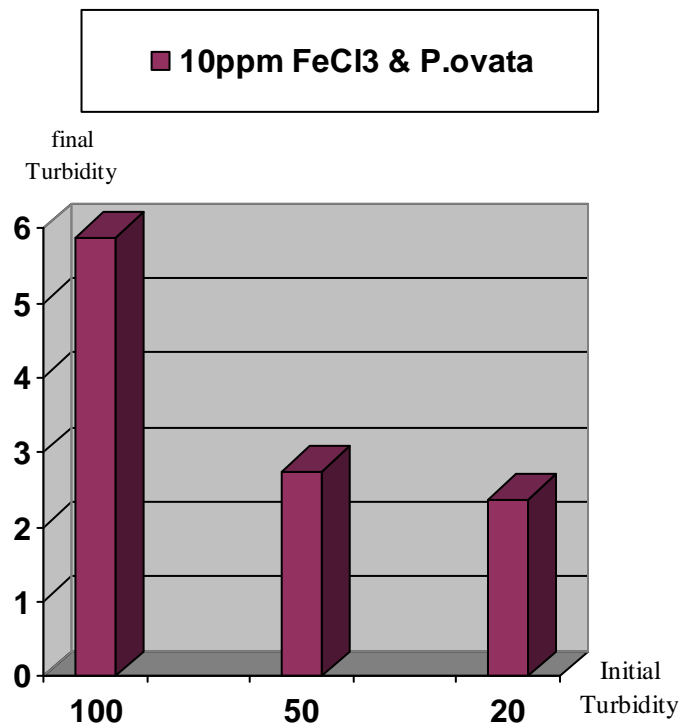


Figure 9. Comparison of final turbidities for the applied turbidities: high, moderate and low in stage: Ferric Chloride coagulant in accompany with P.ovata coagulant aid, pH 7.

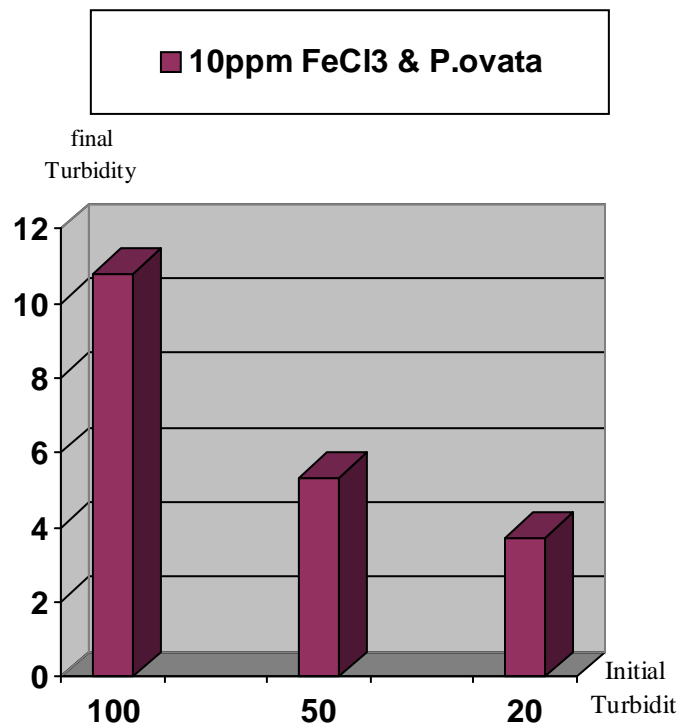


Figure 10. Comparison of final turbidities for the applied turbidities: high, moderate and low in stage: Ferric Chloride coagulant in accompany with P.ovata coagulant aid, pH 8.

Results indicates that turbidity elimination is ideal in pH, 7 and using Ferric Chloride with P.ovata. Figures 7 to10 present the comparison of turbidity elimination for all experiments. The results are as follows:

1) Using 10 ppm Ferric Chloride and 0.2 ppm of P.ovata in 100 NTU turbidity and pH, 7 could remove 94.1% of turbidity, while in pH, 8, turbidity elimination was 89.2%.

2) In moderate turbidity 50 NTU using 10 ppm Ferric Chloride and 0.1 ppm of P.ovata in pH, 7, eliminate 94.5% of the turbidity while in pH, 8 this value was 89.3%

3) In low turbidity of 20 NTU using 10 ppm Ferric Chloride and 0.04 ppm of P.ovata in pH, 7, turbidity reached to 2.37 NTU and elimination rate efficiency was 88.15%. At the same condition in pH, 8 the removal efficiency was 81.45 %.

4) COD measurement results, in all experiment were Nil and it shows that using P.ovata does not have any residual in treated water.

5) TOC in all experiment has been done and there is not any Toc in treated water.

Application of P.ovata plays an important role in turbidity elimination, reducing Ferric Chloride consumption as well as producing sludge significantly.

3.1. Study the Influence of pH Variation on P.ovata Performance

In this section of research, jar test on water sample with pH, 7 was repeated and in each time of injection specified quantity of P.ovata has used as coagulant aid. The results of these tests are presented in Figures 1, 3, 5, 7 and 9.

The influence of P.ovata on coagulation process increases with P.ovata injection enhancement. However, if P.ovata injection exceeds its optimum value, its effect will decrease. Increase in the efficiency of water turbidity removal was observed in low pH values, should be determined under conditions in water treatment plants.

3.2. The Influence of P.ovata Utilization on Sludge Production

The produced sludge from water plant operation is classified as chemical sludge which should be disposed under specific procedures in some countries. Sludge production reduction is the first step to decrease investment cost and sludge transfer and removal operation. One technique is simultaneous utilizations of Ferric Chloride and coagulant aid. When P.ovata is selected as a coagulant aid, consumption of Ferric Chloride decreases that leads to decrease of sludge production.

3.3. Economic Explanation of P.ovata Application in Water Treatment

In this research economized value of variation of consumption of chemical materials was studied. If consumption of P.ovata leads to decrease in Ferric Chloride consumption, with considering global and regional price of this material, it is possible to estimate decreased cost of chemical materials.

Totally, the following results were obtained from the tests:

1) The efficiency of P.ovata seed extract coagulant aid is influenced by pH and optimum pH increases its efficiency.

2) In turbidity of 50 NTU the seed extract of P.ovata in concentration of 0.1 ppm with 10 ppm of Ferric Chloride can eliminate turbidity more than Ferric Chloride in concentration of alone.

3) With turbidity reduction to 20 NTU, efficiency of P.ovata decreases, however leads to standard turbidity level.

4) According to the results presented in figures and tables of this research, the extract of P.ovata does not reduce final pH of water sample, while using Ferric Chloride alone reduces final pH of the samples.

5) pH reduction improves the performance of Ferric Chloride alone as well as Ferric Chloride in accompany with P.ovata.

6) Using coagulant aid promotes the efficiency of Ferric Chloride and reduces the turbidity more than alone situation.

7) The seeds of this plant are much cheaper than artificial coagulant aids. This plant is sowed in Iran and readily accessible. In addition, from health aspect, not only P.ovata does not have any harmful effect in comparison with artificial coagulant aid but also it used as a medicinal plant. Finally it is recommended that the same research is conducted on the influent of water treatment plants in pilot scale.

4. References

- [1] A. G. Kebreab, "Moringa seed and pumice as alternative natural materials for drinking water treatment," KTH Land and Water Resources Engineering University, TRITA, LWR PhD THESIS 1013, 2004.
- [2] R. Menahem and M. Lurie, "Control of organic matter by coagulation and flocculation separation," Water Science and Technology, Vol. 27, No. 11, 1993.
- [3] Water industry standards, "Drinking water quality standard," Vol. 6, July 1987.
- [4] M. C. Amiri, "Water treatment principles," Arkan Publication, Isfahan, 2006.
- [5] HDR Engineering, Inc., "Handbook of public water systems," John Wiley and Sons, Inc., New York, 1991.

- [6] A. A. Shahmansuri and A. A. Neshat, "Comparison among Poly Aluminium Chloride, Aluminium Sulphate and Ferric Chloride in TOC and total Coliform removal," Water and Waste Water Journal, Vol. 48, pp. 39–44, 2003.
- [7] A. A. Tatsi, A. I. Zouboulis, K. A. Matis, and P. Samara, "Coagulation–flocculation pretreatment of sanitary landfill leachates," Chemosphere, Vol. 53, pp. 737–744, 2003.
- [8] D. Wang, W. Sun, Y. Xu, H. Tang, and J. Gregory, "Special stability of inorganic polymer flocculant–PACI," Colloids and Surfaces, Vol. 243, pp. 1–10, 2004.
- [9] D. R. Parker and P. M. Bersch, "Formation of the 'Al₁₃' tridecameric polycation under diverse synthesis conditions," Environment Science Technology, Vol. 26, pp. 914–921, 1992.
- [10] V. K. Lamer and T. W. Healy, "Adsorption–flocculation reactions of micro molecules at the solid-liquid interface," Review of Pure and Applied Chemistry, Vol. 13, pp. 112–132, 1963.
- [11] S. Naseri, "Coagulation and coagulants process: Total principles and practical methods in water treatment industry," Congress Articles Collection of Coagulants in Water Industry, Ahwaz, November 1996.
- [12] S. Kawamura, "Effectiveness of natural polyelectrolytes in water treatment," AWWA, Vol. 83, No. 10, pp. 88, October 1991.
- [13] R. Christopher, S. Daniel, and A. Okun, "Surface water treatment for communities in developing countries," ITDG Publishing, pp. 300, 1992.
- [14] A. Diaz, N. Rincon, A. Escorichvela, and N. Fernandez, "A preliminary evaluation of turbidity removal by natural coagulants indigenous to Venezuela," Process Biochemistry, Vol. 35, pp. 391–395, 1999.
- [15] R. D. Letterman and R. W. Pero, "Contaminant in polyelectrolytes used in water treatment," AWWA, November, 1990.
- [16] S. Kawamura, "Effectiveness of Chitosan for water treatment," Penerbit University Kebangsaan Malaysia, Bang, 1995.
- [17] K. L. Chadho and G. Rajender, "Advances in horticulture medicinal and Aromatic plants," Vol. 11, Maldorta. Pub., New Delhi, 1995.
- [18] B. D. Basudehradun, S. Bisha, and S. Manhendrapol, "Indian medicinal plants," Today and Tomorrow's Publishing, Vol. 1–5. pp. 1–1033, 1989.
- [19] A. Zargari, "Medicinal plants," Published by University of Tehran, Vol. 4, 1997.
- [20] F. A. Ghahraman, "Flour of Iran," Published by Institute of Jungles and Grasslands Research, Vol. 1–18, 1982–1996.
- [21] S. P. Raychaudhuri and J. Ahmad, "Cultivation of important medicinal plants in India," In Glimpses in Plant Research, Today and Tomorrow's Printers and Publishers, New Delhi, Vol. 10. pp. 247–256, 1993.
- [22] L. Hornock, "Cultivation and processing of medicinal plants," Academic Publishing Budapest, 1992.
- [23] Y. Ayinehchi, "Simple substances in medicine and Iran medicinal plants," Published by University of Tehran, 1986.
- [24] N. Kumar, J. B. M. Abdulghader, P. Rangaswami, and I. Irulappen, "Introduction to spices, plantation crops, medicinal and aromatic plants," Oxford and IBH, 1997.

Remove of Phenolic Compounds in Water by Low-Temperature Plasma: A Review of Current Research

Jufang ZHANG¹, Jierong CHEN¹, Xiaoyong LI²

¹School of Energy and Power Engineering, Xi'an Jiao Tong University, Xi'an, China

²School of Science, Xi'an Jiao Tong University, Xi'an, China

E-mail: jrchen@mail.xjtu.edu.cn

Received March 19, 2009; revised April 21, 2009; accepted April 23, 2009

Abstract

Phenolic compounds have very strong toxicity, so it has been paid sharply attention to find an effective way of controlling the wastewater containing phenolic compounds. The work on this subject done by domestic and overseas scholars is studied in this paper, and the progress of researches on low-temperature plasma treatment is summarized through the electrical discharge types, mechanism, kinetics of phenolic compounds decomposition and combination of several methods with low-temperature plasma treatment. In addition, the crucial problem and the developing tendency on low-temperature plasma treatment for phenol-bearing wastewater are briefly discussed.

Keywords: Low-Temperature Plasma Treatment, Phenolic Compounds, Types of Electrical Discharge, Mechanism, Kinetics, Combination of Several Methods

1. Introduction

Phenolic compounds are well-known disinfectants and sterilizers as well as raw materials for synthetic resin, dyes, pharmaceuticals, perfumes, pesticides, tanning agents, solvents or lubricating oils. Long-term exposure to phenol paralyzes the human central nervous system and damages kidneys and lungs [1]. They are the representatives of water soluble. Especially phenol, it is also classified as a teratogenic and carcinogenic agent. Thus, phenol is listed in water hazard class 2 in several countries. Biodegradability is only 90% in surface waters after seven days, and the aquatic toxicity of phenol (LC50) is $12 \text{ mg}\cdot\text{L}^{-1}$ (*Daphnia magna*, 48 h). In EU countries, the maximum concentration of phenol allowed in drinking water is $0.5 \text{ mg}\cdot\text{L}^{-1}$ (Weber *et al.*, 2008) [2]. The removal of phenolic compounds from wastewater is one of the most critical and urgent topics in environmental research.

Plasma is a group of positive particles, negative particles, which includes positive ions, negative ions, electron, free radicals, and a variety of active radicals, etc. Because positive charge is equal to negative charge in this group, it is called plasma. Based on the particle temperature, plasma can be divided into two categories, namely ther-

mal plasma, and non-thermal plasma (low-temperature plasma) [3]. As one of the potential advanced oxidation processes (AOPs), non-thermal plasma production during various discharges has long been exploited for water and wastewater purification. Owing to its virtue of producing in situ oxidative species ($\text{OH}\cdot$, $\text{H}\cdot$, $\text{O}\cdot$, H_2O_2 , H_2 , O_2 , O_3) as well as initiating a variety of chemical and physical processes(a high electric field, intense ultraviolet radiation, overpressure shock waves) [4-7] in water for decomposing toxic compounds, its operational simplicity (realized under the conditions of an ambient temperature and pressure), its variable reactor configuration, and its good-performance degradation of low-concentration organic compounds. This low-temperature plasma treatment has been of great interest in the field of environmental protection. In this review, electrical discharge types, mechanism, kinetics of phenolic compounds decomposition and combination of several methods with low-temperature plasma treatment will be presented.

2. Types of Electrical Discharges

Non-thermal plasma was produced during discharge in the gas, liquid or hybrid liquid-gas phase. Recently, many

types of plasma processes have been developed for the removal of phenolic compounds from water, including pulsed electrical discharge, glow discharge plasma (GDP), gas-liquid gliding arc discharges.

2.1. Pulsed High-Voltage Electrical Discharge

A pulsed high-voltage electrical discharge can begin in gas phase close proximity to the liquid surface, liquid phase and gas-liquid phase. When in liquid, it produces spark, streamers and corona, which are called pulsed spark discharge (PSD), pulsed streamer corona discharge (PSCD), and pulseless corona discharge (PCD) respectively. When it discharges on surface of water (WSP), it can only produce corona, arc and so on [4].

2.1.1. Gas Phase Discharge

L. R. Grabowski *et al.* [8] studied the removal of phenol from a thin layer of water by creating pulsed corona discharges above the water (CAW). The CAW reactor was proved to be an effective source for ozone production, which is capable to remove 45% of phenol in 5 min of a 100 ml 1mM batch. Sun *et al.* [9] found that the removal efficiency of phenol contaminants in the aqueous solution by plasma produced in gas phase discharge was higher when it came to the spark discharge than to the streamer corona discharge. But [4] the specific energy required to decompose phenol was higher in the WSP (Pulsed high-voltage discharges on the water surface) discharge mode than in the corona and streamer discharge modes, but the treatment time required for decomposition in the WSP mode was shorter than in the other modes.

2.1.2. Liquid Phase Discharge

For the pulsed high-voltage electrical discharge in liquid, there are three different types of reactors, which have rod-rod, rod-plate and wire-cylinder electrode constructions. Shinta *et al.* [10] studied the pulsed high voltage discharge in water and degradation properties of three different types of reactors. They found that of the three reactors (rod-rod and rod-plate, wire-cylinder), the highest phenol removal efficiency was obtained with the wire-cylinder reactor, while the removal efficiency with the rod-rod and rod-plate almost the same. Ilie Suarasan *et al.* [11] changed the traditional discharge rod-plate reactor in water to multipoint reactor, and studied many factors affecting the produce of O₃. Wang Fangzheng *et al.* [12] researched a multi-needle-to-plate high voltage pulsed discharge plasma system to degrade phenol. They found that the degradation rate of phenol increases with the decrease of solution conductivity and electrode distance, but with the increase of gas bubbling. In the case of 100 mL•min⁻¹ solution circulation rate, the degradation rate with pH value of 6.4 and electric conductivity of 100 μ s/cm reached 86.2% after 60 min treatment.

Chen, Y. S. *et al.* [13–15] made a series of study on the removal of phenolic compounds (phenol, 4-chlorophenol) in the aqueous solution with pulsed high-voltage corona discharge plasma. They studied the effects of various parameters on the removal efficiency, and found that phenol degradation can be raised considerably by increasing the peak voltage of the pulsed discharge and the repetition rate of pulse, or by increasing pH of the aqueous solution. Furthermore, decreasing the diameter of discharge electrode and electric conductivity of the aqueous solution can increase the degradation efficiency. The addition of gas, especially oxygen through the hollow needle electrode, and of FeSO₄ to the aqueous solution of phenol is found to significantly enhance phenol degradation. L. R. Grabowski *et al.*

Yongjun Shen *et al.* [16] investigated the processes of phenol degradation by pulsed electrical discharges under several kinds of discharge atmospheres (oxygen, argon, nitrogen and ozone) and chemical catalysts (ferrous ion and hydrogen peroxide). It has been found that the effect of various gases bubbling on phenol degradation rate ranked in the following order: oxygen containing ozone > oxygen > argon > nitrogen. However [9], when the argon was used for the electrode-enveloping gas with pulsed discharges on the water surface, a higher phenol decomposition rate was obtained than that for oxygen and air. But when the argon flow rate was increased from 1 to 40 L•min⁻¹, there was no change in the phenol decomposition rate. On the other hand, in the case of oxygen, the decomposition rate decreased with increasing gas flow.

2.1.3. Gas-Liquid Phase Discharge

Electrical discharges in two-phase medium not only combine the advantages of gas-phase discharge (i.e., for ozone O₃ and oxygen radical O[•] formation, UV-radiation generation) with liquid-phase discharge (i.e., for hydroxyl radical OH[•] and hydrogen peroxide H₂O₂ formation), but also have more advantages: increase of the gas-liquid boundary surface area which is exposed to hydrated electrons and free radicals; enhancement of the electric field at the droplet surface; concentration of the organics near the droplet surface [17]. Petr Lukes *et al.* [18] studied the mechanism of phenol degradation through its dependence on the gas phase and liquid phase compositions using pure argon and oxygen atmospheres above the liquid and different initial pH values in the aqueous solution. Phenol degradation was significantly enhanced in the hybrid-series reactor compared with the phenol removal by the single-liquid phase discharge reactor.

The hybrid series gas-liquid electrical dischargereactor was described in detail in Figure 1 [19], which was very typical.

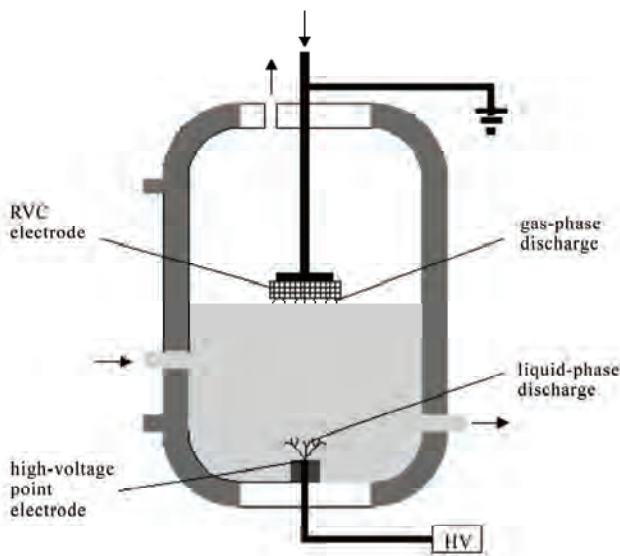


Figure 1. Hybrid series gas-liquid electrical discharge reactor. (HV) pulse power supply.

However, liquid-phase discharge has a problem of consuming an extremely high energy. Kuroki T. *et al.* [20] have investigated phenol decomposition using a gas-liquid interface discharge induced by an ultra-short width (similar to 600 ns) pulse of high voltage. Gas bubbling was employed to enhance both convection and the gas-liquid interface area. A significant improvement in energy efficiency of phenol decomposition was achieved.

2.2. Glow Discharge

Glow discharge plasma (GDP) is one of them where the plasma is sustained by glow discharges across a pointed electrode and the surface of the liquid electrolyte [21].

Gao Jinzhang *et al.* [21–23] made a series study of the oxidative degradation of phenolic compounds (o-chlorophenol; 2, 4-dichlorophenol; 4-chlorophenol (4-CP)); in aqueous solution induced by plasma with submersed glow discharge has been investigated. Various influencing factors such as the initial pH, the concentration of phenolic compounds and the catalytic action of Fe^{2+} were examined. It was showed that degradation of phenolic compounds can be efficiently increased in alkaline conditions with the addition of Fe^{2+} . Liu, Y. J. *et al.* [24] also found that adding appropriate amounts of Fe^{2+} or Fe^{3+} to the solution was favorable for phenol degradation by plasma with submersed glow discharge. Furthermore, carbonate ions or n-butanol in the solution can decelerate the phenol removal. When the treatment time is increased and the pH value of the solution is decreased, leading to an increase in the phenol decomposition.

Wang L. *et al.* [25] investigated the degradation of bisphenol A (BPA) and simultaneous formation of hydrogen peroxide induced by glow discharge plasma in

contact with a queous solution. Experimental results indicated that the BPA degradation rate was higher in sodium chloride solution than that in sodium sulfate or phosphate solutions. However, the formation rates of hydrogen peroxide were on the opposite case.

The schematic diagram of the glow discharge set-up is shown in Figure 2 [22].

2.3. Gliding Arc Discharge

The gliding arc discharge is a simple and inexpensive way to generate non-thermal plasma. It has a dual character of thermal and non-thermal plasma, and can involve relatively high electric powers compared with the corona discharge [26].

Ch. M. Du *et al.* [21–24] has designed a gliding arc reactor in their laboratory with the aim to degrade aqueous phenol solutions and 4-CP solution at atmospheric pressure. They have already made a series study on the various factors affecting the degradation efficiency, including supply voltage, electrode gap distance, and gas–liquid flow properties. The efficiency, which steeply increases when increasing the supply voltage, can reach 96% when the minimum electrode distance is fixed at 3 mm. Experiments show that their degradation efficiency also depends on solution pH, Fe^{2+} addition, gas nature and gas flow rate. Furthermore the chemical oxygen demand (COD) abatement of 4-CP solution with stainless steel electrode is higher than that with aluminum or brass electrode. Increasing gas–liquid mixing rate could also increase the degradation of 4-CP. They also used this method to degrade highly concentrated phenol wastewater [31], about $1000\text{mg}\cdot\text{L}^{-1}$. It was found that the COD removal efficiency is very high, which can reached 88.82% after degradation.

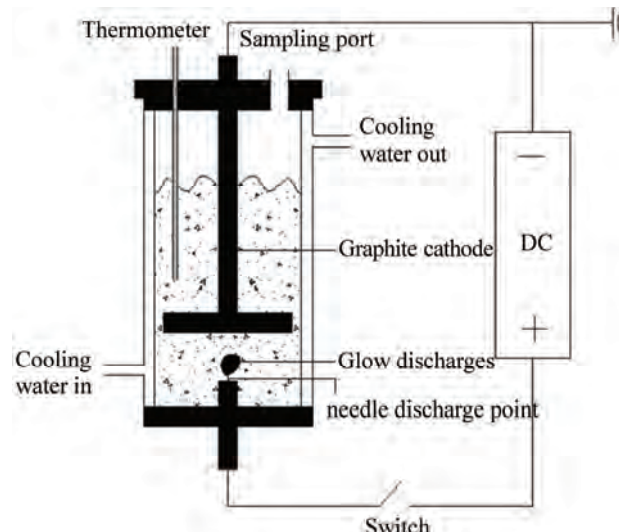


Figure 2. The sketch map of the glow discharge set-up.

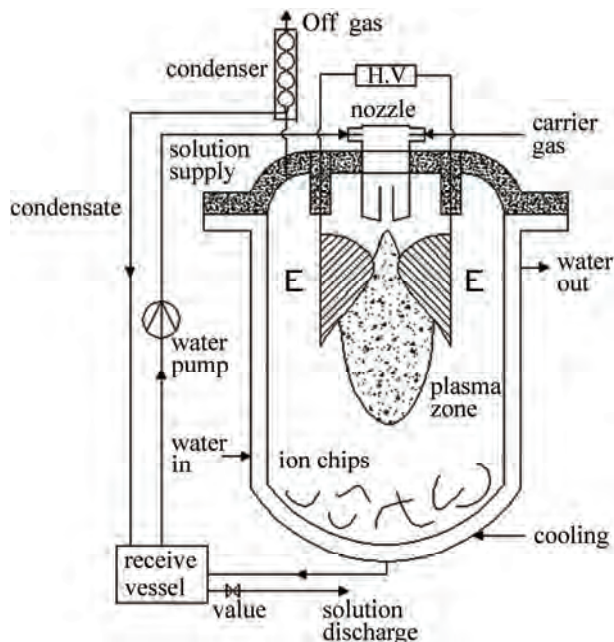


Figure 3. Scheme of the gliding arc discharge reactor.

The schematic diagram of the gliding arc discharge reactor is shown in Figure 3 [30].

3. Mechanism

Pyrolysis, ultraviolet photolysis, electrohydraulic, cavitation and supercritical water oxidation occur in these plasma channels when discharged, and generate various active species such as OH^\bullet , O^\bullet , H^\bullet , O_3 , etc [32]. Petr Lukes *et al.* [18] confirmed that hydroxyl radicals and ozone are the key oxidation species produced by the gas-phase discharge of the hybrid series reactor under argon and oxygen atmospheres, respectively. An electrophilic substitution reaction mechanism was proved by the significant correlation between the relative rates of oxidation of substituted phenols obtained in the hybrid series reactor and the Hammett substituent constants [28]. In conclusion, the mechanism of phenol's degradation was commonly found to be attributed mainly to the oxidation by hydroxyl radicals produced directly by the discharge.

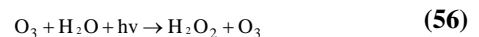
3.1. Mechanism of Discharge Only

Depending on the degradation region, discharge process can be conveniently grouped into two categories of effects: 1) localized and 2) extended. Localized effects occur in the immediate vicinity of the plasma channel and include thermal oxidation within the plasma channel, vacuum UV photolysis at the surface of the plasma channel, and supercritical oxidation within the subsequent steam bubbles. On the other hand, extended effects are due to radical reactions in which active species gen-

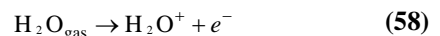
erated in the vicinity of the plasma channel expand outwardly from the circumference [33]. In different discharge types, the radical reactions in localized process are different, but in extended process are nearly the same as each other.

For the pulsed high-voltage electrical discharge in liquid, initial models of the bulk-phase corona-induced chemical reactions were reported by M. Dors *et al* [34]. In that study it was assumed that the pulsed corona discharge leads to the formation of hydrogen peroxide, hydroxyl radicals, and aqueous electrons through reactions (1-3) as shown in Table 1. The other major species produced by the corona reactor were assumed to be the same as those formed in radiation processes such as electron beam radiation and pulse radiolysis as indicated by the propagation and termination reactions given in Table 1. When degrading phenols, the reactions as reactions (57-68) shown in Table 1.

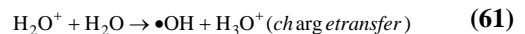
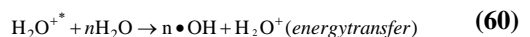
For the pulsed high-voltage electrical discharge in gas and in gas-liquid phase [4,6,19,35], ozone was first produced by gas phase discharge, then went into liquid phase to induce the radical reaction and produced OH radicals (reactions 56-57). Furthermore, reactions between high energetic electrons in discharge streamer and the initial molecules in aqueous solution could form $\cdot\text{OH}$ (as shown in reactions 4-16 given in Table 1).



In the glow discharge, the gaseous water molecules were dissociated into positive water ions and electrons as indicated in reaction [22] (2):



The positive water ions were accelerated in the cathode-fall of the GDP and entered the solution with enough kinetic energy to break up the liquid water molecules to form the following primary species both through energy transfer and through charge transfer (Equations (3)-(5)):



For gliding arc plasma in humid air, it is revealed that OH^\bullet and NO^\bullet radicals are simultaneously present in the discharge [36]

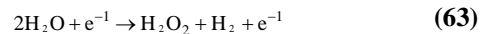
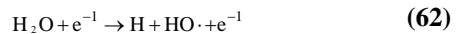
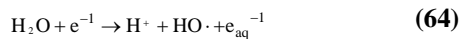


Table 1. The present study utilizes the basic reactions reported by M. Dors *et al.*

No.	Chemical reaction	Reaction rate constant[M ⁻¹ s ⁻¹]
1.	H ₂ O=H· + ·OH	1.7 10 ⁻⁷
2.	2H ₂ O=H ₂ O ₂ +H ₂	3.9 10 ⁻⁶
3.	H ₂ O = H+ + eaq + ·OH	4.2 10 ⁻⁷
4.	eaq + H· = H ₂ + OH ⁻	2.5 10 ¹⁰
5.	eaq + ·OH = OH ⁻	3.01 10 ¹⁰
6.	eaq + HO ₂ = HO ₂ [·]	2.01 10 ¹⁰
7.	eaq + O ₂ ⁻ = HO ₂ [·] + OH ⁻	1.3 10 ¹⁰
8.	eaq + H ₂ O ₂ = ·OH + OH ⁻	1.2 10 ¹⁰
9.	eaq + HO ₂ [·] = O ⁻ + OH ⁻	3.51 10 ⁹
10.	eaq + O ₂ = O ₂ ⁻	1.8 10 ¹⁰
11.	eaq + H ⁺ = ·H	2.31 10 ¹⁰
12.	eaq + H ₂ O = OH ⁻ + H·	1.00 10 ³
13.	2eaq = H ₂ + 2OH ⁻	4.99 10 ⁹
14.	2H· = H ₂	7.82 10 ⁹
15.	H· + ·OH = H ₂ O	2.51 10 ¹⁰
16.	H + HO ₂ = H ₂ O ₂	2.01 10 ¹⁰
17.	H· + O ₂ ⁻ = HO ₂ [·]	2.01 10 ¹⁰
18.	H· + H ₂ O ₂ = H ₂ O + ·OH	8.44 10 ⁶
19.	H· + O ₂ = HO ₂	2.11 10 ¹⁰
20.	OH ⁻ + H = eaq + H ₂ O	2.21 10 ⁷
21.	·OH + ·OH = H ₂ O ₂	5.51 10 ⁹
22.	·OH + O ⁻ = HO ₂ [·]	2.01 10 ¹⁰
23.	OH + HO ₂ = O ₂ + H ₂ O	6.32 10 ⁹
24.	OH + O ₂ ⁻ = O ₂ + OH ⁻	8.22 10 ⁹
25.	OH + H ₂ O ₂ = HO ₂ + H ₂ O	4.07 10 ⁷
26.	OH + HO ₂ [·] = HO ₂ + OH ⁻	7.52 10 ⁷
27.	OH + H ₂ = H + H ₂ O	3.82 10 ⁷
28.	OH + OH ⁻ = O ⁻ + H ₂ O	1.2 10 ¹⁰
29.	2 O ⁻ = OH ⁻ + HO ₂ [·]	1.0 10 ⁹
30.	O ₂ ⁻ + O ⁻ = O ₂ + 2OH ⁻	6.02 10 ⁸
31.	O ⁻ + H ₂ O ₂ = O ₂ ⁻ + H ₂ O	5.01 10 ⁸
32.	O ⁻ + HO ₂ [·] = O ₂ ⁻ + OH ⁻	4.01 10 ⁸

33.	$O^- + H_2 = H + OH^-$	8.02	10^7
34.	$O^- + H_2O = OH + OH^-$	1.76	106
35.	$2 HO_2 = O_2 + H_2O_2$	8.34	10^5
36.	$HO_2 + H_2O_2 = OH + O + H_2O$	2.01	10^{-1}
37.	$O_2^- + HO_2 = HO_2^- + O_2$	9.72	10^7
38.	$HO_2 = H^+ + O_2^-$	7.52	10^5
39.	$2O_2^- = H_2O_2 + O_2 + 2OH^-$	3.01	10^{-1}
40.	$O_2^- + H_2O_2 = OH + O_2 + OH^-$	1.31	10^{-1}
41.	$O_2^- + HO_2^- = O^- + O_2 + OH^-$	1.31	10^{-1}
42.	$H^+ + O_2^- = HO_2$	5.11	10^{10}
43.	$H_2O_2 = 2 \cdot OH$	3.18	10^{-7}
44.	$H_2O_2 + OH^- = HO_2^- + H_2O$	1.0	10^{10}
45.	$HO_2^- + H_2O = H_2O_2 + OH^-$	1.13	10^6
46.	$HO_2^- + H^+ = H_2O_2$	2.01	10^{10}
47.	$H^+ + OH^- = H_2O$	1.4	10^{11}
48.	$H_2O = H^+ + OH^-$	2.54	10^{-5}
49.	$O^- + O_2 = O_3^-$	3.0	10^9
50.	$O^- + O_3^- = 2 O_2^-$	7.0	10^9
51.	$H_2O_2 + O_3^- = O_2^- + O_2 + H_2O$	1.6	10^6
52.	$HO_2^- + O_3 = O_2^- + O_2 + OH^-$	8.9	10^5
53.	$O_3^- = O_2 + O^-$	3.0	10^2
54.	$H_2 + O_3^- = H + O_2 + OH^-$	2.5	10^5
55.	$O^- + H^+ = OH$	1.0	10^{10}
56.	$HO_2 + OH^- = O_2^- + H_2O$	1.0	10^{10}
57.	$Phenol + OH = o\text{-}C_6H_5(OH)_2$	8.0	10^9
58.	$Phenol + OH = m\text{-}C_6H_5(OH)_2$	1.0	10^9
59.	$Phenol + OH = p\text{-}C_6H_5(OH)_2$	6.5	10^9
60.	$CO_3^{2-} + OH^- = CO_3^- + OH^-$	4.0	10^8
61.	$2o\text{-}C_6H_5(OH)_2 = Catechol + H_2O + Phenol$	2.1	10^8
62.	$2m\text{-}C_6H_5(OH)_2 = Resorcinol + H_2O + Phenol$	2.0	10^8
63.	$2 p\text{-}C_6H_5(OH)_2 = Hydroquinone + H_2O + Phenol$	1.0	10^9
64.	$Phenol + H = products$	1.7	10^9
65.	$Phenol + eaq = products$	3.0	10^7
66.	$Catechol + OH = products$	1.1	10^{10}
67.	$Resorcinol + OH = products$	1.2	10^{10}
68.	$Hydroquinone + OH = products$	5.2	10^9



3.2. Intermediate Products and a Discussion of the Degradation Pathways

In many studies [7,37,38], it was revealed by high performance liquid chromatography and ionic chromatography that the main intermediates of phenol decomposition are hydroquinone, pyrocatechol, p-benzoquinone and organic acids. The $\text{OH}\cdot$ radical reacts with phenol to form dihydroxycyclohexadienyl radical $\cdot\text{C}_6\text{H}_5(\text{OH})_2$ (DHCHD). Under the circumstance of oxygen, oxygen will attack these radicals to produce dihydroxycyclohexadienylperoxy (DHCHDP) radicals. The DHCHDP radical may decay in a first-order process to form catechol by elimination of a hydroperoxyl radical. $(\text{HO}_2\cdot)\text{4-CP}$ [39] was mainly converted to 4-chlorocatechol, hydroquinone, 1, 4-benzoquinone, 2, 4-dichlorophenol, 5-chloro-3-nitro-pyrocatechol, and 4-chloro-2-nitrophenol, and then, they all degraded into organic acids, such as formic acid, acetic acid, oxalic acid, etc., which converted into CO_2 and H_2O finally.

The intermediate products are easily oxidized further under the action of the radicals and oxygen. The opening of the aromatic ring leads to the formation of low molecular weight compounds, mainly organic acids. DHCHDP form endoperoxides through repeated scavenges of oxygen. These very unstable intermediates are decomposed by ring cleavage. The intermediate product or organic acids can also be oxidized through hydroxylation and hydration, finally forming carbon dioxide. Figure 1 shows the degradation pathway of phenol by pulsed electrical discharge in the presence of oxygen [38].

3.3. Mechanism and Effect of Oxgen Bubbling

The degradation rates under oxygen gas and oxygen-containing ozone bubbling were greatly improved. When oxygen was bubbled to the aqueous solution in the discharge reactor through the discharge electrode [5], the phenolic compounds in the aqueous solution were degraded through the following steps (As shown by the following equations). First, ozone was formed due to the oxygen discharge in the strong electric field. And then ozone transferred from gas bubble to the aqueous solution

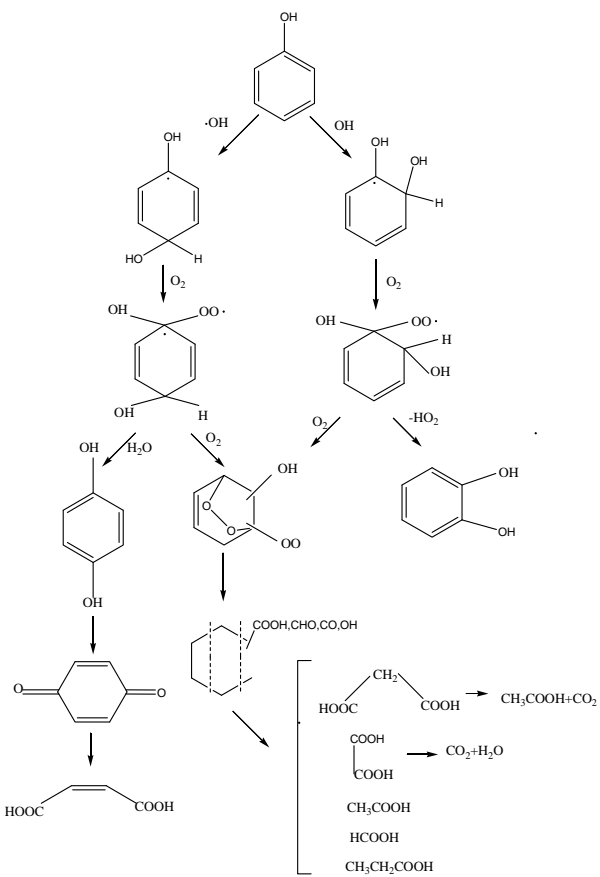


Figure 4. Degradation pathways of phenol by pulsed electrical discharges under conditions of oxygen-containing gas.

containing phenolic compounds, not only lots of $\cdot\text{OH}$ radicals were produced (reaction 56, 57) to degrade phenol, but also other species such as ozone, or superoxide (O_2^-) and singlet oxygen (${}^1\text{O}_2$), participated in the chemical reactions (as shown in Table 1) [16]. The ozone and $\text{OH}\cdot$ radical in the aqueous solution could react with the phenols, which was shown as Figure 4.

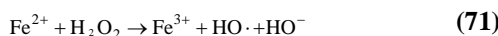
3.4. Mechanism and Effect of Adding H_2O_2

Shinta *et al.* [6] studied the effect of added hydrogen peroxide on phenol removal efficiency. They found that the phenol degradation rate was higher in the presence of hydrogen peroxide. It's rational to assume [10] the reaction scheme where hydroxyl radical would act as the most responsible key-species for the organic degradation in competition with the coupling to hydrogen peroxide. Anto *et al.* [40] found that the addition of a small amount of hydrogen peroxide greatly increased the degradation rate of phenol, in which the ultraviolet light from discharge plasma was considered to be a cause of effective degradation. However [16], since the reaction of phenol with hydrogen peroxide is very slow at the ambient tem-

perature, the degradation process may be due to the reaction of hydroxyl radicals produced by photolysis of hydrogen peroxide, which was caused by UV radiation from electrical discharge plasma. The chemical effects of the electrical discharge plasma are due to direct photolysis (the electrical discharge plasma only), indirect photolysis (combination of chemical additives and the electrical discharge plasma) and pyrolysis destruction in plasma Channels and pyrolysis destruction in plasma Channels [41]. In conclusion, it can be mainly explained by three equations (reaction 36,43,44) as shown in Table 1.

3.5. Mechanism and Effect of Adding Iron Salts

Grymonpre DR *et al.* [42] found that it was useful to add iron salts to enhance hydroxyl radical formation and increase the efficiency of phenol degradation through Fenton's reaction (Equations (3)):



It can be seen that in the presence of Fe^{2+} , more free radicals were produced due to the catalysis of Fe^{2+} , which in turn, accelerated the reaction.

Neyens *et al.* [43] found that by adding Fe^{2+} highly influenced the phenol removal process. With the addition of Fe^{2+} ions the removal increased significantly from 15.45% to 94.94%, but decreased if continuing. Gao Jinzhang *et al.* also found that the removal rate cannot be further enhanced when the concentration of Fe^{2+} is over some value (80mg.l) [22]. However Lei Wang *et al.* [25] demonstrated that Fe^{3+} exhibits a better catalytic effect than Fe^{2+} , which is contradictory to the principles of the Fenton reaction because the reaction rate between ferric ion and hydrogen peroxide is much lower than that ferrous ion with hydrogen peroxide. They thought this phenomenon may be attributed to the following. When the aqueous BPA was exposed to GDP, the BPA initially react with hydroxyl radicals to form the intermediate products through the hydrogen abstraction or electrophilic addition to benzene ring of BPA. Lei Wang *et al.* [44] newly reported that when degrading phenol, one most probable way was by dihydroxycyclohexadienyl radicals, which were resulted from the attack of the hydroxyl radicals on phenol. The dihydroxycyclohexadienyl radicals then can react with Fe^{3+} ions, so Fe^{3+} exhibits a better catalytic effect than Fe^{2+} .

3.6. Mechanism and Effect of Adding Activated Carbon Particles on Phenol Degradation

Activated carbon particles suspended in the liquid phase have been found to play a role in enhancing-phase co-

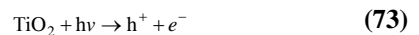
rona reactions, in addition to their role as physical adsorbents [19]. There exists also the possibility of reactions occurring on the surface of the activated carbon-induced by the electrical discharge, thus continually regenerating the activated carbon [45]. David R. *et al.* [46] also found that there was a strong possibility that the activated carbon participates in catalytic reactions with phenol and its primary byproducts. This occurs by adsorption of the organic molecules and possible reactions of the phenol on the carbon surface. After the carbon particles have been suspended in the solution treated by the pulsed corona, the physical properties of the carbon remain unchanged. An analysis of the carbon showed that little of the phenol initially adsorbed on the activated carbon was still present after treatment was completed.

3.7. Mechanism and Effect of Adding TiO_2 on Phenol Degradation

Lukes *et al.* [47] and Hao, X L *et al.* [48] both studied the non-thermal plasma-induced degradation of phenols in the presence of photocatalytically active TiO_2 . It was found that the phenols removal efficiency with TiO_2 was obviously increased. The main effect of TiO_2 addition was in the utilizing of ultraviolet radiation from the plasma resulting in the photocatalytical formation of OH radicals on the surface of TiO_2 particles and, thus, in the increase of the yield of OH radicals available for phenolic compounds degradation [49]. Farre *et al.* [50] suggested that the OH radical was produced by reaction of absorbed H_2O molecule with photogenerated holes at the illuminated TiO_2 particle. Equation (4).



Because when discharged, there will be much O_3 produced. It can also generate OH^\cdot radicals through the formation of an ozonide radical ($\text{O}_3^\bullet-$) in the adsorption layer. Equation (5) [51].



Hao, XL *et al.* compared the 4-CP removals between original TiO_2 and TiO_2 (used thrice), and found no obvious differences

4. The Kinetics of Phenol Decomposition

It is commonly believed that the phenol degradation with pulsed high-voltage discharge in aqueous solution shows a first-order kinetics: $C = C(0) e^{(-kt)}$ [7, 10–12].

M. Dors *et al.* [34] build a chemical kinetics model of phenol decomposition in water. The densities of the species participating in the chemical reactions were calculated with a set of first order, differential equations describing the chemical conversions. Results of their calculations are in good agreement with experimental and modelling results obtained by Joshi *et al.* Shunsuke *et al.* [52] studied the mechanism of phenol degradation by means of contact glow discharge electrolysis. They found that the rate of disappearance followed the first order rate law when the initial concentration of phenol was lower than 100 mM. As the initial concentration increased, the rate equation gradually deviated from the first-order and eventually shifted to zero-order above 250 mM. Grymonpré *et al.* [54] developed models including chemical reaction kinetics, and determined the rates of function of hydrogen peroxide, hydroxyl radicals and aqueous electrons by fitting the experimental data of phenol degradation to the model. Le C. Lei *et al.* [55] established a kinetic model to compare three different discharge systems (pulsed spark discharge, PS; pulsed streamer corona discharge (PSCD), and pulseless corona discharge (PCD), and predict the degradation pathway. The model results are in good agreement with the experimental observations on hydrogen peroxide and ozone formation, 4-CP degradation, and intermediates formation.

5. Combination of Several Methods with Low-Temperature Plasma Treatment

Wen Yuezhong *et al.* [54] used the combination of high voltage pulse discharge and ozone as an advanced oxidation technology was used to investigate the degradation of 4-chlorophenol (4-CP) in water. The factors that affect the rate of degradation were discussed. The 1.95×10^{-3} mol•L⁻¹ solutions of 4-CP were almost completely (96%) degraded after the discharge treatment of 30min.

Lukes *et al.* [47] investigated the non-thermal plasma-induced degradation of phenol by pulsed high-voltage discharge generated in water using point to plane geometry of electrodes in the presence of photocatalytically active TiO₂. They found that the phenol removal attributed directly to the effects of plasma chemical activity of the discharge was enhanced in the presence of TiO₂. Hao, XL *et al.* [48] also used this method to degrade para-chlorophenol (4-CP), including other compounds phenol and methyl red in water. The experimental results showed that rate constant of 4-CP degradation, energy efficiency for 4-CP removal and TOC removal with TiO₂ were obviously increased. Pulsed high-voltage discharge process with TiO₂ had a promoted effect for the degradation of these pollutants under a broad range of liquid conductivity.

Bubnov *et al.* [55] studied the decomposing phenol in aqueous solutions under the action of an atmospheric pressure. Oxygen dielectric barrier discharged in the presence or absence of catalysts in the plasma zone, and tested two types of catalysts, NiO and TiO₂. It was found that both materials exhibited catalytic properties. The action of NiO accelerated the step of phenol destruction while the action of TiO₂ catalyst resulted in a more preferable composition of decomposition products and provided a higher degree of carboxylic acid conversion into carbon dioxide than the NiO catalyst.

6. Conclusions

Although non-thermal plasma produced by different types of electrical discharges have recently attracted particular interest as a promising method of water treatment without pollution or less pollution. Report on basic research are too less and not have been used to the practical application. Moreover, the final byproducts and the reaction mechanisms involved in the destruction of phenolic compounds have not been sufficiently clarified up until now. Therefore, it is need a lot of basic research for the application of technology to industrial implementation. Finally, a combination of other methods (activated carbon particles, TiO₂, H₂O₂, O₃, and so on) with low-temperature plasma treatment to treat phenolic compounds will become more popular.

7. Acknowledgments

We gratefully acknowledge the financial support from National Natural Science Foundation of China and Shanxi Province, “2008ZDKG-78”technology innovation project, major scientific and technology in Suzhou, Jiangsu Province.

8. References

- [1] F. X. Zhang, “Disposal and utilization of phenolic wastewater,” Chemical Industry Press, Beijing, pp. 1–10, 1983.
- [2] B. Iurascu, I. Siminiceanu, D. Vione, and M. A. Vicente, “Phenol degradation in water through a heterogeneous photo-fenton process catalyzed by pretreated laponite,” Journal of Water Research, pp. 1313–1322, 2009.
- [3] J. R. Chen, “Chemistry of low-temperature plasma and its applications,” Science press, Beijing, 2001.
- [4] M. Sato, T. Tokutake, and T. Ohshima, “Aqueous phenol decomposition by pulsed discharges on the water surface,” IEEE Transactions on Industry Applications, pp. 1397–140, 2008.
- [5] P. Lukes and B. R. Locke, “Plasmachemical oxidation processes in a hybrid gas-liquid electrical discharge

- reactor," *Journal of Physics D: Applied Physics*, Vol. 38, pp. 4074–4081, 2005.
- [6] S. Tomizawa and M. Tezuka, "Kinetics and mechanism of the organic degradation in aqueous solution irradiated with gaseous plasma," *Journal of Plasma Chemistry and Plasma Process*, Vol. 27, pp. 486–495, 2005.
- [7] Y. S. Chen, X. S. Zhang, S. Chang, et al, "Study on the degradation mechanism of organic compounds in the aqueous solution by pulsed high-voltage discharge plasma," *Acta Scientiae Circumstantiae*, Vol. 25, pp. 113–116, 2005.
- [8] L. R. Grabowski, E. M. van Veldhuizen, A. J. M. Pemen, and W. R. Rutgers, "Corona above water reactor for systematic study of aqueous phenol degradation," *Plasma Chemistry and Plasma Processing*, Vol. 26, pp. 3–17, 2006.
- [9] B. Sun, M. Sato, J. S. Clements, "Oxidative processes occurring when pulsed high voltage discharges degrade phenol in aqueous solution," *Journal Environment Science*, Vol. 34, pp. 509–513, 2000.
- [10] S. Kunitomo and B. Sun, "Removal of phenol in water by pulsed high voltage discharge," *Journal of Pulsed Power Plasma Science*, IEEE ,Vol. 6, pp. 1138–1141, 2001.
- [11] I. Suarasan and L. Ghizdavu, "Experimental characterization of multipoint corona discharge devices for direct ozonization of liquids," *Journal of Electrostatics*, Vol. 54, pp. 207–214, 2002.
- [12] F. Z. Wang, J. Li, Wu Yan, Wang Huijuan, and Li Guofeng , "Degradation of phenol in aqueous solution by high voltage pulsed discharge plasma," *High Voltage Engineering*, Vol. 33, pp. 124–127, 2007.
- [13] Y. S. Chen, X. S. Zhang and W. K. Yuan, "A preliminary study of pulsed high-voltage corona discharge plasma for the degradation of phenol in aqueous solution," *Acta Scientiae Circumstantiae*, Vol. 22, pp. 566–569, 2002.
- [14] Y. S. Chen, Y. S. Chen, Y. C. Dai, and W. K. Yuan, "Degradation of 4-chlorophenol in aqueous solution with pulsed high-voltage discharge plasma," *Journal of Chemical Industry and Engineering*, Vol. 9, pp. 1269–1273, 2003.
- [15] Y. S. Chen, Y. S. Chen, and Y. C. Dai, "Pulsed high-voltage discharge plasma for degradation of phenol in aqueous solution," *Separation and Purification Technology*, Vol. 34, pp. 5–12, 2004.
- [16] Y. J. Shen, L. C. Lei , X. W. Zhang, M. G. Zhou, and Y. Zhang, "Effect of various gases and chemical catalysts on phenol degradation pathways by pulsed electrical discharges," *Journal of Hazardous Materials*, Vol. 150, pp. 713–722, 2008.
- [17] P. Lukes, A. T. Appleton, and B. R. Locke, "Hydrogen peroxide and ozone formation in hybrid-gas-liquid electrical discharge reactors," *IEEE Transactions on Industry Applications*, Vol. 40, No. 1, pp. 60–67, 2004.
- [18] P. Lukes and B. R. Locke, "Plasmachemical oxidation processes in a hybrid gas-liquid electrical dischar-
- gereactor," *Physics D: Applied Physics*, Vol. 38, pp. 4074–4081, 2005.
- [19] P. Lukes and B. R. Locke, "Degradation of substituted phenols in a hybrid gas-liquid electrical discharge reactor," *Industrial & Engineering Chemistry Research*, Vol. 44, pp. 2921–2930, 2005.
- [20] T. Kuroki, K. Yoshida, and Watanabe, "Decomposition of trace phenol in solution using gas-liquid interface discharge," *Japanese Journal of Applied Physics Part 1-Regular Papers Brief Communications & Review Papers*, Vol. 45, pp. 4296–4300, 2006.
- [21] Y. Q. Mo, L. M. Pu, H. G. Liang, J. Zhao, Q. Zhang, J. Z. Gao, "Degradation of o-chlorophenol in aqueous solution by contact glow discharge electrolysis," *Journal of Gansu Agricultural University*, Vol. 40, 2005.
- [22] L. M. Pu, J. Z. Gao, W. Yang, Y. Li, J. Yu , and D. L. Huang, "Oxidative degradation of 4-chlorophenol in aqueous induced by plasma with submersed glow discharge electrolysis," *Plasma Science & Technology*, Vol. 75, 2005.
- [23] Q. F. Lu, J. Yu, J. Z. Gao, "Degradation of 2,4-dichlorophenol by using glow discharge electrolysis," *Journal of Hazardous Materials*, Vol. B136, pp. 526–531, 2006.
- [24] Y. J. Liu and X. Z. Jiang, "Phenol degradation by a nonpulsed diaphragm glow discharge in an aqueous solution," *Environmental Science & Technology*, Vol. 39, pp. 8512–8517, 2005.
- [25] L. Wang, X. Z. Jiang, and Y. J. Liu, "Degradation of bisphenol A and formation of hydrogen peroxide induced by glow discharge plasma in aqueous solutions," *Journal of Hazardous Materials*, Vol. 154, pp. 1106–1114, 2008.
- [26] A. Czenichowski, *Pure and Applied Chemistry*, Vol. 66, pp. 1301, 1994.
- [27] C. M. Du, J. H. Yan, X. D. Li, Z. Bo, X. D. Sun, and K. F. Cen, "Gas-liquid two phase gliding arc plasma for degradation of phenol in aqueous solution," *Journal of Engineering Thermophysics*, 2005.
- [28] C. M. Du, J. H. Yan, X. D. Li, K. F. Cen, M. J. Ni, Y. L. Wei, and B. G. Cheron, "Treatment of 4-chlorophenol solution by gas-liquid gliding arc discharge," *Proceedings of the CSEE*, Vol. 13, 2006.
- [29] J. H. Yan, C. M. Du, X. D. Li, et al., "Degradation of phenol in aqueous solutions by gas-liquid gliding arc discharges," *Plasma Chemistry and Plasma Processing*, Vol. 26, pp. 31–41, 2006.
- [30] C. M. Du, J. H. Yan, and B. G. Cheron, "Degradation of 4-chlorophenol using a gas-liquid gliding arc discharge plasma reactor," *Plasma Chemistry and Plasma Processing*, Vol. 27, pp. 635–646, 2007.
- [31] X. D. Sun, J. H. Yan, X. D. Li, C. M. Du, and J. L. Yang, "The study of circulating degradation of highly concentrated phenol wastewater by gas-liquid phase gliding arc discharge," *Energy Engineering*, Vol. 1, pp. 32–35, 2006.

- [32] Power Plasma Science, IEEE, Vol. 6, pp. 1138–1141, 2001.
- [33] D. R. Grymonpre, “An experimental and theoretical analysis of phenol degradation by Pulsed corona discharge,” The Florida State University, Doctor thesis, USA, 2001.
- [34] M. Dors, G. V. Nichipor, and J. Mizeraczyk, “Modeling of phenol decomposition induced by pulsed corona discharge in water,” Dielectric Liquids, IEEE International Conference, 2005.
- [35] W. F. L. M. Hoeben, “Pulsed corona-induced degradation of organic materials in water,” PhD thesis, Technische Universiteit Eindhoven, June 2000.
- [36] Y. N. Liu, J. H. Yan, X. D. Li, C. M. Du, and S. L. Dai, “Progress in research of application of Gl iding arc discharge to wastewater treatment,” High Voltage Engineering, Vol. 33, pp. 159–162, 2007.
- [37] D. R. Grymonpre, “An experimental and theoretical analysis of phenol degradation by Pulsed corona discharge,” The Florida State University, Doctor thesis, USA, 2001.
- [38] A. A. Joshi, B. R. Locke, P. Arce, and W. C. Finney, “Formation of hydroxyl radicals, hydrogen peroxide and aqueous electrons by pulsed streamer corona discharge in aqueous solution,” Journal of Hazardous Materials, Vol. 41, pp. 3–30, 1995.
- [39] NIST Chemical Kinetics Database, <http://kinetics.nist.gov/>
- [40] A. T. Sugiarto and M. Sato, “Pulsed plasma processing of organic compounds in aqueous solution,” Thin solid Films, Vol. 386, pp. 295–299, 2001.
- [41] C. R. Huang and H. Y. Shu, “The reaction kinetics, decomposition pathways and intermediate formations of phenol in ozonation,UV/O₂,and UV/H₂O₂ processes,” Journal of Hazardous Materials, Vol. 41, pp. 47–64, 1995.
- [42] D. R. Grymonpre, A. K. Sharma, W. C. A. Finney, and B. R. Locke, “The role of fentons reaction in aqueous phase pulsed streamer corona reactors,” Chemical Engineering Journal, Vol. 82, pp. 189–207, 2001.
- [43] E. Neyens and J. Baeyens, “A review of classic fentons peroxidation as an advanced oxidation technique.”, Journal of Hazardous Materials, Vol. 98, pp. 33–55, 2003.
- [44] L. Wang and X. Z. Jiang, “Unusual catalytic effects of iron salts on phenol degradation by glow discharge plasma in aqueous solution,” Journal of Hazardous Materials, Vol. 161, pp. 926–932, 2009.
- [45] D. R. Grymonpre , W. C. Finney, and B. R. Locke, “Aqueous-phase pulsed streamer corona reactor using suspended activated carbon particles for phenol oxidation: model-data comparison,” Chemical Engineering Science, Vol. 54, pp. 3095–3105, 1999.
- [46] D. R. Grymonpre, W. C. Finney, R. J. Clark, and B.R. Locke, “Suspended activated carbonparticles and ozone formation in aqueous-phase pulsed corona discharge reactors,” Industrial & Engineering Chemistry Research, Vol. 420, pp. 5117–5134, 2003.
- [47] P. Lukes, M. Clupek, P. Sunka, et al, “Degradation of phenol by underwater pulsed corona discharge in combination with TiO₂ photocatalysis,” Research on Chemical Intermediates, Vol. 31, 2004.
- [48] X. L. Hao, M. H. Zhou, and L. C. Lei, “Non-thermal plasma-induced photocatalytic degradation of 4-chlorophenol in water,” Journal of Hazardous Materials, Vol. 141, pp. 475–482, 2007.
- [49] H. J. Wang, J. Li, X. Quan, and Y. Wu, “Enhanced generation of oxidative species and phenol degradation in a discharge plasma system coupled with TiO₂ photocatalysis,” Applied Catalysis B: Environmental, Vol. 83, pp. 72–77, 2008.
- [50] M. J. Farre, M. I. Franch, S. Malato, J. Ayllon, J. Peral, and X. Domenech, Chemosphere, 2004.
- [51] L. Sanchez, J. Peral, and X. Domenech, Applied Catalysis B: Environmental, Vol. 19, pp. 59–65, 1998.
- [52] H. Tomizawa and M. Tezuka, “ Kinetics and mechanism of the organic degradation in aqueous solution irradiated with gaseous plasma,” Plasma Chemistry and Plasma Processing, Vol. 27, 2007.
- [53] L. C. Lei, Y. Zhang, X. W. Zhang, Y. X. Du, Q. Z. Dai, and S. Han, “Degradation performance of 4-chlorophenol as a typical organic pollutant by a pulsed high voltage discharge system,” Applied Chemistry, Vol. 46, pp. 5469–5477, 2007.
- [54] Y. Z. Wen, X. Z. Jiang, and W. P. Liu, “Degradation of 4-Chlorophenol in Aqueous Solution by high-voltage pulsed discharge-ozone technology,” Environmental Science, Vol. 23, pp. 73–76, 2002.
- [55] A. G. Bubnov, E. Y. Burova, V. I. Grinevich, et al., “Comparative actions of NiO and TiO₂ catalysts on the destruction of phenol and its derivatives in a dielectric barrier discharge,” Plasma Chemistry and Plasma Processing, Vol. 27, pp. 177–187, 2007.

Water Quality Analysis of the Songhua River Basin Using Multivariate Techniques

Yang LI¹, Linyu XU^{1*}, Shun LI²

¹*State Key Laboratory of Water Environment Simulation, School of environment, Beijing Normal University, Beijing, China*

²*College of resources science & technology, Beijing Normal University, Beijing, China*

E-mail: xly@bnu.edu.cn

Received November 29, 2008; revised January 13, 2009; accepted February 14, 2009

Abstract

Multivariate statistical techniques, including cluster analysis (CA), principal component analysis (PCA), factor analysis (FA) and discriminant analysis (DA), were used to evaluate temporal and spatial variations and to interpret a large and complex water quality data sets collected from the Songhua River Basin. The data sets, which contained 14 parameters, were generated during the 7-year (1998-2004) monitoring program at 14 different sites along the rivers. Three significant sampling locations (less polluted sites, moderately polluted sites and highly polluted sites) were detected by CA method, and five latent factors (organic, inorganic, petrochemical, physicochemical, and heavy metals) were identified by PCA and FA methods. The results of DA showed only five parameters (temperature, pH, dissolved oxygen, ammonia nitrogen, and nitrate nitrogen) and eight parameters (temperature, pH, dissolved oxygen, biochemical oxygen demand, ammonia nitrogen, nitrate nitrogen, volatile phenols and total arsenic) were necessarily in temporal and spatial variations analysis, respectively. Furthermore, this study revealed the major causes of water quality deterioration were related to inflow of effluent from domestic and industrial wastewater disposal.

Keywords: Water Quality, Multivariate Statistical Analysis, the Songhua River Basin, the North-Eastern Region Of China

1. Introduction

Rivers are among the most vulnerable water bodies to pollution because of their role in carrying municipal and industrial wastes and run-offs from agricultural lands in their vast drainage basins. Detailed hydrochemical research is needed to evaluate the different processes and mechanisms involved in polluting water [1]. Furthermore, due to temporal and spatial variations in water qualities, monitoring programs that involve a large number of physicochemical parameters and frequent water samplings at various sites are mandatory to produce reliable estimated topographies of surface water qualities [2]. The results are usually compiled into a large data matrix, which requires sophisticated data interpretations [3].

A variety of mathematical assessment models, including water quality index models [4], structurally dynamic

models [5], fuzzy synthetic evaluation approach [6], generalized logistic models [7], Bayesian models [8], etc, have been used to study the physicochemical interrelationships and processes. However, these methods aren't useful for large-scale and long-term monitoring database. Because of the limitations of these methods, the multivariate statistical analysis methods have the advantage of explaining complex water quality monitoring data to get a better understanding of the ecological status of the studied systems [9]. The multivariate statistical analysis has been successfully applied in a number of hydrogeochemical studies [10-13]. All the studies show that multivariate statistical analysis can help to interpret the complex data sets and assess the water quality, and it is useful in verifying temporal and spatial variations caused by natural and anthropogenic factors linked to seasonality.

In the study, the large database analyzed, was obtained during a 7-year (1998-2004) monitoring program (5,320

*Corresponding author.

observations) of the Songhua River Basin. It was subjected to different multivariate statistical techniques (cluster analysis (CA), principal components analysis (PCA), factor analysis (FA) and discriminant analysis (DA)) with a view to extract information about the similarities or dissimilarities among the sampling sites. Latent factors in river water quality were identified and the water quality variables responsible for temporal and spatial variations explained the structure of the data sets. Further, the hidden factors revealed the influence of possible sources on the water quality parameters and pollution levels of sampling stations in the Songhua River Basin.

2. Materials and Methods

2.1. Study Area

The Songhua River Basin is one of the biggest river basins in China, which consists of Nen River, Second Songhua River, and Songhua River. The basin area is 556,800 km² and the main stream spans 2,308 km long, in the north-eastern region of the China (Figure 1). The rivers are the major freshwater source for industries, farms, and millions of residents along their expansions [14,15]. The area of the Songhua River Basin is China's largest aggregate of oil shale, borax and steatite, accounting for more than half of the nation's total reserve. The region's total population amounts are 62 million, 50% of which live in urban areas. At the end of 2004, the

rate of urban sewage treatment was less than 40% in cities, such as Harbin, Changchun, Daqing and Mudanjiang. At 2006, the average sewage treatment of the whole basin is only about 15% [15].

2.2. Monitoring Sites

To accurately represent the water quality of the river systems, a sampling strategy was designed to cover a wide range of determinants at the key sites. In the present study, total 14 sampling stations (Figure 1). The location information of the 14 monitoring sites is showed in Table 1.

2.3. Data Preparation

The data sets of the 14 water quality monitoring stations, which comprised 14 water quality parameters monitored quarterly over 7 years (1998-2004), were obtained from the Ministry of Environmental Protection (MEP) of China. Although there were more than 20 water quality parameters available, only 14 parameters were selected because of their continuity in measurement at all selected water quality monitoring stations. The selected water quality parameters included temperature, pH, suspended solids, dissolved oxygen, chemical oxygen demand (manganese), biochemical oxygen demand after 5 days, ammonia nitrogen, nitrate nitrogen, volatile phenol, petroleum oil, total cyanide, total arsenic, total mercury and chromium VI. The water quality parameters with units and basic statistics are summarized in Table 2.

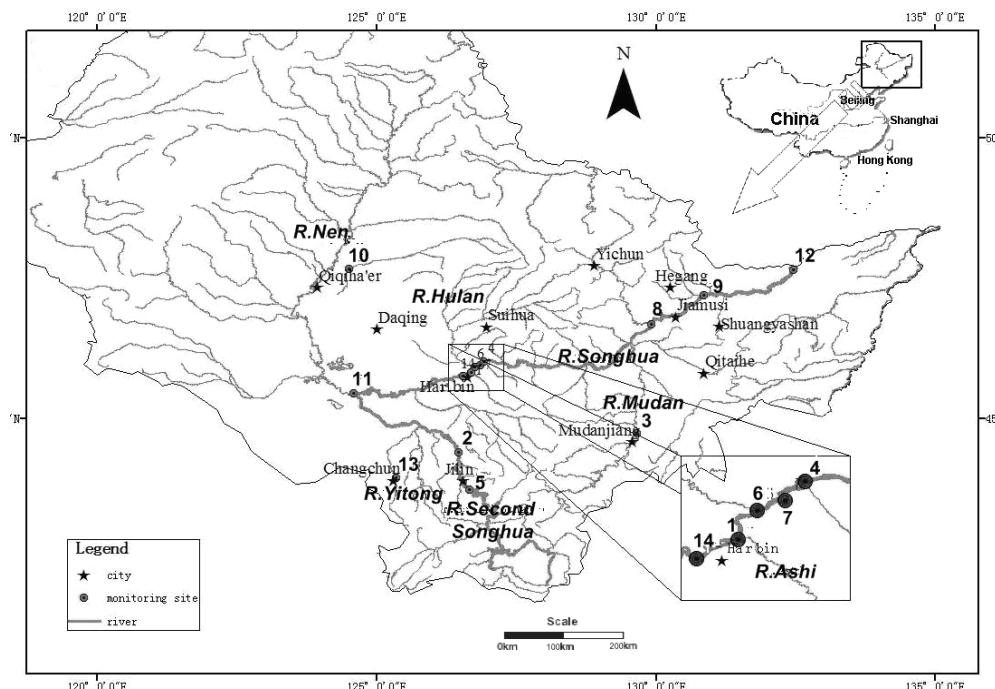


Figure 1. Map of study area and surface water quality monitoring stations.

Table 1. Basic situation of the 14 monitoring stations.

Code	Station	River	City
1	Ashihekounei	R. Ashi	Harbin
2	Baiqi	R. second Songhua	Jilin
3	Chaihetiluqiao	R. Mudan	Mudanjiang
4	Dadingzishan	R. Songhua	Harbin
5	Fengman	R. second Songhua	Jilin
6	Hulanhekounei	R. Hulan	Harbin
7	Hulanhekouxia	R. Songhua	Harbin
8	Jiamusishang	R. Songhua	Jiamusi
9	Jiangnantun	R. Songhua	Jiamusi
10	Liuyuan	R. Nen	Qiqihaer
11	Nenjianghekounei	R. Nen	Zhaoyuan
12	Tongjiang	R. Songhua	Tongjiang
13	Yangjiaweizi	R. Yitong	Changchun
14	Zhushuntun	R. Songhua	Harbin

Table 2. Water quality parameters and summary basic statistics of the Songhua River Basin^{a,b}.

Parameters	Abbreviation	Minimum	Maximum	Mean	Stand. dev.
Temperature	WT	-1.000	26.000	11.770	8.901
pH	pH	4.950	9.300	7.493	0.461
Suspended solids	SS	0.000	1031.700	69.435	106.008
Dissolved oxygen	DO	0.000	14.000	6.948	3.069
Chemical oxygen demand (Mn)	CODMn	0.000	189.000	9.140	11.235
Biochemical oxygen demand after 5 days	BOD5	0.000	302.000	9.590	21.611
Ammonia nitrogen	NH4-N	0.000	22.339	1.111	3.335
Nitrate nitrogen	NO3-N	0.000	2.963	0.563	0.474
Volatile Phenols	VP	0.000	5.695	0.032	0.317
Petroleum oil	Oil	0.000	6.890	0.249	0.839
Total cyanide	CN	0.000	1.07E-01	3.14E-03	8.73E-03
Total arsenic	As	0.000	5.00E-02	3.35E-03	5.73E-03
Total mercury	Hg	0.000	1.23E-03	5.03E-05	1.24E-04
Chromium VI	Cr(VI)	0.000	0.046	0.002	0.003

^azero means no detected. ^bconcentration units in mgL⁻¹; temperature units in Celsius.

The K-S statistics were used to test the goodness-of-fit of the data to log-normal distribution. According to the K-S test, all the variables are log-normally distributed with 95% or higher confidence. Similarly, to examine the suitability of the data for principal component analysis/factor analysis, KMO and Bartlett's test were performed, which also indicates that there are significant relationships among variables.

2.4. Multivariate Statistical Methods

The multivariate analyses of the river water quality data sets were performed through CA, PCA, FA and DA. CA, PCA and FA were applied to experimental data, standardized through z-scale transformation to avoid misclassification due to wide differences in data dimensionality [16–18], whereas DA was applied to raw data [19, 20].

Then, with Equation (1) and Equation (2) the authors calculated the component scores (CS) and composite factor score (CFS) of each sampling station. The values of CFS reflected the pollution levels of sampling stations whereas the CS of each site revealed the sources of pollutants.

$$f_i = \sum_{k=1}^{14} \beta_{ik} \chi_k \quad (i = 1, 2, \dots, 5) \quad (1)$$

$$F = \sum_{i=1}^5 \eta_i f_i \quad (2)$$

where f is the component score of sampling station, F the composite factor score, β the factor score (get from FA), χ the standardized measured value of a variable, η the % variance of the principal component (get from PCA), i the component number, k the variable number.

In this study, CA was performed on the normalized data sets by means of the Ward's method, using squared Euclidean distances as a measure of similarity. The spatial variability of water quality in the whole river basin was determined by CA, using the linkage distance ($D_{\text{link}}/D_{\text{max}}$), which represented the quotient between the linkage distances for a particular case divided by the maximal linkage distance. The quotient was then multiplied by 100 to standardize the linkage distance represented on the y-axis.

PCA is designed to transform the original variables into new, uncorrelated variables (axes), called the principal components, which are linear combinations of the original variables. The new axes lie along the directions of maximum variance. FA follows the PCA. The main purpose of the FA is to extract a lower dimensional linear structure from the data sets. It further reduces the contribution of less significant variables obtained from

the PCA. And the new group of variables known as vari-factors (VFs) is extracted through rotating the axis defined by the PCA.

The DA was applied to raw data by using the Bayesian model to construct the discriminant functions to evaluate both the temporal and spatial variations in river water quality.

All mathematical and statistical computations were carried out using Microsoft Office Excel 2003 and SPSS 11.5.

3. Results and Discussion

3.1. Site Similarity

The result of CA is shown in Figure 2. All the 14 sampling sites on the rivers were grouped into three statistically significant clusters at $(D_{\text{link}}/D_{\text{max}}) \times 100 < 60$: Cluster 1 (site 3, site 4, site 6, site 7, site 8, site 9, site 11, site 14), cluster 2 (site 2, site 5, site 10, site 12) and cluster 3 (site 1 and site 13). These clusters of sampling stations indicated that each cluster had a water quality of its own which was different from the other clusters. The CA results revealed that this approach was useful in offering reliable classifications of surface waters in the whole region and optimizing the design of a future spatial sampling strategy. Thus it can be said that for quick spatial assessments of water quality, one site sampled in each cluster is sufficient to determine the water quality of the entire network.

3.2. Data Structure Determination and Source Identification

The PCA and FA were performed on the normalized [16] data sets (14 variables). Five principal components (PC) were obtained with Eigenvalues > 1 summing more than 85% of the total variance in the water data sets (Table 3).

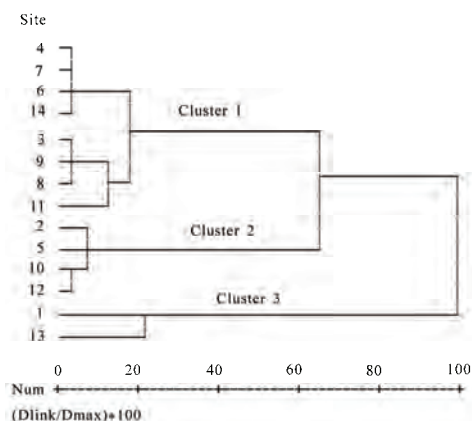


Figure 2. Dendrogram showing clustering of sampling sites.

The first component (PC1), accounting for 33.3% of the total variance in the data sets of the river water, was correlated with COD_{Mn}, BOD₅ and VP to represent “organic” pollution [8,10,11]. This “organic” factor can be interpreted as influences from point sources such as discharges from wastewater treatment plants, domestic wastewater and industrial effluents. The same interpretation was also suggested by the other studies [21,22]. The second component (PC2) that accounted for 21.01% of the total variance represented the “inorganic” parameters, which included SS, NO₃-N, AS and CN in the solution and demonstrated similar behaviors as in the river water samples [19,20]. The third component of the total variance (PC3, 15.29%) had a strong positive loading on NH₄-N and Oil and a moderate negative loading on DO. It was, therefore, a group of “petrochemical” source pol-

lution indicator parameters [18]. The fourth component (PC4) associated to 9.89% of the total variance, was weighted on WT and pH and represented the “physico-chemical” source of variability. The former study also supports the idea [23]. Finally, the fifth component (PC5) of PCA and FA that had strong positive loadings on Hg and Cr(VI) presented the last 7.18% of the total variation. The authors reckoned that PC5 could be associated with “heavy metals” pollution from metal activities and industrial effluents. The same conclusion was drawn by at least one other research [24,25].

Therefore, as the “organic” factor (PC1) has the largest proportion of the total variance, we have come to the conclusion that anthropogenic pollution mainly due to the domestic and industrial wastewater disposal, was the major source of river water contamination.

Table 3. Varimax rotated factor matrix for the whole data sets^a.

Parameter	PC				
	1	2	3	4	5
WT	-0.122	0.071	0.069	0.815	0.184
pH	0.121	0.047	-0.183	0.725	-0.166
SS	0.091	0.693	0.02	0.202	0.094
DO	-0.372	-0.324	-0.546	0.099	-0.053
CODMn	0.870	0.354	0.098	0.007	-0.009
BOD	0.885	0.135	0.31	-0.014	-0.008
NH ₄ -N	0.135	-0.09	0.847	-0.028	-0.065
NO ₃ -N	-0.002	0.793	-0.126	0.004	-0.24
VP	0.924	0.003	-0.134	0.016	0.022
Oil	0.092	0.331	0.807	-0.046	-0.026
CN	0.125	0.753	0.21	-0.02	0.013
As	0.016	0.806	0.138	-0.118	0.072
Hg	0.083	-0.128	0.281	0.054	0.736
Cr(VI)	-0.004	0.052	-0.063	0.033	0.942
% variance	33.30	21.08	15.29	9.89	7.18
Cumulative % variance	33.30	54.38	69.66	79.56	86.74

^a Significant factor loadings are bold faced.

Table 4. Sampling stations score matrix.

Site	PC					CFS
	1	2	3	4	5	
1	4.152	1.303	2.181	0.375	0.941	2.095
2	-0.900	-0.902	-1.014	-1.010	-0.754	-0.799
3	-0.446	-0.122	-0.664	0.302	-0.200	-0.260
4	-0.582	-0.064	-0.892	0.455	-0.371	-0.325
5	-1.118	-1.378	-1.200	-1.240	-0.649	-1.015
6	0.342	0.385	0.012	0.467	0.067	0.248
7	-0.535	-0.049	-0.802	0.466	-0.297	-0.286
8	-0.583	-0.082	-0.536	0.216	-0.249	-0.290
9	-0.504	-0.348	-0.527	0.457	-0.245	-0.294
10	-1.119	-1.661	-1.272	0.115	-0.243	-0.923
11	-0.736	-1.053	-0.338	0.283	1.428	-0.388
12	-0.914	-1.175	-0.614	-0.667	0.551	-0.672
13	3.693	5.104	6.976	-0.809	0.384	3.320
14	-0.875	-0.069	-1.342	0.274	-0.524	-0.522

3.3. Pollution Level Analysis

With Equation (1) and Equation (2) the authors calculated the component score (CS) and composite factor score (CFS) of each sampling station. The values of CFS reflected the pollution levels of sampling stations whereas the CS of each site revealed the sources of pollutants. The results of the 14 sampling stations are presented in Table 4, which showed high pollution levels at site 1 and 13, especially site 13.

Water quality of site 13 was rated as "heavily polluted" due to pollutions from domestic wastewater, wastewater treatment plants, and from industrial effluents located in the city of Changchun. Compared to the upstream samples at station 14, severe pollution seen at site 1 indicated rapid deterioration of water quality while the Songhua River flowed through the city of Harbin. Both of the cities are big cities, and whose municipal sewage and industrial waste water not meeting the discharge standards [15,26,27] were found to be the immediate cause.

Site 4, site 6 and site 7 were situated at the lower peripheries of the city of Harbin. The pollution levels of

these stations were moderate. Site 11 had a high value of PC5 which pointed heavy metals such as Hg and Cr(VI) in its samples. This station placed at the Nen River estuary, so the Nen River was a source of the heavy metal pollution of the Songhua River [28]. In the rivers network, site 3, site 8 and Site 9 were located in the medium-sized cities (Mudanjiang and Jiamusi). These sites also had medium values of CFS. According to the CFS values, site 2, site 5, site 10 and site 12 of cluster 2 showed low pollution levels. Let's recall the Figure 1, site 2, 5 and 10 were located at upstream whereas site 12 was at the most downstream location of the rivers. This observation that site 12 demonstrated a low degree of pollution may suggest a strong self purifying and assimilating capability of the rivers. Meanwhile, the above results also showed that the big cities had great impacts on the water quality of the Songhua River Basin.

Referring to the result of the CA technique (Figure 1), cluster 1 (sampling stations 3, 4, 6-9, 11, 14), Cluster 2 (sampling stations 2, 5, 10, 12) and cluster 3 (sampling stations 1, 13) corresponded to relatively moderate pollution (MP), low pollution (LP) and high pollution (HP) regions, respectively.

Table 5. Classification functions for discriminant analysis of temporal variations.

Parameter	Coefficient			
	1st Quarter	2nd Quarter	3rd Quarter	4th Quarter
WT	-0.613	0.078	0.351	-0.178
pH	38.72	38.62	37.32	39.379
DO	0.564	1.061	0.954	1.088
NH ₄ -N	0.681	0.891	0.849	0.89
NO ₃ -N	-1.919	-1.142	-0.109	-1.35
(Constant)	-143.902	-152.634	-147.697	-155.293

Table 6. Classification matrix for discriminant analysis of temporal variations.

Quarter	% Correct	Quarter assigned by DA			
		1st	2nd	3rd	4th
1st	90.4	85	0	0	9
2nd	70.1	6	68	16	7
3rd	86.3	4	9	82	0
4th	73.5	7	16	3	72
Total	79.9	102	93	101	88

3.4. Temporal and Spatial Variations in River Water Quality

A total of 5,320 observations were categorized into four known groups (1st Quarter: January 1–March 31, 2nd Quarter: April 1–June 30, 3rd Quarter: July 1–September 30, and 4th Quarter: October 1–December 31) and analyzed statistically using DA technique. The discriminant functions (DFs) and classification matrices (CMs) obtained from the Bayesian model of DA are listed in Tables 5 and 6, respectively. The DA gave the CMs with 79.9% correct assignations using only five discriminant parameters. Thus, the temporal DA results suggested that WT, pH, DO, NH₄-N and NO₃-N were the most significant parameters to discriminate between the four different quarters, which means that these five parameters account for most of the expected temporal variations in the river water quality.

Box and whisker plots of the selected parameters showing quarterly trends are given in Figure 3. The variation of water temperatures (Figure 3(a)) showed a clear-cut seasonal effect. The water pH values (Figure 3(b)) are higher in 2nd Quarter and Quarter 4th compared to 1st Quarter and 3rd Quarter. The average con-

centration of DO (Figure 3(c)) was observed to be lowest in 1st Quarter when parts of the river were frozen over. During 2nd Quarter to 4th Quarter, the inverse relationship between temperature and DO was a natural process because warmer water became more easily saturated with oxygen and it can hold less DO. A decrease in average NH₄-N concentration (Figure 3(d)) from 1st Quarter to 3rd Quarter followed by an increase in 4th Quarter was observed. Similar temporal variations in concentration of NH₄-N were also reported by [29]. The average concentration of NO₃-N (Figure 3(f)) was highest in 3rd Quarter. It should be attributed to the influences from non-point sources such as agricultural runoff and atmospheric deposition. This fact was also supported by other studies [21,29].

Spatial DA was performed with the raw data after dividing the whole data sets into three spatial groups (LP region, MP region and HP region) obtained through the CA technique. The station (clustered) was the grouping (dependent) variable, while all the measured parameters constituted the independent variables. The DFs and CMs obtained from the Bayesian model of DA are listed in Tables 7 and 8, respectively. The DA gave the CMs with 78.6% correct assignations using only eight discriminant parameters. Thus, the result showed that only WT, pH,

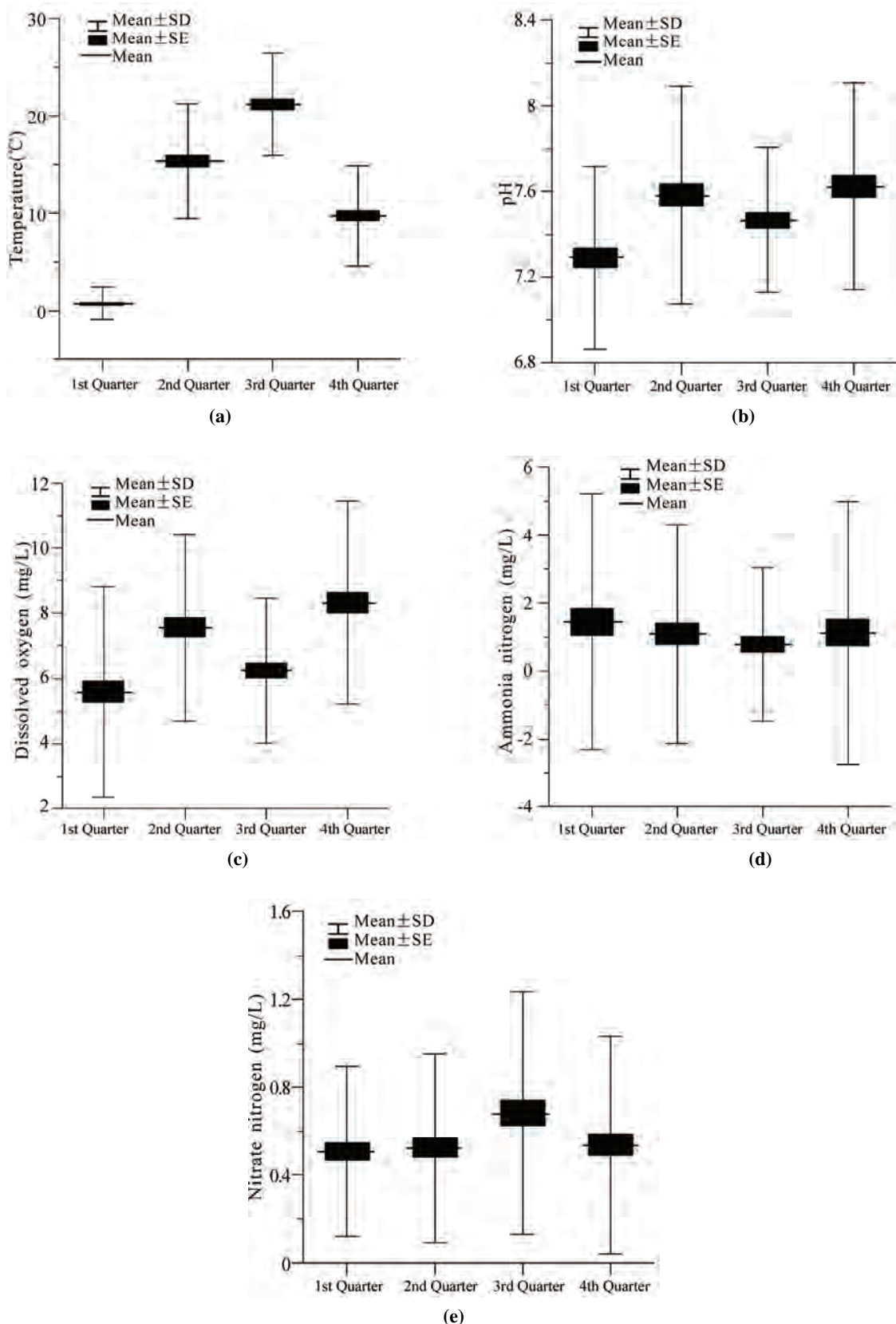


Figure 3. Temporal variations: (a) WT, (b) pH, (c) DO, (d) NH₄-N, (e) NO₃-N in water quality of the Songhua River Basin.

Table 7. Classification functions for discriminant analysis of spatial variations.

Parameter	Site		
	LP coefficient	MP coefficient	HP coefficient
WT	-0.191	-0.134	-0.057
pH	41.194	43.78	44.74
DO	-0.584	-1.075	-1.986
BOD	0.058	0.076	0.282
NH ₄ -N	0.604	0.724	1.561
NO ₃ -N	0.981	2.253	3.436
VP	-10.647	-11.866	-17.763
As	4.877	9.99	333.564
(Constant)	-147.292	-163.931	-177.389

Table 8. Classification matrix for discriminant analysis of spatial variations.

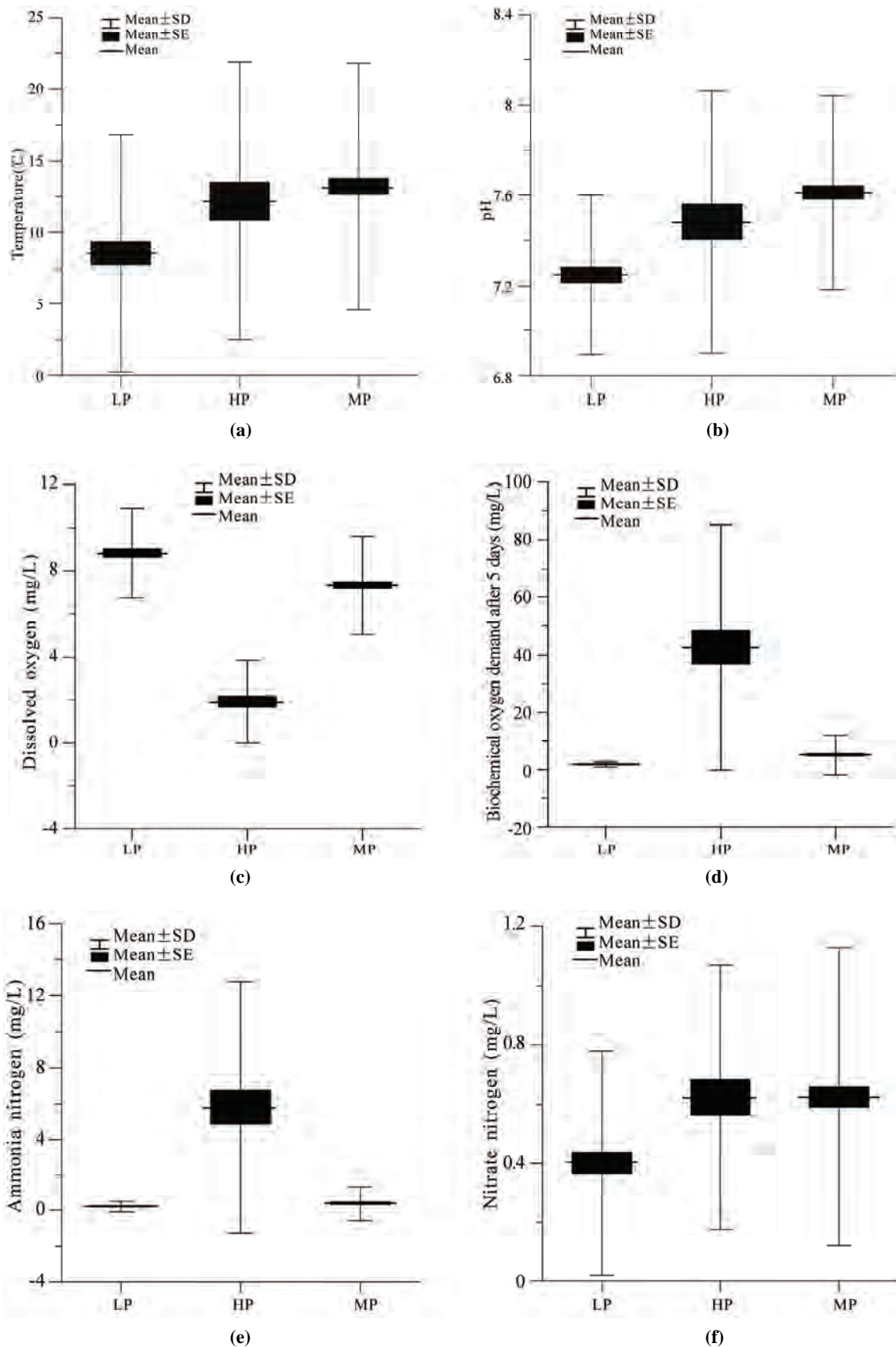
Monitoring Region	% Correct	Region assigned by DA		
		LP	MP	HP
LP	75	168	51	5
MP	83.8	17	88	0
HP	83.6	9	0	46
Total	78.6	194	139	51

DO, BOD₅, NH₄-N, NO₃-N, VP and As were the discriminate parameters in space. And there were significant differences between these three categories (LP, MP and HP), which were expressed in terms of eight differentiating parameters. Hence, DA made a considerable data reduction.

Box and whisker plots of discriminating parameters identified by spatial DA were constructed to evaluate different patterns associated with spatial variations in river water quality (Figure 4). The river water temperatures (Figure 4(a)) were the highest at the MP sites as discharges of municipal wastewater merged. The water pH values (Figure 4(b)) were highest in the MP region and lowest in the LP region. The trends for DO (Figure 4(c)), BOD₅ (Figure 4(d)) and NH₄-N (Figure 4(e)) suggested a large load of dissolved organic matter at the HP sites where domestic wastewater from treatment plants and industrial effluents were injected. The MP sites had a high average concentration of NO₃-N (Figure 4(f)), which should be attributed to the use of nitrogenous fertilizers in orchard and agricultural areas [15]. Similar trends of spatial variations observed for VP (Figure 4(g)) and As (Figure 4(h)) suggested vast difference in pollution load and sources in regions of the river.

4. Conclusions

In this study, different multivariate statistical techniques were used to evaluate variations in surface water quality of the Songhua River Basin. CA grouped the 14 sampling stations into three clusters of similar water quality characteristics. PCA and FA helped to identify that the parameters responsible for water quality variations were mainly related to trace organic, inorganic, petrochemical, physiochemical and heavy metals, and the principal components revealed the Songhua River Basin water quality was mainly controlled by domestic wastewater and industrial discharges. DA rendered an important data reduction, as it used only five parameters (WT, pH, DO, NH₄-N and NO₃-N) affording more than 79% correct assignations in temporal analysis, while eight parameters (WT, pH, DO, BOD₅, NH₄-N, NO₃-N, VP and As) affording more than 78% right assignations in spatial analysis. Therefore, DA showed a reduction in the dimensionality of the large data sets, by delineating a few indicator parameters of the water quality. Consequently, this study illustrated the usefulness of multivariate statistical techniques for interpretation of complex data sets, identification of pollution sources, understanding tem-



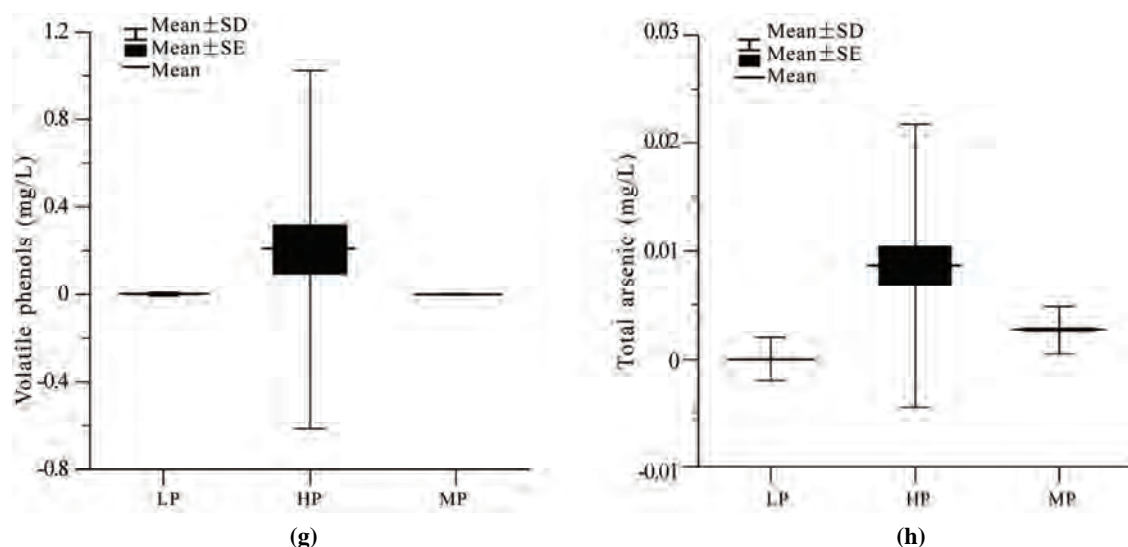


Figure 4. Spatial variations: (a) WT, (b) pH, (c) DO, (d) BOD, (e) NH₄-N, (f) NO₃-N, (g) VP, (h) As in water quality of the Songhua River Basin.

poral and spatial variations in water quality, analysis of pollution levels and design of monitoring strategy for effective river water management.

7. Acknowledgements

The research was supported by the National Natural Science Foundation of China (No. 40871262) and by National Science and Technology Project (No. 2007BAC08B03). The authors sincerely thank Bing Chen, Jian-su Mao *et al.* from Beijing Normal University and Bo Zhang, Qiang Sun *et al.* from Ministry of Environmental Protection of China for their suggestions and help.

8. References

- [1] B. A. Helena, M. Vega, E. Barrado, R. Pardo, and L. Fernandez, "A case of hydrochemical characterization of an alluvial aquifer influenced by human activities," *Water, Air, and Soil Pollution*, Vol. 112, No. 3, pp. 365–387, 1999.
- [2] W. Dixon and B. Chiswell, "Review of aquatic monitoring program design," *Water Research*, Vol. 30, No. 9, pp. 1935–1948, 1996.
- [3] D. Chapman, "Water quality assessment," Chapman & Hall Press, London, 1992.
- [4] S. B. Jonnalagadda and G. Mhere, "Water quality of the Odzi river in the eastern highlands of Zimbabwe," *Water Research*, Vol. 35, No. 10, pp. 2371–2376, 2001.
- [5] J. Zhang, S. E. Jorgensen, C. O. Tan, and M. Beklioglu, "A structurally dynamic modelling—Lake Mogan, Turkey as a case study," *Ecological Modelling*, Vol. 164, No. 2, pp. 103–120, 2003.
- [6] Y. T. Liou and S. L. Lo, "A fuzzy index model for trophic status evaluation of reservoir waters," *Water Research*, Vol. 39, No. 7, pp. 1415–1423, 2003.
- [7] C. O. Tan and M. Beklioglu, "Catastrophic-like shifts in shallow Turkish lakes: A modeling approach," *Ecological Modelling*, Vol. 183, No. 4, pp. 425–434, 2005.
- [8] M. E. Borsuk and C. A. Stow, "Bayesian parameter estimation in a mixed-order model of BOD decay," *Water Research*, Vol. 34, No. 6, pp. 1830–1836, 2000.
- [9] M. Vega, R. Pardo, E. Barrado, and L. Debán, "Assessment of seasonal and polluting effects on the quality of river water by exploratory data analysis," *Water Research*, Vol. 32, No. 12, pp. 3581–3592, 1998.
- [10] V. Simeonov, J. A. Stratigis, C. Samara, G. Zachariadis, D. Voutsas, A. Anthemidis, M. Sofoniou, and T. Kouimtzis, "Assessment of the surface water quality in Northern Greece," *Water Research*, Vol. 37, No. 17, pp. 4119–4124, 2003.
- [11] K. P. Singh, A. Malik, and S. Sinha, "Water quality assessment and apportionment of pollution sources of Gomti river (India) using multivariate statistical techniques: A case study," *Analytica Chimica Acta*, Vol. 538, No. 1–2, pp. 355–374, 2005.
- [12] T. Kowalkowska, R. Zbytniewska, J. Szpejnbab, and B. Buszewski, "Application of chemometrics in river water classification," *Water Research*, Vol. 40, No. 4, pp. 744–752, 2006.
- [13] H. Boyacioglu, "Water pollution sources assessment by multivariate statistical methods in the Tahtali Basin, Turkey," *Environmental Geology*, Vol. 54, No. 2, pp. 275–282, 2008.

- [14] L. L. Ren, M. R. Wang, C. H. Li, and W. Zhang, "Impacts of human activity on river runoff in the northern area of China," *Journal of Hydrology*, Vol. 261, No. 3, pp. 204–217, 2002.
- [15] Ministry of Environmental Protection of China, "Planning of comprehensive water pollution control the Songhua River Basin," 2006. <http://wirmc.sepa.gov.cn/info/hbdxj/200612/W020061207298075130105.pdf>.
- [16] D. A. Wunderlin, M. P. Diaz, M. V. Ame, S. F. Pesce, A. C. Hued, and M. A. Bistoni, "Pattern recognition techniques for the evaluation of spatial and temporal variations in water quality. A case study: Suquia river basin (Cordoba, Argentina)," *Water Research*, Vol. 35, No. 12, pp. 2881–2894, 2001.
- [17] S. A. A. Wahab, C. S. Bakheit, and S. M. A. Alawi, "Principal component and multiple regression analysis in modelling of ground-level ozone and factors affecting its concentrations," *Environmental Modelling & Software*, Vol. 20, No. 10, pp. 1263–1271, 2005.
- [18] K. P. Singh, A. Malik, S. Sinha, D. Mohan, and S. Sinha, "Chemometric analysis of groundwater quality data of alluvial aquifer of Gangetic plain, North India," *Analytica Chimica Acta*, Vol. 550, No. 1, pp. 82–91, 2005.
- [19] C. W. Liu, K. H. Lin, and Y. M. Kuo, "Application of factor analysis in the assessment of groundwater quality in a Blackfoot disease area in Taiwan," *Science of the Total Environment*, Vol. 313, No. 1, pp. 77–89, 2003.
- [20] P. George, D. Gerasimoula, and L. Nicolaos, "A long-term study of temporal hydrochemical data in a shallow lake using multivariate statistical techniques," *Ecological Modelling*, Vol. 193 No. 3, pp. 759–776, 2006.
- [21] D. H. Wang, Y. Wang, and Z. Lin, "The control and damage of organic pollutant in Songhua River to the ecological environment," *Environmental Science and Management*, Vol. 32, No. 6, pp. 67–69, 2007.
- [22] Y. P. Liu, L. H. Wang, W. Liu, and Q. B. Liu, "Research of organic pollution's character in Songhua River," *Environmental Science and Management*, Vol. 31, No. 3, pp. 73–75, 2006.
- [23] Q. L. Yang and T. Ma, "Water quality analysis and forecast of the Songhua River (Harbin)," *Heilongjiang Science and Technology of Water Conservancy*, Vol. 34, No. 1, pp. 71–74, 2006.
- [24] L. M. Shen, C. K. Zhang, and H. K. Wang, "Water quality analysis of the Songhua River," *Heilongjiang Science and Technology of Water Conservancy*, Vol. 35, No. 2, pp. 116–117, 2007.
- [25] S. H. Guo, X. L. Wang, Y. Li, J. J. Chen, and J. C. Yang, "Investigation on Fe, Mn, Zn, Cu, Pb and Cd fractions in the natural surface coating samples and surficial sediments in the Songhua River, China". *Journal of Environmental Sciences*, Vol. 18, No. 6, pp. 1193–1198, 2006.
- [26] X. Q. Li, J. W. Zhang, Q. J. Wang, H. F. Zhang, and N. Qiu, "Analysis of mechanism of water purification by nature and strategy of protection of water environment in Songhua River through Harbin city," *Urban Environment & Urban Ecology*, Vol. 16, No. 6, pp. 233–235, 2003.
- [27] J. R. Liu, H. W. Dong, X. L. Tang, X. R. Sun, X. H. Han, B. Q. Chen, C. H. Sun, and B. F. Yang, "Genotoxicity of water from the Songhua River, China, in 1994–1995 and 2002–2003: Potential risks for human health," *Environmental Pollution*, Vol. 157, No. 2, pp. 357–364, 2009.
- [28] S. K. Jiang and H. Liu, "Analysis for the present situation and development trend of the water quality in the downstream of Nenjiang River," *Jilin Water Resources*, Vol. 265, No. 9, pp. 1–2, 2004.
- [29] W. D. Yang and H. L. Jiang, "Cause analysis and control measure of water pollution in zhaoyuan section of Songhua River," *Environmental Science and Management*, Vol. 32, No. 7, pp. 61–63, 2007.

Modeling and Control of pH in Pulp and Paper Wastewater Treatment Process

Jiayu KANG, Mengxiao WANG, Zhongjun XIAO

Shannxi University of Science & Technology, Xi'an, China

Email: kangjiayu@sust.edu.cn

Received March 24, 2009; revised April 12, 2009; accepted April 16, 2009

Abstract

Pulp and paper industry is responsible for large discharge of highly polluted effluents, which often be treated by biological treatment process. For biological treatment system, pH is an important environmental factor that can influence the activity of microorganisms. In general, the optimal pH for aerobic processes is around neutral pH (7~7.8) and for the anaerobic process is between 6.8~7.2. The control of pH is a difficult link in the biological treatment system due to its nonlinearity and large time-delay. Aiming at the difficult point in the pH control of the biological wastewater treatment system, a mathematical model of pH control is established in the essay. On this basis, a traditional PID control and a cascade control are adopted to carry out simulation and comparison with MATLAB. The results show that the cascade control has better comprehensive effect in terms of response speed, stability and disturbance resistance.

Keywords: Biological Treatment, pH, MATLAB, Cascade Control

1. Introduction

Pulp and paper industry is the greatest industrial polluter in terms of wastewater volumes and organic discharges. The general characteristics of the pulp and paper industry effluent can be listed as: 1) high lignin content, 2) high absorbable organic halide concentration, 3) color, 4) low biodegradability which is indicated by their high chemical oxygen demand to biochemical oxygen demand ratios, and 5) potential toxicity problems.

The typical treatment processes for pulp and paper effluents are chemical precipitation, lagooning, activated sludge, and anaerobic treatment. It should be mentioned that the liquors from alkaline pulping, wood resins, and tannins are potentially toxic to methane bacteria. Moreover, the degradation of lignin by the anaerobic consortium is limited to the low molecular weight fraction. Until now aerobic treatment systems are the most widely used method to treat effluents from pulp plants. However when the economic concerns and the rate of treatment are considered, anaerobic treatment is an alternative that must be considered [1].

The anaerobic process has been successfully applied in the treatment of nontoxic and easily biodegradable wastewaters from pulp and paper plants, such as the effluents from mechanical pulping, from paper recycling and from evaporation condensates. In fact anaerobic reactor followed by aerobic reactor is more successful at reducing toxicity [2]. Reductive dechlorination may occur in anaerobic stage and produce less chlorinated organics. These organics may be further biotransformed in conventional aerobic stage.

Biological treatment such as aerobic and anaerobic process is indisputably the most effective, economical way used for treating pulp and paper effluents [2]. In biological treatment living organisms are used for purifying waste, which can be solid, liquid or gas. The substance that is degraded acts as a source of building blocks and/or energy source for the microorganisms so they can fulfill their goal in life, which is to multiply.

There are a lot of factors that influence the well being of microorganisms, such as temperature, pH, nutrient, etc. And pH is one of the most important factors. It should not be allowed to vary too much during a short time period since variations of the pH can be of big influence on the

behaviour of bacteria, low pH(<6.8) and high (>8.2) as well as sudden increase or decrease of the pH, should be avoided. In general the optimal pH for aerobic processes is around neutral pH (7~7.8) [2~3] and for the anaerobic process is between 6.8~7.2 [4~5].

For pulp and paper wastewater, pH may vary considerably, depending on the raw material and manufacturing process utilized. For control of the pH in the system, an automatic dosing system is installed and strong acid (HCl) and strong base (NaOH) are adopted as neutralizing liquid in the system.

2. Basis and the Difficult Point of pH Control

As shown in the acid-base titration curve [6], the changes at the two ends of the curve are gentle, that is to say, the pH varies very little with the addition of strong acid (or strong base); however, the sensitivity is very high around the neutral point, and the pH is to change dramatically even when a little strong acid (or strong base) is added in. the sensitivity is very high near the neutral point, while is extremely low at the place far from the neutral point, and it has been proven by experiments that the nonlinearity of a strong acid-strong base neutralization process is more obvious than that of a weak acid-strong base process.

As for the pH control system in biological wastewater treatment, the target range of pH is required to be controlled within 7~7.8 for aerobic processes and 6.8~7.2 for the anaerobic process, which are just located in the vicinity of the neutral point of the titration curve, thus the sensitivity of change is high; on the one hand, a controller is required to have relatively high control precision, on the other hand, control difficulty is raised as the controller becomes more sensitive to lagging.

The pH control of the biological wastewater treatment system is an indispensable measurement item; however, it is difficult to control, for there are numerous phenomena that can not be described quantitatively. The main reasons are as follows:

1) Wastewater from pulp and paper mill may be either acidic or basic at different moments; therefore, two neutralization reagents are needed. The pH in the neutralization reaction has typical nonlinearity [7~8].

2) The acidic and basic ingredients contained in wastewater are complex, which causes the pH curve of the measured object to be difficult to determine.

3) There is pure lagging at the mixing, measuring and other links in the pH control process [9~10], so that the regulated amount fails to reflect the perturbation borne by the system in time. Even if a measuring signal reaches an adjustor and the adjustor receives a regulatory signal to take action instantly, it is not until after a pure lagging period that the regulated amount can be concerned and controlled. Therefore, such a process will inevitably gen-

erate a more significant overshoot and a longer control period. The existence of pure lagging also contributes to the difficulty of pH control.

3. Modelling of pH Control System

3.1. Model Building of pH Control Process in the Biological Wastewater Treatment System

For the reasons described above, it is necessary to carry out preliminary model building to a concerned object before a pH control proposal is put forward so as to facilitate the research and to further study the characteristics of the object.

If the relation between the flow rate u of a neutralization flow and the flow rate F of a process flow in the neutralization process is assumed to be that: $u \ll F$, the following input/output relation can be worked out [11]:

$$V \frac{dX}{dt} = u - FX \quad (1)$$

$$T(pH) = X \quad (2)$$

Wherein: F represents the flow rate of the process flow; u represents the flow rate of the neutralization flow; V represents the volume of the preparation pool; X represents the state variable of the model; $T(pH)$ represents the back-titration curve of the process flow, the nonlinearity of the process is just contained in the back-titration curve $T(pH)$ of the process flow, and the $T(pH)$ is related to ingredients and concentration of all chemical substances added in the preparation pool; if all chemical ingredients in the whole system are known, the nonlinearity of the process can be expressed as follows:

$$\frac{A(pH) + \sum_{i=1}^n a_i(pH)c_i}{\sum_{i=1}^n a_i(pH)x_i} = X \quad (3)$$

Wherein: n represents the number of the ions in the preparation pool, c_i represents the ion concentration of the i th kind of process flow, and x_i represents the concentration of the i th kind of neutralizing liquid,

$$A(pH) = 10^{(-pH_{sv})} - 10^{(pH_{sv}-14)} \quad (4)$$

$a_i(pH)$ Represents an acid-base weight factor, and it is equal to -1 for strong monacid and +1 for strong monoacidic base. Therefore, when there are only strong acid solution and strong alkaline solution, the concentration of solution can be directly combined; only when there are weak acid and weak base, a weight factor, $a_i(pH_{sv})$, needs to be multiplied. The required volume of solution

when it reaches a set point is determined by a weight sum, that is, $\sum_{i=1}^n a_i(pH)x_i$. The weight sum is named as a strong acid equivalent which can directly reflect the amount of the neutralizing agent required for titrate the pH to a set value, and it can be taken as a control objective and has larger practical significance than the pH.

In the process of neutralization titration, the difference value between an actually measured pH and a set value is in line with a non-linear conversion process, and the numeral value is [12–13]:

$$Y = T(pH_{sv}) - T(pH) \quad (5)$$

The process is dynamic balance output of pH; as long as there is a one-to-one relation between the pH and T (pH), the pH is controlled to be pH_{sv} , which is equivalent to the control of Y, and the Y is set to be 0. In this way, the control problem of pH is converted into a linear problem.

The following study on pH control is based on the Formula (1) and the Formula (2) described above.

4. pH Control

As remarked above, the adjustment of the pH in the an

aerobic wastewater treatment is completed in the preparation pool, and strong acid (HCl) and strong base (NaOH) are generally adopted as neutralizing liquid in a project. The flow chart of pH neutralizing process is shown as Figure 1. In the Figure 1, F represents the flow rate of the process flow; u_1 and u_2 represent the flow rate of the neutralizing flow; a_1 and a_2 represent the concentration of the neutralizing flow; F_{T1} represent the flow rate of the wastewater in a branch loop of the preparation pool; F_{T2} is the flow rate of the swage sent to the reactor.

The concentration of the acid liquor or alkali liquor to be added is calculated and adjusted according to the technology. It is prevented from fluctuating, so that we can focus on the stabilization of the flow rate of acid or base. We can take the acid adding single feeding process when the pH is too high as the study object to carry out further analysis so as to obtain a structural diagram of the system as shown in the Figure 2.

As shown in the Figure 2, the cascade control system forms two closed loops in terms of the structure, the flow loop and the pH loop, which are called auxiliary ring and main ring respectively. The flow PID controller controls the flow control valve according to the pH PID controller, thus ensuring that the pH can still meet the requirements under the condition of feeding disturbance.

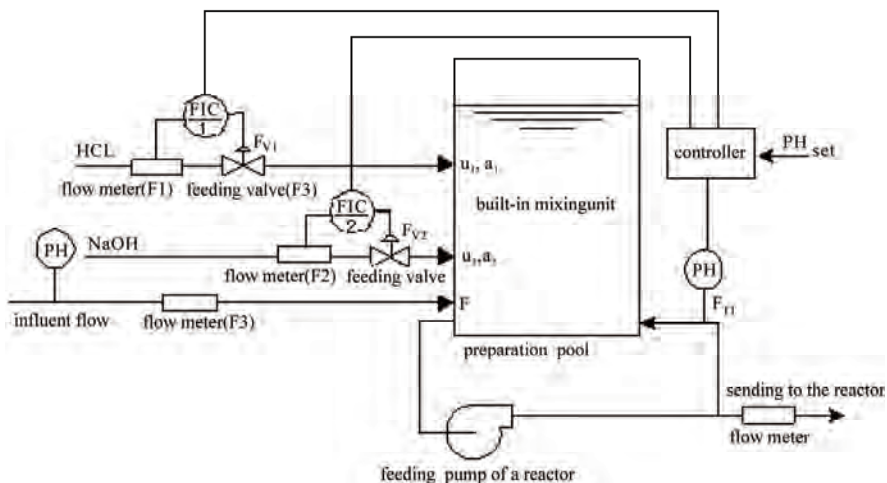


Figure 1. Flow chart of pH neutralizing control system.

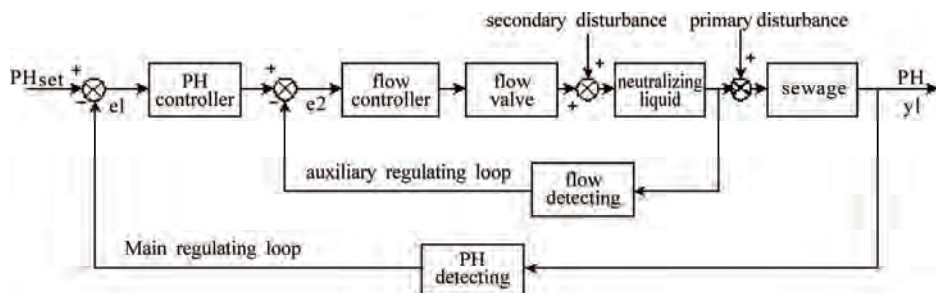


Figure 2. pH cascade control system.

Nevertheless, in the actual production process, it is inevitable that the mixing concentration of the neutralizing liquid has small difference and fluctuation in different times, however, the method described above can effectively eliminate the influence on pH adjustment caused by the fluctuation; as the flow self stabilization system can act quickly, the fluctuation of the concentration of the neutralizing liquid can be eliminated in a short time.

5. Simulation of the pH Cascade Control System

5.1. Building a Simulation Model

1) Model building of a main controlled object and an auxiliary controlled object in the cascade loops

According to the preliminary model building of the neutralization process in section II, a first order model can be obtained:

$$V \frac{dX}{dt} = u - FX \quad \& \quad T(pH) = X$$

The study on the pH control is based on the above two formulas; similarly, let's take the acid adding process when the pH is too high as an example. The formulas are subject to Laplace transformation to obtain the following transfer function:

$$G_p(S) = \frac{1}{Vs + F} \quad (6)$$

Given the pure lagging caused by the pipeline and the detection process of a measuring instrument as well as a delay factor, the transfer function is converted into:

$$G_p(S) = \frac{1}{Vs + F} e^{-\tau s} \quad (7)$$

The Formula (7) shows the model of the pH neutralizing process; according to the actual situation, the parameters in the formula are respectively as follows:

$$V = 102m^3; \quad F = 250m^3/h = 0.069m^3/s; \quad \tau = 4s$$

All the parameters are written into the formula which is simplified into a standard form:

$$G_p(S) = \frac{K_0}{Ts + 1} e^{-\tau s} = \frac{14.49}{1478.26s + 1} e^{-4s} \quad (8)$$

As for the flow adjusting process in the cascade control loops, the objective transfer function is as:

$$G_{p2}(S) = \frac{1}{2s} \quad (9)$$

2) Selection of a main adjuster and an auxiliary adjuster in the cascade loops

In the cascade control system, the main adjuster and the auxiliary adjuster have different tasks; their type se-

lection, that is, the selection of adjusting action law, also have different requirements. The task of the auxiliary adjuster is to take quick action to offset the secondary disturbance in the auxiliary ring, and non-error adjustment of auxiliary parameters is not required, thus a P adjuster is adopted in the model building. However, the task of the main adjuster is to accurately maintain the regulated variable to meet production requirements, therefore, a PI adjuster is selected to eliminate residual error.

5.2. Setting the Parameters of the Adjusters

A step-by-step method is employed for the parameter setting of the cascade loop; in the method, the main ring and the auxiliary ring are set in sequence, and then the process is repeated to approach the optimal setting. The basic steps thereof include: setting the auxiliary ring, cutting off the main ring, working out the setting parameters of the auxiliary adjuster according to the setting method of a single loop, taking the just set auxiliary ring as a link of the main ring, and working out the setting parameters of the main adjuster according to the setting method of a single loop.

The relevant parameters of the main adjuster obtained through the method described above are as follows:

The parameter of the auxiliary adjuster is: $K_C = 15$;

The parameter of the main adjuster is: $K_C = 12$, $T_i = 15$.

According to above parameters, we carry out the following simulation; wherein the ordinate axis represents pH, the horizontal axis represents time, and the unit is second (s):

1) Only under the action of PID, the step response curve of the pH control loop is in line with the Figure 3: From the Figure 3, we can know the overshoot $\delta_1\%$ of the system is relatively large, while the adjusting time t_{sl} is relatively long.

2) Only when the pH control loop is under the action of PID and is affected by inlet water pH, fluctuation of the flow rate of the neutralizing fluid, and other disturbing factors, the system response cure is as shown in the Figure 4: We can learn that disturbance resisting capacity of the system is rather poor; when disturbed, the overshoot basically remains unchanged; however, the system still cannot enter a steady state 300 s later.

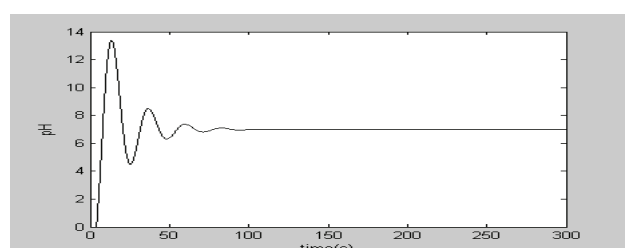


Figure 3. Simulation response curve of PID control

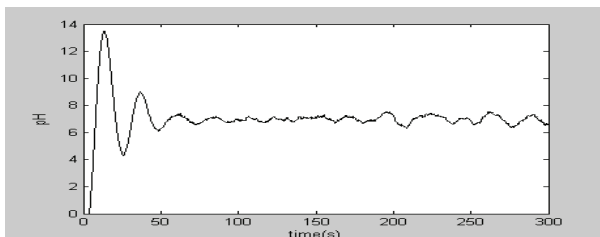


Figure 4. Simulation response curve under PID control when disturbed

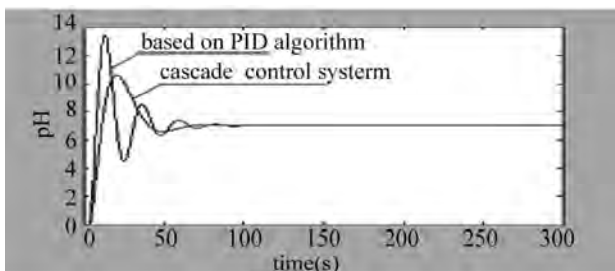


Figure 5. The curve of cascade control system

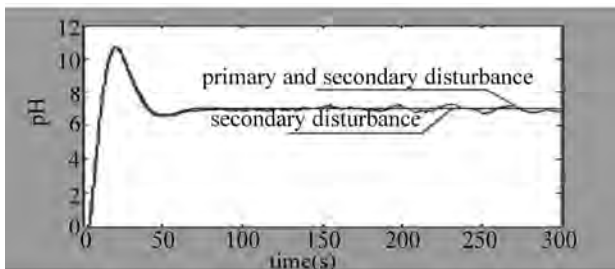


Figure 6. The curve of cascade control system with interference

3) The system step response curve under the action of the cascade control loop based on PID is as shown in the

Figure 5. We can know that: the overshoot of the cascade control system based on PID is $\delta_2\% < \delta_1\%$, and the adjusting time t_{s2} is significantly shortened $t_{s2} < t_{s1}$.

4) When the pH control system is under the action of the cascade control loop based on PID and is affected by inlet water pH, fluctuation of the flow rate of the neutralizing fluid, and other disturbing factors, the system response curve is as shown in the Fig.6: We can know that the anti-disturbing capacity of the system is dramatically improved, and especially has strong inhibiting function on the secondary disturbance in the flow control loop. Though it still takes a long time for the system to completely enter a steady state after being disturbed, the fluctuation is small and is basically within the acceptable range in an industrial site.

6. Conclusions

From the above simulation figure, we can know that: the cascade control system based on PID can contribute to excellent control effect and facilitate engineering application. Compared with a simple PID control, not only the capacity adaptive to the change of the controlled parameters is strong, but also good control effect can still be achieved when the structure of the objective model is intensively disturbed. The step response curve of the cascade control system based on PID has the advantages of quick raising, short adjusting time, high adjusting precision, excellent steady state performance and small overshoot, and can competently fulfill the automatic control of pH. The runtime curve of the pH control system used in a pulp and paper wastewater treatment process is showed in Figure 7. We can know that it worked well.



Figure 7. The runtime curve of the pH control system.

7. References

- [1] U. Tezel, E. Guven, T. H. Erguder, and G. N. Demirer, "Sequential (anaerobic/aerobic) biological treatment of dalaman SEKA pulp and paper industry effluent," *Waste Management*, Vol. 21, pp. 717–724, 2001.
- [2] X. F. Yang, "Wastewater treatment in pulp paper making sector," Chemical Industry Press, Beijing, 2001.
- [3] Biothane System International, Enclosure F: Aerobic Microbiology [M], 2006.
- [4] Biothane System International, Enclosure F: Anaerobic Microbiology [M], 2006.
- [5] "An expert system for monitoring and diagnosis of anaerobic wastewater treatment plants," *Water Research*, Vol. 36, pp. 2656–2666, 2002.
- [6] S. B. Wu, "Water pollution control and treatment technology in the paper industry," Chemical Industry Press, Beijing, Vol. 5, 2001.
- [7] J. F. Bieteaua, "Modelling of anaerobic digestion in a fluidised bed with a view to control," *Biochemical Engineering Journal*, Vol. 24, pp. 255–267, 2005.
- [8] G. Ulvsson and B. Newell, "The model building, diagnosis and control of the wastewater treatment system," Chemical Industry Press, Beijing, 2004.
- [9] J. C. Wang and H. Y. Zhu, "Chemical process control [M]," Chemical Industry Press, Beijing, 1991.
- [10] S. Regunath and V. Kadirkamanathan, "Design of a pH control system using fuzzy non-uniform grid scheduling and evolutionary programming," *Applied Soft Computing*, pp. 91–104, 2001.
- [11] W. W. Tan, F. Lu, A. P. Loh, and K. C. Tan, "Modeling and control of a pilot pH plant using genetic algorithm," *Engineering Applications of Artificial Intelligence*, Vol. 18, pp. 485–494, 2005.
- [12] R. A. Wright and C. Kravaris, "On-line identification and nonlinear control of an industrial pH process," *Journal of Process Control*, Vol. 11, pp. 361–374, 2005.
- [13] H. H. Lee and J. W. Yang, "A new method to control electrolytes pH by circulation system in electrokinetic soil remediation," *Journal of Hazardous Materials* B77, pp. 227–240, 2000.

Health Risk Assessment on Rural Drinking Water Safety

—A Case Study in Rain City District of Ya'an City of Sichuan Province

Fuquan NI^{1,2}, Guodong LIU², Huazhun REN³, Shangchuan YANG¹, Jian YE¹, Xiuyuan LU^{1,2}, Min YANG¹

¹College of Information & Engineering, Sichuan Agricultural University, Ya'an, China

²College of Water Resources & Hydropower, Sichuan University, Chengdu, China

³College of Hydrology & Water Resources, Hohai University, Nanjing, China

E-mail: nfg1965@163.com

Received March 31, 2009; revised May 28, 2009; accepted May 31, 2009

Abstract

Taking Rain City District of Ya'an for example, this paper based on ComGIS (Component Object Model Geographic Information System) platform takes comprehensive and systematic detection on the exposure dose of chemical carcinogens and non-carcinogens from drinking water sources in this region and discusses health risk assessment of single factor and the whole health risk assessment. As, Hg, Cr, Pb, Cd and fluorides in some drinking water sources of Rain City District are analyzed according to Standards For Drinking Water Quality (GB5749-2006). A health risk assessment model called USEPA is also applied to drinking water health risk assessment and management countermeasure is proposed.

The results show that the greatest health risk for individual person per year is caused by Cr(VI). The health risk of carcinogens is much higher than that of non-carcinogens: the greatest risk value due to non-carcinogen pollutants is caused by fluoride (F), achieving $1.05 \times 10^{-8}/\text{a}$. The ranking of risk values due to non-carcinogen pollutants by drinking water is Pb>fluoride (F)>Hg, within Pb accounting for 44.77%, fluoride (F) accounting for 34.30% and Hg accounting for 20.92%. The average individual carcinogenesis annual risk of Cr(VI) is the greatest, achieving $8.91 \times 10^{-4}/\text{a}$. The ranking of risk value due to chemical carcinogen by rural drinking water of Ya'an is Cr⁶⁺>As>Cd, within Cr⁶⁺ accounting for 91.12%, As accounting for 5.89% and Cd accounting for 3.00%. Based on this, the strategy and measures of the health risk management are put forward.

This study has worked efficiently in practice. Compared with the same kind of methods which have been found, the paper has the outstanding results for the health risk assessment of the rural drinking water safety.

Keywords: Rural Drinking Water Safety, Health Risk Assessment, ComGIS, Ya'an

1. Introduction

At present, water safety and water environment health risk assessment is mainly focused on the polluted fields in certain areas, the drinking water of city, reuse of wastewater in city, groundwater, etc. The rural drinking water safety is being paid more and more attention.

The report from UN points out that there are 80% human diseases caused by unsafe drinking water in poor areas and about 25 thousand people died of unsafe drinking water every day. Besides, the report from World Health Organization (WHO) points out that there are

1/3 people living in the city of developing countries could not get safe drinking water in the world [1,2].

In China, there are about 300 million rural residents have no safe water supply, so the drinking water safety is important. It is not only the problem of resources and environment, but also the strategic problem, which have influence on the national economy, sustainable development of society, as well as the harmony between water and human. The factors influencing rural drinking water are multitudinous, which have non-determinism and the spatial variability characteristics. Based on this, the paper coupled the ComGIS technology and the health risk as-

essment model together, carries out the spatial analysis and the system research of rural drinking water safety problem in typical mountainous region of Ya'an, Sichuan [3,4].

In the whole water safety assessments which are based on water standard, health risk assessment only describes whether hazardous pollutants exceeded seriously. It doesn't directly reflect the effect of water on human health. This paper aims at how to quantify severity of pollutants in drinking water so that risk degree can be used directly to represent hazard to human health.

This paper takes Rain City District of Ya'an in Sichuan Province for example. According to the analysis of detection result for the 8 water sources, carcinogenic risk and non-carcinogenic risk of transnormal items in water are calculated and analyzed using health risk assessment model recommended by USEPA. Risk level of rural drinking water environment in research area, the primary-secondary of pollutants and the priority order of governance are also demonstrated in this paper, providing scientific foundation for drinking water risk management in research area.

2. Material and Methods

2.1. Overview of the Study Area

Rain City District of Ya'an locates in western edge of the basin where sits in the middle Qingyi River, with longitude of $102^{\circ}51' E - 103^{\circ}12' E$ and latitude of $29^{\circ}40' N - 30^{\circ}14' N$ and covering $1,066.99 \text{ km}^2$. It locates in the northern slope of Erlang branch range which belongs to Qionglai Mountains, at $515.97 - 2,629.4 \text{ m}$ altitude. It belongs to middle-low mountain region that the west area is higher than east. The mountains occupied 91% of the whole region including 45% low mountains which altitude is less than 1,000m, 46% middle mountains which altitude is more than 1,000m and 9% flatland. In this area, the climate type belongs to subtropical humid monsoon climate except a few high mountain regions. The annual precipitation is 1,732mm. The maximum is 2,367.3mm (in 1966) and the minimum is 1,204.2mm (in 1974). The main rivers in this area are Qingyi River, Zhougong River, Longxi River, Fen River, Gaoqiang River, Yanchang River and Yanqiao River. The amount of their total length is 197.4 Km. The main runoff of these rivers is $580.5 \text{ m}^3/\text{s}$ and the amount of total runoff is 15.1 billion m^3 .

The population in this area is 320 thousand including 207.326 thousand in rural. The investigation in 2004 points out that unsafe rural drinking water affects 657.88 million people in this area. And 354.02 million people drink untreated surface water whose bacteriological index exceeds standard seriously. Besides, the untreated and seriously polluted groundwater affects 1,517 people

and other drinking water affects 101.04 million people. It is urgent and essential to make health risk assessment actively and improve the rural drinking water conditions in this area.

2.2. Samples Investigation

8 water samples were collected in 2005 according to terrain, landform, geology, hydrology, water system, drinking water sources, distribution of waterborne infectious disease and types of water supply project. According to related standards of water quality detection methods, there are 21 indexes of these water samples which are detected, such as physics water quality indexes (color, turbidity, odor, visible material by bare eye), hydrochemistry index (PH, COD, total hardness, total dissolved solids, chloride, sulfate), toxicological indexes (Fe, Mn, fluoride, As, Hg, Cd, Cr, Pb, nitrate), bacteriological index (total bacterial count, total coliform count). 6 hydrochemistry toxicological indexes need health risk assessment according to if the detected water quality indexes are harmful to human. And the 6 indexes are As, Hg, Cr, Pb, Cd and fluoride.

The sampling sites and mainly water quality problems of rural drinking water safety in Rain City District of Ya'an can be seen in Figure 1.

The monitoring data of pollutants of rural drinking water in Rain City of Ya'an can be seen in Table 1. In the study area, the pollutants concentration scopes of the water sampling are as follows: As: 0.004mg/l, Hg: 0.001 mg/l, Cr^{6+} : 0.005~0.015 mg/l, Pb: 0.01 mg/l, Cd: 0.005 mg/l, fluoride (F): 0.01~1.4 mg/l. Compared with the *Rural Surface Water Environment Quality Standard* (GB3838-2002), each indicator achieves I~III sort of standard except fluoride (F).

2.3. Health Risk Assessment Models and Parameters

There are many researches of dosage-reaction relation to human health risk assessment at present [5,6,7], which are calculated from the basis of various investigation and experiment data. The first choice is the survey materials of human epidemiology, and the second one is the experiment materials of sensitive animal close to the mankind. In the light of the hazard effect by pollutants and a large number of research results from hazard substance (including the carcinogen and non-carcinogen) for several decades, the risk models that are applied to the human health hazard affected by different contaminations (including the drinking approach) may be established. These models include the carcinogenic risk model, the non-carcinogenic risk model and the total hazard risk model of health.

The carcinogenic risk model:

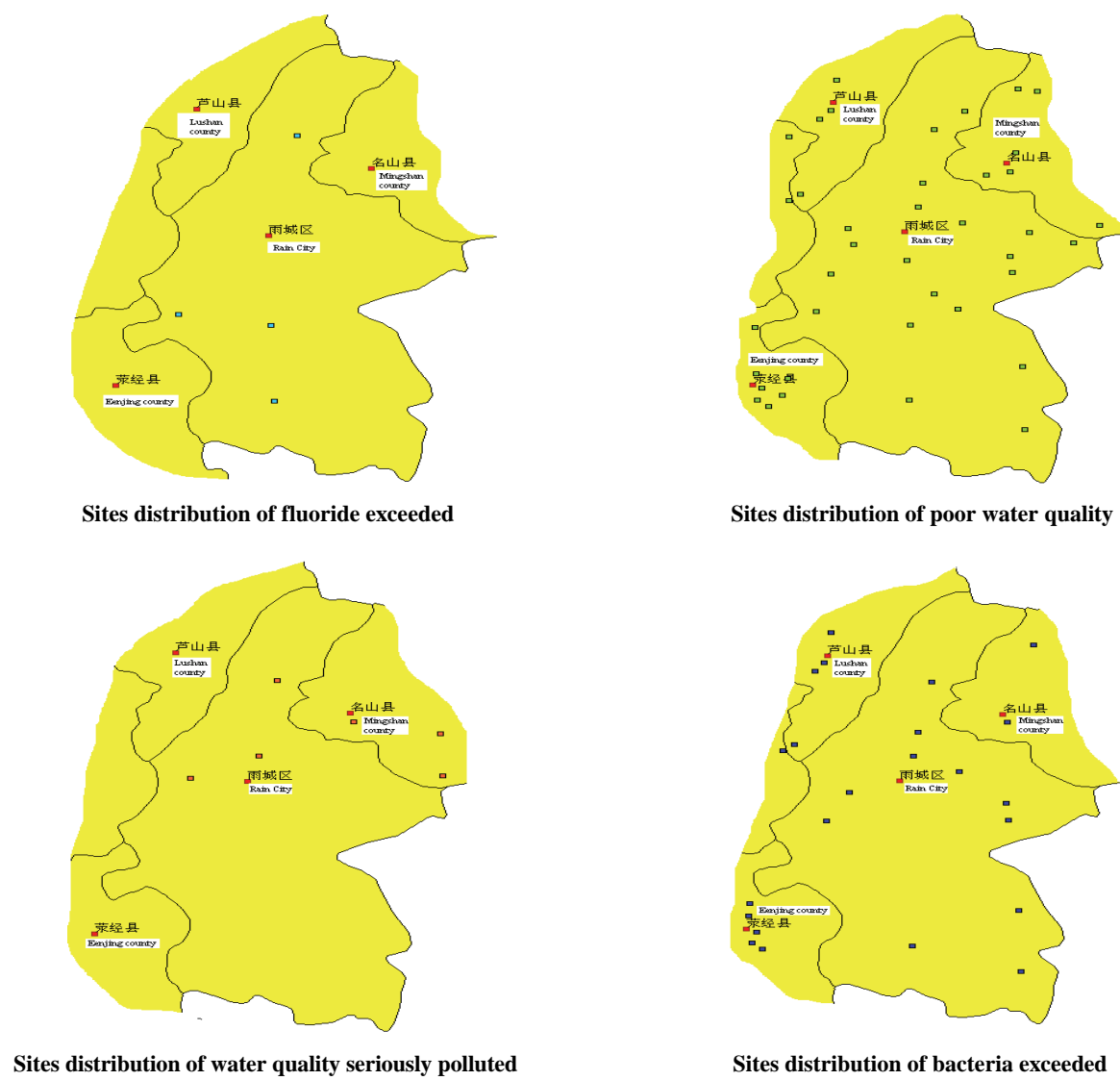


Figure 1. The map of water quality problems in Rain City District of Ya'an.

Table 1. Exposure concentrations of the sampling sites in Rain City of Ya'an (mg/l) .

Serial Number	Sample Sites	As	Hg	Cr ⁶⁺	Pb	Cd	fluoride(F)
1	Fuping village	0.004	0.001	0.05	0.01	0.005	0.1
2	Liujiavillage	0.004	0.001	0.05	0.01	0.005	1.4
3	Kanpo village	0.004	0.001	0.05	0.01	0.005	0.1
4	Liuliang village	0.004	0.001	0.015	0.01	0.005	0.39
5	Pingshi village	0.004	0.001	0.005	0.01	0.005	0.32
6	Liba village	0.004	0.001	0.006	0.01	0.005	0.12
7	Zhanggou village	0.004	0.001	0.005	0.01	0.005	0.16
8	Baishu village	0.004	0.001	0.005	0.01	0.005	0.36

$$R^c = \sum_{i=1}^k R_i^c \quad (1)$$

$$R_i^c = [1 - \exp(-D_i q_i)] \quad (2)$$

where, R_i^c is assigned the carcinogenic contamination i to the average individual carcinogenesis annual risk by pathway-intake, a^{-1} ; D_i is assigned the carcinogenic contamination i to the daily average exposure dosage per unit weight by the pathway-intake, mg/(kg·d); q_i is assigned the carcinogenic contamination i to the carcinogenic by the pathway-intake, mg/(kg·d); 70 is average span of human, a. The D_i can be expressed:

$$D_i = 2.2 \times C_i / 70 \quad (3)$$

where, 2.2 is average daily intake from drinking water for an adult, L; C_i is the concentration of carcinogenic contamination i , mg/L; 70 is average weight of human, kg).

The non-carcinogenic risk model:

$$R_i^n = (D_i / RfD_i) \times 10^{-6} / 70 \quad (4)$$

where, R_i^n is assigned the non-carcinogenic contamination i to the average individual health hazard annual risk by pathway-intake, a^{-1} ; D_i is assigned the non-carcinogenic contamination — to the daily exposure dosage per unit weight by pathway-intake, mg/(kg·d); RfD_i is assigned the non-carcinogenic contamination i to reference dosage, mg/(kg·d); 70 is average span of human, a.

Total risk model of water environment health assessment:

The cumulative effects of the toxic substances which damage the physical health of human include addition relation, cooperating relation and resisting relation. Cumulative effects analysis (CEA) is a very complicated and uncertainty work. To obtain reliable result, it is nec-

essary to get enough successive historical and current observation data. At present, the developed countries are paying great attention to CEA, and also have carried out a lot of real researches. But the systematic theory and method have not formed.

The concentrations of toxic substances are very low in the daily drinking water source. It is assumed that the effect which each compound causes is independent and the relation among between cumulative effects of the toxic substances which damage the physical health of human is addition relation, but not cooperating relation or resisting relation. So the total water environmental health risk (R_h) can be expressed as following:

$$R_h = R^c + R^n \quad (5)$$

Formula (5) is the total risk model of rural drinking water safety health assessment.

Health risk assessment parameters [8,9,10]:

According to the taxonomy of the International Cancer Development Facility (IARC) and the World Health Organization (WHO) which is established through the comprehensive appraisal chemical substance carcinogenicity reliability level, the chemical substances in Group 1 or Group 2A are chemistry carcinogen. Their carcinogenicity assurance factors can be found in Table 2.

Regarding to the health risk appraisal resulting from the non-carcinogen, the reference dosage is an important parameter. According to the relevant data, the reference dosages are found and can be seen in Table 3.

3. Results and Discussion

3.1. Results

According to health risk assessment models recommended by USEPA and the evaluation parameters, the average individual health hazard annual risk of the non-carcinogens and the average individual carcinogenesis annual risk of the chemical carcinogens through the drinking water in this district in 2005 can be calculated.

Table 2. Carcinogenicity intensity coefficient of chemical carcinogen q_i [mg/(kg·d)].

chemical carcinogen	Cd	As	Cr ⁶⁺
q_i	6.1	15	41

Table 3. The reference doses of non-carcinogens RfD_i [mg/(kg·d)].

Non-carcinogen	Hg	Pb	fluoride(F)
RfD_i	3.0×10^{-4}	1.4×10^{-3}	6.0×10^{-2}

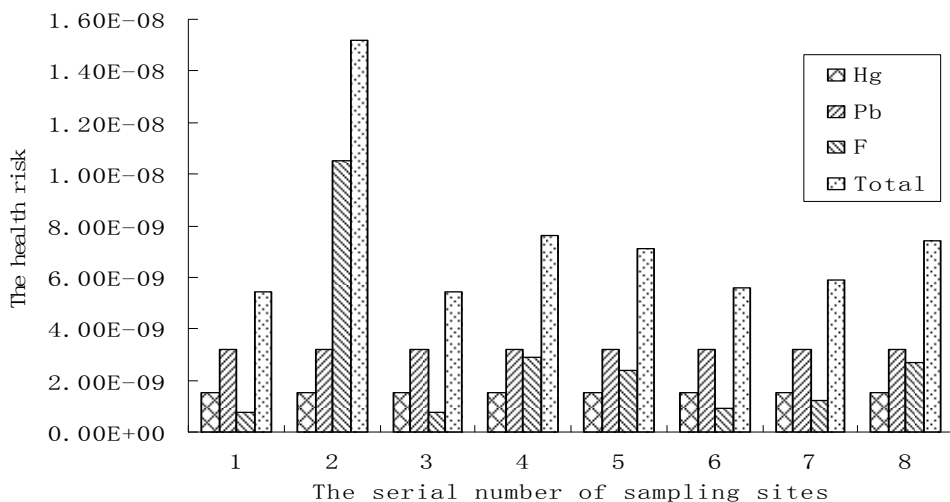


Figure 2. The average individual health hazard annual risk of the non-carcinogens.

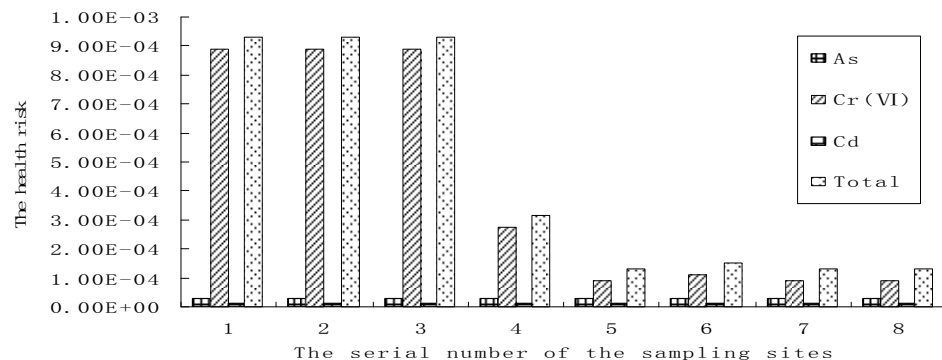


Figure 3. The average individual carcinogenesis annual risk of the carcinogens.

The average individual health hazard annual risk of the non-carcinogens can be seen in Figure 2. In the investigation area, the greatest risk value due to non-carcinogen pollutant is caused by fluoride (F), achieving $1.05 \times 10^{-8}/\text{a}$. The ranking of risk value due to non-carcinogen pollutant by drinking water is Pb>fluoride (F)>Hg, within Pb accounting for 44.77%, fluoride (F) accounting for 34.30% and Hg accounting for 20.92%. The average risk values order of the 8 sampling points caused by the non-carcinogen pollutants is as follows: Number 2 > Number 4 > Number 8 > Number 5 > Number 7 > Number 6 > Number 3 = Number 1.

The average individual carcinogenesis annual risk can be seen in Figure 3. Among the three kinds of chemical carcinogens, the average individual carcinogenesis annual risk of Cr^{6+} is the greatest, achieving $8.91 \times 10^{-4}/\text{a}$. The ranking of risk values due to chemical carcinogen by rural drinking water of Ya'an is $\text{Cr}^{6+} > \text{As} > \text{Cd}$, within Cr^{6+} accounting for 91.12%, As accounting for 5.89% and Cd accounting for 3.00%. The order of risk values of the 8 investigation sampling sites caused by the chemical

carcinogen is as follows: Number 1 = Number 2 = Number 3 > Number 4 > Number 6 > Number 5 = Number 7 = Number 8.

3.2. Discussion

The level of human health hazard individual annual risk caused by non-carcinogens virulent chemical material concentrates in $10^{-8} \sim 10^{-10}/\text{a}$. Namely, because of the drinking water's non-carcinogens pollutants, human health risk or the death population in each ten million people is less than one person. This indicates that the human health risk caused by the non-carcinogenicity chemical substances is slighter and will not be harmful to human health obviously. The level of human health individual annual risk caused by carcinogens virulent chemical substances concentrates in $10^{-4} \sim 10^{-5}/\text{a}$. Namely, because of the drinking water's carcinogenic pollutants, the health dangers (or deaths) in each ten million are more than 100 or 1000 people. Thus, the health danger individual annual risk caused by carcinogenic toxic sub-

stances is much bigger than one caused by total non-carcinogen toxic substances in the research area. The American Environmental Protection Bureau (EPA) carcinogenicity risk assessment guide points out that the risk is acceptable if the risk level is lower than $10^{-4}/\text{a}$ in one year. The health danger individual annual risk resulting from each kind of pollutant of rural drinking water source in Ya'an is on this level. But it surpasses the acceptable maximum ($5 \times 10^{-5}/\text{a}$), which is recommended by International Commission on Radiological Protection (ICRP).

Thus, chemical carcinogens are primary and should be removed accordingly. The effective way of decreasing the health risk is to control and dispose the rural drinking water containing Cr(VI), Pb and fluoride (F). The results can provide important information of the early warning for rural drinking water quality management.

3.3. Risk Management

Enhance the conservation of water sources

Technical measures: In order to ensure the drinking water quality, the drinking water source of Qingyi River should be protected according to the relational laws in *Regulations of pollution control to the Drinking Water Source Conservation Areas*, etc.

Construction contents: The conservation areas are determined and the signs are set. The point source pollution in conservation areas, such as rubbish, toilet, are removed. In conservation areas, the organic agriculture and water protection forest are developed to avoid non-point pollution caused by pesticide and fertilizer and to reduce the soil and water losses and preserve the water resources.

Construction standards: The water quality is improved and reaches the drinking water standard. The groundwater quality reaches *standards of groundwater quality* (GB/T14848) and the surface water quality reaches *environmental quality standards of surface water* (GB3838).

Construction of drinking water supply

The construction of drinking water supply contains water sources, facilities of water treatment, pipe network of water delivery and distribution, water quality detection and so on. The construction of each part should reach the requirements of relational regulations.

The selection and distribution of water sources: The exploration and demonstration of water source selection should be so deep and meticulous that can reduce the investment of water supply system and the cost of water. In addition, the exploration and demonstration should ensure that the technologies are feasible, operation and management are convenient and water supplying is safe and reliable. When there are more than two water sources to select, the different schemes should be compared according to their water qualities, water volume,

engineering investments, operation cost, constructions, managements and the conditions of healthy protection. Then, the best scheme is decided. The regional water resources allocation should be optimized well. The high quality water is priority as drinking water for daily life.

Engineering type selection: According to the local conditions of water source, water demand, landform and the residential area density and the engineering types are determined reasonably by comparing their technologies and investment.

Selections of water treatment measures: the following conventional water treatments are adopted to process the original water which reaches the standards of water source quality. The groundwater with good quality only needs disinfection treatment. If the original water's permanent turbidity is less than 20NTU and the instant one is less than 60NTU, the technology of slow filtering with disinfection or contact filtration with disinfection will be adopted. In addition, the ultrafiltration membrane technology can be taken to process the original water. If the original water's permanent turbidity is less than 500NTU and the instant one is less than 1000NTU, the technology of coagulation sedimentation (or clarification) and filtration with the disinfection will be adopted. If the original water's sediment concentration changes greatly or its turbidity is usually more than 500NTU, the facilities of pre-precipitation and rough filtration or infiltration will be added before the conventional water treatment technology.

If there is no qualified water source indeed, the following special water treatment measures should be adopted. For brackish water desalination, the treatment measures, such as electrodialysis, reverse osmosis, electric absorption should be adopted. For reducing the fluoride in high fluoride water, the treatment measures, such as medium adsorption, electrodialysis, reverse osmosis, electric absorption should be adopted. For the treatment of micro-polluted water, the enhanced conventional water treatment technology should be adopted. In addition, the following measures added into the conventional water treatment technology are adopted, such as air floatation technology, biological pretreatment, chemical pre-oxidation treatment, activated carbon treatment, the ozone activated carbon advanced treatment.

Selection of material and equipment: Comparing the technology and investment, the material and equipment in water supply engineering are determined according to the concrete engineering situation. The material and equipment should have reliable performance and reach the relational national standards and requirements of hygienic and safety. The products which are corrosion resistant, aging resistant, energy-saving, water-saving and good for environmental protection should be given priority to be used.

Water quality monitoring

According to the requirements of *The Drinking Water Health Standards* (GB5749), laboratory has been built which is equipped with the appropriate water quality monitoring equipment to monitor the water quality coming from the water resources, the waterworks and peripheral water of pipe network. For the water supply project in smaller scale, automatic test equipment or simple testing equipment should be adopted or can be also tested by the entrusted with drinking water quality testing units.

Establishment and effective implementation for water safety emergency mechanism

For the study of the emergency measures to unexpected events water safety, the comprehensive emergency preparedness should be formulated from the legal system, institutional settings, the application of information technology, multi-sector participation, professional research, capital protection, etc. The main contents of the rural water safety emergency mechanism include as follows: forecasting the large-scale flood and drought disaster and possible rural water safety emergency events based on the regional climate and water resources status; designing the corresponding emergency preparedness according to rural water safety emergency calculation water quantity; setting up a special inter-departmental water safety emergency control and implementation agencies to enhance reaction speed and achieve the "emergency" requirement really.

5. Conclusions

Combining the rural drinking water quality with public health hazards, this paper quantitatively analyzes the degree of water environmental pollution on public health hazards and obtains the synthesized results of the water environmental quality based on the health risk calculated results. And it also determines the primary-secondary water pollutions, gives the control priority, and provides a scientific basis and decision-making objects of the environmental risk management.

In the study area, the mainly problems of the water environmental health risks are as follows: rural water source pollutant risk, the outburst water source pollutant risk, simple supply structures and the weak ability to resist risks, unexpected geological disasters increasing the risk of the rural water supply system, water treatment risk, water sources health risk of surrounding areas, etc. The calculated results show that the greatest health risk for individual person per year is caused by Cr(VI). The health risk of carcinogens is much higher than that of non-carcinogens. The greatest risk value due to non-carcinogen pollutants is caused by fluoride (F), achieving $1.05 \times 10^{-8}/\text{a}$. The ranking of risk values due to non-car-

cinogen pollutants by drinking water is Pb>fluoride (F)>Hg, within Pb accounting for 44.77%, fluoride (F) accounting for 34.30% and Hg accounting for 20.92%. The average individual carcinogenesis annual risk of Cr(VI) is the greatest, achieving $8.91 \times 10^{-4}/\text{a}$. The ranking of risk values due to chemical carcinogen by rural drinking water of Ya'an is Cr⁶⁺ > As > Cd, within Cr⁶⁺ accounting for 91.12%, As accounting for 5.89% and Cd accounting for 3.00%. Based on this, this study pointed out that the effective way of decreasing the health risk is to control and dispose the rural drinking water containing Cr(VI), Pb and fluoride (F). The results can provide important information of the early warning for rural drinking water quality management.

In the study area, the mainly control measures of the water environmental health risk are as follows: conserving the water resources, constructing supply water project, monitoring water quality, investigating and constructing emergency water sources, establishing and implementing of water safety emergency mechanism effectively.

The rural water source water quality health risk assessment shows the relationship between water quality and human health. It can provide much more scientific information for the management and protection of rural water sources to apply this method to evaluate the water quality safety of rural water source and detect the relationship between the source water quality and human health.

This study has uncertainty to some extent and mainly showing as follows. On one hand, following the risk assessment method of the effect of drinking water pollutants on human used by EPA, the exposure way just takes average drinking intake into consideration which excludes other toxic substances and their routes, for instance, inhaling by dermal touch and the form of steam and dieting. Actually, the exposure risk of pollutants is underestimated. On the other hand, the exposure risk by drinking is also closely bound up with residence time of water in domestic pipe network, consumer's life style, consuming habit and career. So more complicated exposure assessment method is needed to get the average exposure dose by consumer touch, the daily distribution of pollutants exposure dose and the main exposure chance that individual is affected by pollutants. Therefore, this study on the pollutants exposure risk in water is elementary which need to be developed further in future [11].

6. Acknowledgements

This study is financed jointly by Sichuan Agricultural University youth science and technology innovation fund (00530300) and Sichuan Agricultural University introduces the talented person fund (00530301).

7. References

- [1] F. Wang, "Water pollution, unnegelectable point," *Ecological Economy*, No. 7, pp. 142–145, July, 2006.
- [2] M. Luo, "Analysis of the relationship between drinking water and health," *Guide of Chinese Medicine*, Vol. 6, No. 14, pp. 160–161, July 2008.
- [3] F. Ni, *et al.*, "Drinking water safety decision support system for rural areas in Ya'an city of China," in *Proceedings of the 5th International Conference on Urban Watershed Management & Mountain River Protection and Development*, Vol. 2, Sichuan University Press, pp. 669–677, April 3–5, 2007.
- [4] D. Wang, *et al.*, "Applications of the health hazard assessment for the environmental quality," *Environmental Pollution & Control*, No. 5, pp. 91–92, July 1995.
- [5] U. S. National Research Council, "Risk assessment in the federal government: Managing the process," National Academy Press, Washington, D. C., 1983.
- [6] USEPA, "The risk assessment guidelines of 1986," EPA Report, No. EPA/600/18-87/045, Washington, D. C..
- [7] "Superfund Public Health Evaluation Manual," USEPA/540/186060, EPA.
- [8] J. Gao, L. Zhang, S. Huang, *et al.*, "Preliminary health risk assessment of heavy metals in drinking waters in Beijing," *Environmental Science*, Vol. 25, No. 2, pp. 47–50, 2004.
- [9] G. Zeng, L. Zhuo, Z. Zhong, *et al.*, "Assessment models for water environmental health risk analysis," *Advances in Water Science*, No. 3, pp. 212–217, September 1998.
- [10] H. Luo, R. Xu, X. Liu, *et al.*, "The system design of water environmental health risk assessment in river," in *Proceedings of the 5th International Conference on Urban Watershed Management & Mountain River Protection and Development*, Vol. 1, Sichuan University Press, pp. 189–198, April 3–5, 2007.
- [11] H. Chen, F. Liu, *et al.*, "Health-based risk assessment of contaminated sites: A case study," *Earth Science Frontiers*, Vol. 13, No. 1, pp. 230–235, 2006.

Uncertainty Analysis of Interpolation Methods in Rainfall Spatial Distribution—A Case of Small Catchment in Lyon

Tao TAO^{1,*}, Bernard CHOCAT², Suiqing LIU¹, Kunlun XIN¹

¹*State key laboratory of Pollution Control and Resources Reuse, Tongji University, Shanghai, China*

²*U.R.G.C. Hydrology Urbane, I.N.S.A. de Lyon, 69621 Villeurbanne Cedex, France*

E-mail: taotao@mail.tongji.edu.cn

Received April 7, 2009; revised May 15, 2009; accepted May 18, 2009

Abstract

Quantification of spatial and temporal patterns of rainfall is an important step toward developing regional water sewage models, the intensity and spatial distribution of rainfall can affect the magnitude and duration of water sewage. However, this input is subject to uncertainty, mainly as a result of the interpolation method and stochastic error due to the random nature of rainfall. In this study, we analyze some rainfall series from 30 rain gauges located in the Great Lyon area, including annual, month, day and intensity of 6mins, aiming at improving the understanding of the major sources of variation and uncertainty in small scale rainfall interpolation in different input series. The main results show the model and the parameter of Kriging should be different for the different rainfall series, even if in the same research area. To the small region with high density of rain gauges (15km^2), the Kriging method superiority is not obvious, IDW and the spline interpolation result maybe can be better. The different methods will be suitable for the different research series, and it must be determined by the data series distribution.

Keywords: Rainfall, Spatial Distribution, Kriging, Interpolation

1. Introduction

Precipitation is in many cases the most important input factor in hydrological modeling [1]. The role of rainfall is essential for urban hydrology: it is the driving phenomenon of runoff mechanisms, particularly in an urban context. Its variability constitutes a significant source of uncertainty for hydrological modeling. Assessing rainfall variability is an important element to developing conceptual and predictive models of runoff, pollutant loading, and river dynamics. Quantification of spatial and temporal patterns of rainfall is an important step toward developing regional water sewage models. For example, the intensity and spatial distribution of rainfall can affect the magnitude and duration of pollutant washoff to the ocean [2,3], which are also an input for hydrological models. The small size of the urban catchments and the hydrological purposes (especially for real time applications) oblige us to consider rainfall at small scales: on the

order of 6 min in time and 5 km in space. Hence urban hydrology requires rainfall measurements with high temporal and spatial resolution.

However, this input is subject to uncertainty, as a result of measurement errors, systematic errors in the interpolation method and stochastic error due to the random nature of rainfall. In addition to the stochastic nature of rainfall, the precipitation pattern may be influenced by the irregular topography. The large variability in altitude, slope and aspect may increase variability by means of processes such as rain shading and strong winds. Accurate estimation of the spatial distribution of rainfall and extrapolation of point measurements over large areas is complicated.

The best method to improve the quality of spatial rainfall estimation is to increase the density of the monitoring network. However, traditionally used rain gauges data are sparse and do not always provide adequate spatial representation of rainfall. This is very costly, and in many cases practically infeasible. And even for dense networks, interpolation remains necessary in order to

*Corresponding author. Foundation item: The Major Science and Technology Project-Water Pollution Control and Treatment (NO.2008ZX7421-001)

calculate the total rainfall over a certain area [4]. Therefore, both the design of an adequate monitoring network and choice of an interpolation method require insight in the patterns of rainfall variability and the sources of uncertainty. To provide optimal input for distributed hydrological modeling, the best strategy is probably a combination of all available information on rainfall, including data from hourly point observations, radar data, denser daily measurements, physiographic factors like elevation, and applying sophisticated interpolation or merging methods [5].

Rainfall has been interpolated using averaged values ranging from daily, monthly or annual aggregation levels. And quite a number of modern interpolation methods have been proposed for rainfall. Besides geostatistical approaches, such as ordinary Kriging, Kriging with external drift and co-Kriging [6,7], other techniques based on splines [8,9] or genetic algorithms [10,11] have been applied. These studies concluded that the Kriging method yields a more realistic spatial behaviour of the climatological variable of interest. The use of auxiliary variables in order to improve the spatial interpolation of rainfall variables has been analyzed. Some authors use elevation as an auxiliary variable improving the spatial interpolation of monthly rainfall data, and showing that the interpolation of daily events is improved by the use of elevation as a secondary variable even when these variables show a low correlation [12].

For years various correlation and Semi-Variogram techniques have been used to evaluate both the temporal and spatial structure of rainfall events. Apart from correlation techniques, use of a semi-variogram model for two-dimensional (2-D) interpolation with Kriging approach has been a common practice in different engineering applications, especially in the fields of mining and hydrogeology [13]. By its definition, a semi-variogram function has the capability of estimating the disassociation between measurements from the different gauge locations. In hydrologic engineering applications, the semi-variogram development has been applied to estimate the mean precipitation over a catchment by Matheron (1971), Creutin and Obled (1982), Bastin, Larent and Gevers (1984).

In this study, we analyze some rainfall series from 30 rain gauges located in the Great Lyon area (Figure 1), including annual, monthly, daily and intensity of 6mins, which is more useful to water drainage model. Lyon possesses one of the densest rain gauge networks in an urban area within Europe, having 52 gauges in an area of 460 km². Most of the pluviometers belong to the urban community of Lyon, with 30 tipping bucket rain gauges working in this area. This creates a density of more than 1 pluviometer for every 15 km². They are spread all over the Lyon area, although with a lower density in the eastern part of the agglomeration. The first rain gauges were

set up in 1985, but the actual network density of the present day was reached in 1989. The data is available every 6 minutes although this is variable according to the tip of the bucket.

This paper focuses on three interpolation methods for the different rainfall series. The study is aimed at improving our understanding of the major sources of variation and uncertainty in small scale rainfall interpolation in the time series with different time resolution. This is achieved by means of a spatial characterization and data analysis of the rainfall series. The difference in uncertainty between three interpolation methods that differ strongly in complexity, IDW, Spline and Kriging, is assessed by means of cross validation and validation. This allows us to evaluate the amount of complexity allowed in interpolation, in view of the available data.

2. Methods

Ground-based rain gauge networks supply a reliable source of precipitation data used in many analyses associated with the development of rainfall models. Three methods for the interpolation are used: IDW, Spline and ordinary Kriging. The methods are chosen because they represent two kinds of interpolation methods -- deterministic and geostatistical methods. Each interpolated location is given the value of the closest measurement point, resulting in a typical polygonal pattern and discontinuities at the borders of the polygons. IDW and Spline are deterministic, while Kriging is a geostatistical method. The Inverse Distance Weighted (IDW) and Spline methods are referred to as deterministic interpolation methods because they assign values to locations based on the surrounding measured values and on specified mathematical formulas that determine the smoothness of the resulting surface. Inverse distance weighted (IDW) interpolation determines cell values using a linearly weighted combination of a set of sample points. The weight is a function of inverse distance. The surface being interpolated should be that of a locationally dependent variable. The Spline method is an interpolation method that estimates values using a mathematical function that minimizes overall surface curvature, resulting in a smooth surface that passes exactly through the input points. It fits a mathematical function to a specified number of nearest input points while passing through the sample points. This method is best for generating gently varying surfaces such as elevation, water table heights, or pollution concentrations.

A second family of interpolation methods consists of geostatistical methods, such as Kriging, that are based on statistical models that include autocorrelation (the statistical relationship among the measured points). Because of this, not only do geostatistical techniques have the



Figure 1. The location of rain gauges in Great Lyon.

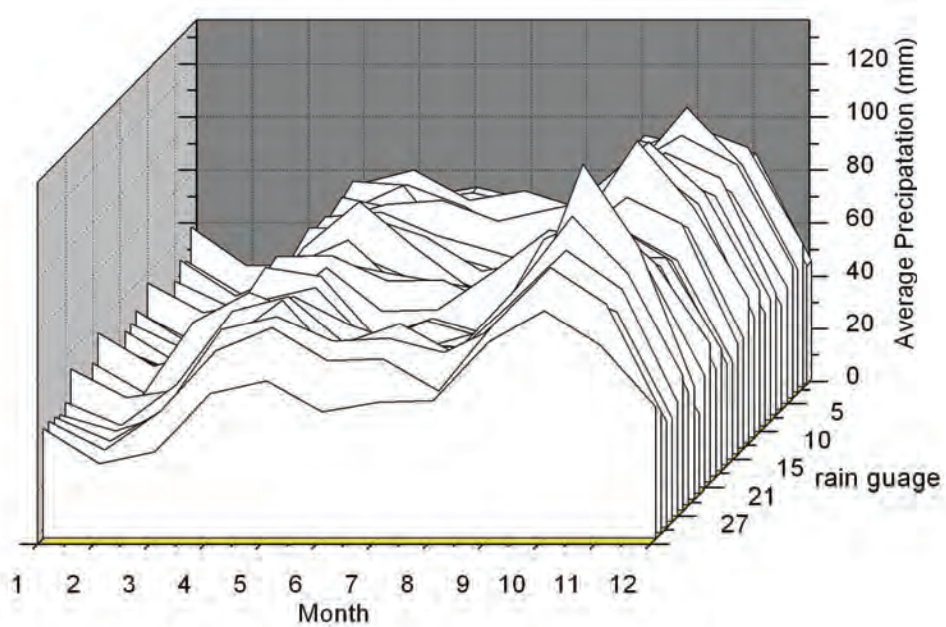


Figure 2. Average monthly precipitation of 30 rain gauges.

capability of producing a prediction surface, but they also provide some measure of the certainty or accuracy of the predictions. Geostatistical Analyst uses sample points taken at different locations in a landscape and creates (interpolates) a continuous surface. The sample points are measurements of some phenomenon such as radiation leaking from a nuclear power plant, an oil spill, or elevation heights. Geostatistical Analyst derives a surface using the values from the measured locations to predict values for each location in the landscape. Kriging is an advanced, computationally intensive, geostatistical estimation method that generates an estimated surface from a scattered set of points with z-values [6,14,15]. Kriging involves an interactive investigation of the spatial behavior of the phenomenon represented by the z-values before the best estimation method is selected for generating the output surface.

Kriging, like most interpolation techniques, is built on the basis that things that are close to one another are more alike than those farther away (quantified here as spatial autocorrelation). The semivariogram is a means to explore this relationship. Pairs that are close in distance should have a smaller difference than those farther away from one another. The extent that this assumption is true can be examined in the semivariogram. Semivariogram measures the strength of statistical correlation as a function of distance.

The semivariogram function is defined as: $Y(si, sj) = \frac{1}{2} \text{var}(Z(si) - Z(sj))$, where var is the variance. si and sj are two locations, Z(si) and Z(sj) are their values.

If two locations are close to each other in terms of the distance measure of $d(si, sj)$, then they are expected to be

more similar, so the difference in their values $Z(si) - Z(sj)$, will be small. As si and sj get farther apart, they become less similar, so the difference in their values will become larger. Notice that the variance of the difference increases with distance, so the semivariogram can be thought of as a dissimilarity function.

3. Results and Discussion

The results include three parts: one is to analyze the data, deeper understanding of data will be useful to make decision of model and results analysis; two is to make decision of parameters, such as the choice of semivariogram model, lag size, and search neighborhood, and then according to the cross validation, and comparison of different models, choose the appropriate model for ordinary Kriging interpolation; three is to use the validation to compare the three interpolation methods in annual, monthly, daily and intensity data, and analyze the uncertainty of different methods to different rainfall series.

3.1. Data Analysis

Rainfall data collected from January 1, 1986 to December 31, 2005 on 30 available stations in the whole study area were analyzed with interpolation technologies. Data with different time span may also have different spatial and temporal distribution. Furthermore, different analysis method should be selected for different data series. In this study, four types of data series were studied, which were annual, monthly, daily, and maximum 6-min precipitation data. Average precipitation in November were

selected as monthly rainfall data, because precipitation in this month is always the highest one over 20 years. Precipitation on December 2, 2003 is selected as the one-day rainfall data, because the storm event was happened at this period, and all stations have non-zero rainfall data.

As the distribution of data will affect the selection of methods, we firstly analyzed the Statistical Characteristics of rainfall data. As shown in table 1, the distribution difference of the annual rainfall is not very big, and the C_s (Skewness Coefficient) is only 0.0557. While for the rainfall intensity, the range of variation is bigger and C_s is 0.194, and the biggest C_s is of the rainfall intensity.

3.2. Original Kriging Analysis

This section discusses the impact of different approaches for the estimation of the semivariogram on the original Kriging interpolation performance for different rainfall data series. Because Kriging is a more complicated interpolation process, one special problem for geostatistical interpolation of whole time series is the effective and

reliable estimation of the variograms for each time step [5], so special attention is given to the analysis of the impact of the semivariogram estimation on the interpolation performance. First we should have a deeper understanding of the phenomena investigated so that we can make better decisions on issues relating to our data, and then by cross validation and comparing the different models, to choose an appropriate model and parameters.

1) Fit a model—to create a surface and to choose the definition and refinement of an appropriate model.

In the process of Kriging analysis, the semivariogram plays a central role in the analysis of geostatistical data. A valid semivariogram model is selected and the model parameters are estimated before Kriging analysis is performed.

According to the history data spatial analysis, notice that the values of the annual rainfall change more slowly in the north-south direction than in east-west the direction. This is because the terrain in east-west direction changes greatly from high to low while the north-south direction

Table 1. of the data series from 30 stations.

Results	Annual(mm)	Month(mm)	Day(mm)	Intensity of 6min(mm/h)
Mean	798.966	105.565	63.479	94.062
Minimum	719.64	77.44	46.6	66
Maximum	877.98	130.87	86.2	140.5
Sd($y_{Er\pm}$)	44.5	9.226	10.111	18.28
C_s	0.0557	0.0874	0.159	0.194

$Sd(y_{Er\pm})$: Standard Deviation

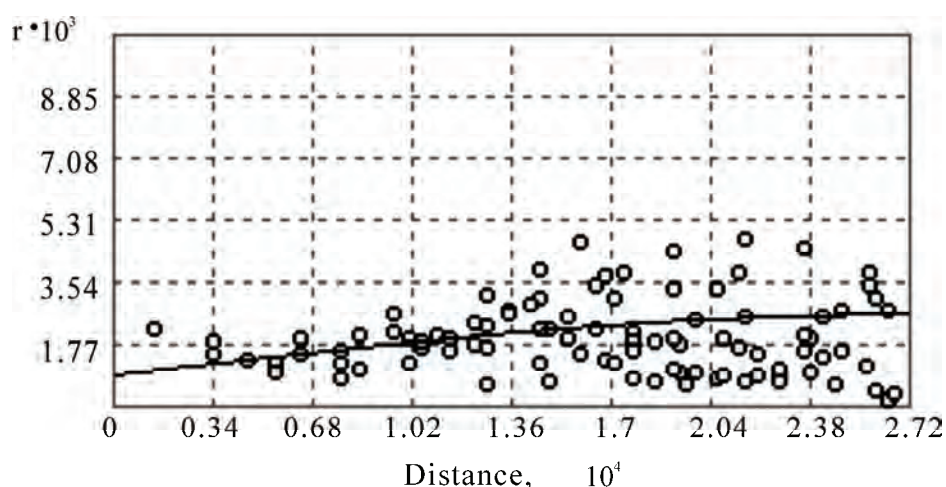


Figure 3. Semivariogram result of annual data.

Table 2. Interpolation model parameters and results of different rainfall series.

Model and results	Annual	Month	Day	Intensity
Model	spherical	exponential	spherical	Gaussian
Anisotrop	yes	yes	no	yes
Root-Mean-Square(mm)	33.36	8.311	6.48	15.29
Average Standard Error(mm)	38.24	8.945	6.776	16.48
Mean Standardized	-0.01779	-0.05089	-0.007049	-0.0018
Root-Mean-Square Standardized	0.898	0.9329	0.985	0.936

is more flat. So the anisotropy method is chose. Anisotropy is a characteristic of a random process that shows higher autocorrelation in one direction than another. Annual semivariograms are inferred from annual data considering anisotropic behavior using automatic and manual fitting procedures. Figure 3 shows the semivariogram result of the annual precipitation data, and the parameters of different rainfall series are shown in Table 2.

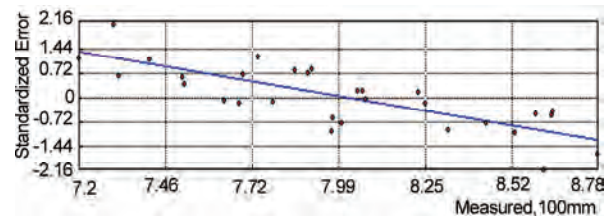
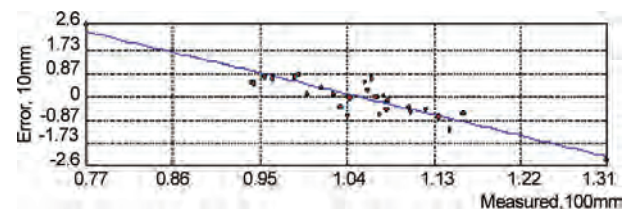
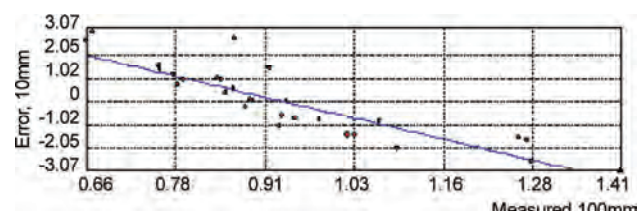
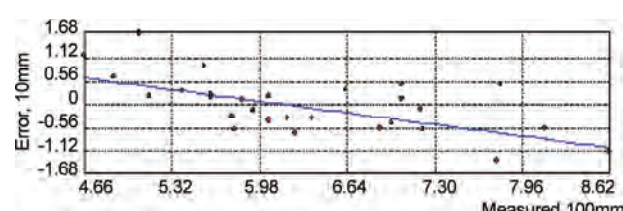
2) Perform diagnostics—the output surface using cross-validation method, which will help understand how well the model predicts the values at unmeasured locations.

Cross-validation uses the following idea—removes one data locations and then predicts their associated data using the data at the rest of the locations. In this way, we compared the predicted value to the observed value and obtained useful information about some of our previous decisions on the Kriging model. The most rigorous way to assess the quality of an output surface is to compare the predicted values with those measured in the field.

Cross-validation is used to determine "how good" the model is. The goal should be to have standardized mean prediction errors near 0, small root-mean-squared prediction errors, average standard error near root-mean-squared prediction errors, and standardized root-mean-squared prediction errors near 1.

Table 2 lists the different rainfall series estimation models, parameters and results that are compared here.

Figure 4 shows the standardized error of Kriging interpolation on annual rainfall data. We may conclude from the analysis result that, for the annual rainfalls series from 30 stations, the majority of results of Kriging interpolation is very good with $\pm 5\%$ limits of relative errors. Although the maximum and minimum interpolation errors are a little high, the results are reasonably accepted, because Kriging interpolation is based on the measured value so that the predicted value can not surpass this scope.

**Figure 4. Standardized error of Kriging in annual rainfall.****Figure 5. Error of Kriging interpolation in monthly rainfall(mm).****Figure 6. Error of Kriging interpolation in intensity rainfall(mm).****Figure 7. Error of Kriging interpolation in daily rainfall(mm).**

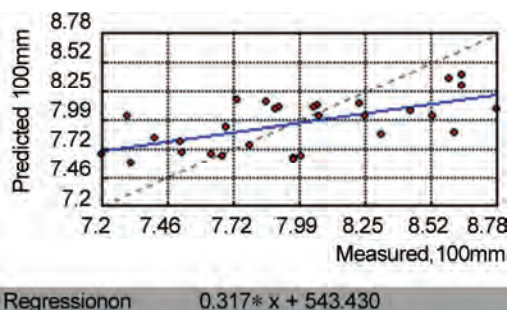


Figure 8. Measured value and predicted value of IDW for annual rainfall.

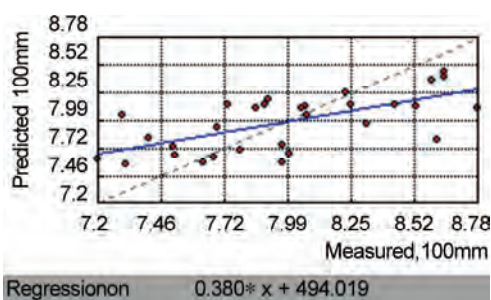


Figure 9. Measured value and predicted value of Kriging for annual rainfall.

The same spatial analysis was carried out in monthly rainfall, daily rainfall and rainfall intensity data, as shown in Figure 5, Figure 6, and Figure 7. The result shows that interpolation on the monthly data series is obviously better than the results on the intensity series and the daily series. The relative errors of monthly series are about within $\pm 8\%$ limits, and we also noticed that the Cs of monthly data serie is obviously smaller than that of the intensity data serie and the daily data seire. Therefore, for the Kriging interpolation method, where there is smaller data variation, there is better interpolation result.

3.3. Results of Three Interpolation Methods

The annual rainfall interpolation results of Kriging and IDW method are shown in Figure 8 and Figure 9. From the regression line of interpolation result, we could see that both methods show good outputs, while the Kriging result (the regression line slope is 0.38) is slightly better than IDW (the regression line slope is 0.317). More detailed analysis results are shown in Table 3-1. For Kriging method, the relative error and std_dev of results are 3.9 and 2.273, while for IDW the values are 2.192 and 3.959. It is believed that the difference of results from these two methods is acceptable. Although neither of these two methods has remarkable advantage in handling with the average annual rainfall data, the spline method will surely get worse results than the above two methods.

Table 3-1. Validation results of three methods in annual rainfall.

Method	Relative Error of Annual rainfall			
	Low	High	Mean	Standard deviation
IDW Spline	0.512	8.186	3.900	2.273
Kriging-ordinary	1.043	7.498	3.959	2.192
	0.322	10.342	5.848	3.168

Table 3-2. Validation results of three methods in monthly rainfall.

Method	Relative Error of Monthly rainfall			
	Low	High	Mean	Standard deviation
IDW Spline	0.0013	21.24	7.052	5.638
Kriging-ordinary	0.6327	20.017	6.698	4.528
	0.0196	21.132	6.068	5.454

Table 3-3. Validation results of three methods in the daily rainfall.

Method	Relative Error of Daily rainfall			
	Low	High	Mean	Standard deviation
IDW Spline	0.337	20.01	7.282	5.139
Kriging-ordinary	0.127	22.159	6.817	6.410
	0.001	20.951	8.969	7.981

Table 3-4. Validation results of three methods in the intensity (6mins).

Method	Relative Error of Intensity (6mins)			
	Low	High	Mean	Standard deviation
IDW Spline	2.640	25.691	11.829	7.046
Kriging-ordinary	1.759	34.533	12.217	8.961
	5.902	52.392	16.699	14.213

For the average monthly rainfall data, result from spline method is comparatively better(shown in Table 3-2), the relative error and std_dev of which are respec-

tively 6.068 and 5.454, while the Kriging result (7.052, 5.638) is inferior to the IDW result. For daily rainfall data, IDW method is the best one (shown in Table 3-3), while spline is obviously worst. For intensity of 6-minute data series, none of the three methods produce high-quality result. Kriging is comparatively good, while the average relative error approaches 11.829 (shown in Table 3-4).

3.4. Uncertainty in Interpolation

These results suggest that most of the uncertainty involved in the interpolation is related to the different basic data statistics. In this view, Kriging is not a better method, as it relies strongly on the assumption of stationarity in the means and thus, a lack of external trends.

In fact, for different rainfall series, it is difficult to determine which method is better. It is not changed with the variation of measured value, its essence should be closely related to the space and temporal distribution of different series. For this study region, because the rainfall station distributed in high density with a small area, the Kriging method cannot show an obvious advantage. At the same time, results from kriging and IDW interpolation are not much different. But for the spline method, the interpolation results in daily rainfall and intensity are not very good. According to statistics analysis of data, we can consider that the spline method is not favorable for data with big Cs.

Although some researchers proposed that in order to reduce the uncertainty of spatial rainfall information, the basic way is to introduce other relative variations with high sample density [6], and to integrate them in interpolation methods. But this suggestion is only suitable for the big area with low distribution density of rain gauges. The choice of those relative variations and their integration with interpolation methods will be one of the main directions of the future research in rainfall interpolation.

4. Conclusions

In this study, different interpolation approaches are compared for the different precipitation series. Special attention is given to the impact of the variogram estimation approach on the interpolation performance. The main results can be summarized as follows:

a) As a kind of geostatistical interpolation methods, the application of the Kriging method obtained the widespread promotion, but in the application process it still had the choice of multi parameters and the model. For the different rainfall series in the same area, its model and the parameter choice of Kriging method may be different.

b) The impact of the semivariogram on interpolation performance is also discussed in this paper. And anisotropy and isotropy are all present in the data, also leading to the little difference in prediction performance. The best results can be obtained using an automatic fitting procedure except isotropic and anisotropic varigrams from all precipitation series.

c) Given the small region with high density of rain gauges (15km^2), the Kriging method superiority is not obvious, and to some data series, IDW and the spline interpolation result can be better. Therefore we may obtain, to the different rainfall series, they will be suitable for the different methods, and it must be determined by the data distribution.

In this paper, we have analyzed the connection between data variance and the different interpolation methods, but this kind of data variance that we analyzed is only in the magnitude, not involved spatial distribution. From the characteristic of spatial interpolation, the spatial distribution can be influential to the method selected, so it still needs further to study in this point. Although we concluded that the different data series possibly can be more suitable for different method, the detailed relations between the data and method, at present still has not been able to analyze. Therefore to the small region, if there is no relative information to be applied, selecting the appropriate method will be the key research point.

5. References

- [1] F. Fabry, "Meteorological value of ground target measurements by radar," *Journal of Atmospheric and Oceanic Technology*, Vol. 21, pp. 560–573, 2004.
- [2] L. L. Tiefenthaler and K. C. Schiff, "Effects of rainfall intensity and duration on first flush of storm water pollutants," In S. B. Weisberg, & D. Elmore (Eds.), *Southern California Coastal Water Research Project Annual Report 2001–2002*, CA' Westminster, pp. 209–215, 2003.
- [3] J. Vaze and F. H. S. Chiew, "Study of pollutant wash off from small impervious experimental plots," *Water Environment Research*, Vol. 39, pp. 1160–1169, 2003.
- [4] P. Goovaerts, "Geostatistics for natural resources evaluation," Oxford University Press, New York, Oxford, Vol. 483, 1997.
- [5] U. Haberlandt, "Geostatistical interpolation of hourly precipitation from rain gauges and radar for a large-scale extreme rainfall event," *Journal of Hydrology*, Vol. 332, pp. 144–157, 2007.
- [6] P. Goovaerts, "Geostatistical approaches for incorporating elevation into the spatial interpolation of rainfall," *Journal of Hydrology*, Vol. 228, No. 1–2, pp. 113–129, 2000.

- [7] C. D. Lloyd, "Assessing the effect of integrating elevation data into the estimation of monthly precipitation in Great Britain," *Journal of Hydrology*, Vol. 308, No. 1–4, pp. 128, 2005.
- [8] M. F. Hutchinson, "Interpolation of rainfall data with thin plate smoothing splines: Analysis of topographic dependence," *Journal of Geographic Information and Decision Analysis*, Vol. 2, No. 2, pp. 152–167, 1998.
- [9] M. F. Hutchinson, "Interpolation of rainfall data with thin plate smoothing splines: Two dimensional smoothing of data with short range correlation," *Journal of Geographic Information and Decision Analysis*, Vol. 2, No. 2, pp. 139–151, 1998.
- [10] V. Demyanov, M. Kanevski, S. Chernov, E. Savelieva, and V. Timonin, "Neural network residual Kriging application for climatic data," *Journal of Geographic Information and Decision Analysis*, Vol. 2, No. 2, pp. 215–232, 1998.
- [11] Y. Huang, P. Wong, and T. Gedeon, "Spatial interpolation using fuzzy reasoning and genetic algorithms," *Journal of Geographic Information and Decision Analysis*, Vol. 2, No. 2, pp. 204–214, 1998.
- [12] J. J. C. Hernandez and S. J. Gaskin, "Spatial temporal analysis of daily precipitation and temperature in the Basin of Mexico," *Journal of Hydrology*, doi:10.1016/j.jhydrol.2006.12.021, 2007.
- [13] K. Umakhanthan and J. E. Ball, "Estimation of rainfall heterogeneity across space and time scale," *Urban Drainage*, 2002.
- [14] P. A. Burrough and R. A. McDonnell, "Principles of geographical information systems," Oxford University Press, 1998.
- [15] C. T. Haan, "Statistical methods in hydrology," Second Edition, Iowa State Press, 2002.
- [16] G. Bastin, B. Lorent, C. Duque, and M. Gevers, "Optimal estimation of the average area rainfall and optimal selection of raingauge locations," *Water Resource Research*, Vol. 20, No. 4, pp. 463–470, 1984.
- [17] J. D. Creutin and C. Obled, "Objective analysis and mapping techniques for rainfall fields: An objective comparison," *Water Resource Research*, Vol. 18, No. 2, pp. 251–256, 1982.
- [18] G. F. Lin and L. H. Chen, "A spatial interpolation method based on radial basis function networks incorporating a semivariogram model," *Journal of Hydrology*, Vol. 288, 288–298, 2004.
- [19] G. Matheron, "The theory of regionalized variables and its applications," Ecole des Mines, Cahiers du Centre de Morphologie Mathématique, Paris, Vol. 5, 1971.
- [20] N. P. Nezlin, E. D. Stein, "Spatial and temporal patterns of remotely-sensed and field-measured rainfall in southern California," *Remote Sensing of Environment*, Vol. 96, pp. 228–245, 2005.
- [21] W. Buytaert, R. Cellier, and P. Willems, "Spatial and temporal rainfall variability in mountainous areas: A case study from the south Ecuadorian Andes," *Journal of Hydrology*, Vol. 329, pp. 413–421, 2006.

Screening and Domestication of High Effective Microorganism Used in Oil Containing Wastewater Remediation

Xinyang XU, Xi CHEN, Yindi FAN

School of Resources and Civil Engineering, Northeastern University, Shenyang, China

E-mail: chenxineu@mail.neu.edu.cn

Received March 31, 2009; revised May 22, 2009; accepted May 25, 2009

Abstract

According to the characteristics of oil containing wastewater, four strains of microorganism, named TA-11, TA-17, HA-9, HD-1, were picked out from the oil contaminated soil and activated sludge of biochemical treatment system of an asphalt plant wastewater in Panjin. They can degrade oil and COD_{Cr} in oil containing wastewater. The research result showed that each strain of microorganisms can remove oil and COD_{Cr} in oil containing wastewater effectively when the pH value was 7.0, the temperature was 30 degree Celsius, the rotation speed was 140r/min and the inoculation amount was 10%. Especially the highest removal ratio of COD_{Cr} was 68% after growth of 64 hours. The removal ratio of COD_{Cr} in oil containing wastewater of mixed bacilli was much higher than that of unitary bacilli, and mixing a certain amount of domestic sewage with the oil containing wastewater will also improve the removal rate of COD_{Cr}.

Keywords: Oil Containing Wastewater, Screening, Domestication, COD_{Cr}, Removal Ratio

1. Introduction

The source of oily wastewater is very extensive, mainly including the oil industry, the oil processing, refining, storage and transportation, the emulsified oil waste water owing to the machinery manufacturing and processing, car washing in the transport industry, railway maintenance of the wash tank, and other oily waste water emissions of restaurants, food processing, textile industry and other manufacturing wastewater [1]. The main pollutant in oily wastewater is oil, as well as the sulfide, volatile phenol and so on.

According to the existing form of oil in the oily wastewater, it can be divided into floating oil, dispersed oil, emulsified oil, dissolved oil and so on. In the processing of oily wastewater, first of all, most of the floating oil, dispersed oil and emulsified oil are removed by physical or physical-chemical methods. And then biochemical method is used in further treatment. At last, the treated water was discharged after reaching standard [2-5]. However, the oily wastewater is poor biodegrad-

ability, and problems such as running instability and low efficiency commonly exist in the bio-chemical process. Consequently, it is academic and practical significance that we should develop screening and domestication of microorganism which is used in oil containing wastewater remediation.

2. Material and Methods

2.1. Experimental Strains

Strains of microorganism used in the experiment were isolated from the oil contaminated soil and activated sludge of biochemical treatment system of an asphalt plant wastewater in Panjin. Four strains of microorganism, which can degrade oil and COD_{Cr} of oil containing wastewater effectively, were obtained through screening and domestication [6-8]. In the laboratory they were named TA-11(short rod-like, yellow, gram positive bacteria), TA17 (globular, pink, gram positive bacteria) isolated and purified from the oil contaminated soil of Panjin

Table 1. Water quality of oil containing wastewater sample (mg/L).

Oil	COD _{Cr}	Sulfur	Phenol	NH ₃ - N
63	1125	6.41	34.31	29.80

asphalt plant and HA-9 (rod-like, yellow, gram positive bacteria), HD-1 (rod-like, pink, gram positive bacteria) from activated sludge of biochemical treatment system of an asphalt plant wastewater in Panjin.

2.2. Experimental Wastewater Sample

The oily wastewater is from biochemical treatment system of an asphalt plant wastewater in Panjin, of which the water quality is listed in Table 1.

2.3. Screening and Domestication of Strains

2.3.1. Preliminary Screening Method of the Strains

Through esterase decomposition test, strains which can highly degrade oil were screened out. Pick one purified strain, streak in prepared lipid culture medium, then put it into biochemical incubator with the temperature of 30 °C, finally observe the color of medium after static culture for 64h. If it became red, it would suggest that the strain can degrade oil. The deeper the color showed, the stronger the ability of oil degradation was.

2.3.2. Secondary Screening Method of Strains

After obtaining strains in preliminary screening, secondary screening was based on ability of single strain degradation of COD in oil containing wastewater.

2.3.3. Domestication Methods of Strains

Domestication processes were divided into three phases. In the first phase, sterilized culture solution was filled into erlenmeyer flasks with 70 ml in each, and inoculation amount in each erlenmeyer flask was 5 ml. They were cultivated in shaking cultivation at the speed of 130~140r/min, in the temperature of 30°C and for 72h. At the same time, the OD₅₅₀ was measured every 6 hours. In the second phase, the condition was the same as first phase except that culture medium formula was different. In the third phase, sterilized culture solution was filled into the erlenmeyer flasks with 30 ml in each, and Inoculation amount of each erlenmeyer flask was 2 ml. The

culture condition was the same as the two phrases before.

2.4. Determination of Growth Curve of Strains

Turbidimetry was applied to determine concentration of bacterial suspension in order to decide the growth curve. 2ml of bacterial suspension was inoculated in newly prepared and sterilized basic culture medium, and cultivated in 30°C. The OD₅₅₀ was measured every 2h.

2.5. Medium-Related

Medium: beef extract 3g, peptone 10g, NaCl 5g, agar 15~20g, distilled water 1000 ml, pH value 7.0~7.2.

Oil medium: beef extract 3g, peptone 10g, NaCl 5g, agar 15~20g, 90# diesel 1ml, the concentration of 1.6% neutral red solution 1ml, distilled water 1000ml, pH value 7.0~7.2.

Domesticated medium: components of domesticated medium shown in Table 2.

Seed Media: glucose 12.5g, yeast extract 2.5g, NH₄NO₃ 1g, MgSO₄·7H₂O 0.2g, KCl 0.2g, distilled water 1000ml, pH value 7.0~7.2.

Proliferated medium: glucose 30g, yeast extract 4g, beef extract 1g, NH₄NO₃ 1g, MgSO₄·7H₂O 0.2g, KCl 0.2g, distilled water 1000ml, pH value 7.0~7.2.

2.6. Test Method of COD_{Cr}

COD_{Cr} in wastewater was determined by COD_{Cr} instrument with the principle of potassium dichromate method.

2.7. Test Method of OD₅₅₀

OD₅₅₀ was determined by 722E spectrophotometer at 550nm wavelength.

3. Results and Discussion

3.1. Screening of Strains

3.1.1. Primary Screening of Strains

Screen out the strains which can degrade the oil containing wastewater according to the esterase decomposition experiment. The result is shown in Table 3.

Table 2. Culture medium component of high oil domesticating at different stages (g/L).

Stage of culture	diesel	yeast extract	NH ₄ NO ₃	MgSO ₄ ·7H ₂ O	KCl
1	1.0	3.0	1.0	0.2	0.2
2	5.0	1.0	1.0	0.2	0.2
3	10.0	1.0	1.0	0.2	0.2

Table 3. Esterase decompound experiment.

Flat culture time	12h	24h	36h	48h	64h
TA-11	++	+++	++++	++++	++++
TA-17	++	++	+++	++++	++++
TA-15	+	++	++	+++	++++
HA-9	+	+	++	+++	++++
HB-7	-	+	++	+++	+++
HD-1	-	-	+	++	+++
HC-16	-	-	+	+	++
TB-5	-	-	-	+	+
TC-11	-	-	-	+	+
HD-3	-	-	-	+	+

①: TA-11、TA-17、TA-15、TB-5、TC-11 are strains of microorganism separated from the oil contaminated soil of an asphalt plant in Panjin; HA-9、HB-7、HD-1、HC-16、HD-3 are strains of microorganism isolated from activated sludge of an asphalt plant in Panjin.

②: The results were divided into five grades according to shade: -、+、++、+++、++++, the deeper of the colour, the stronger of the degradation ability.

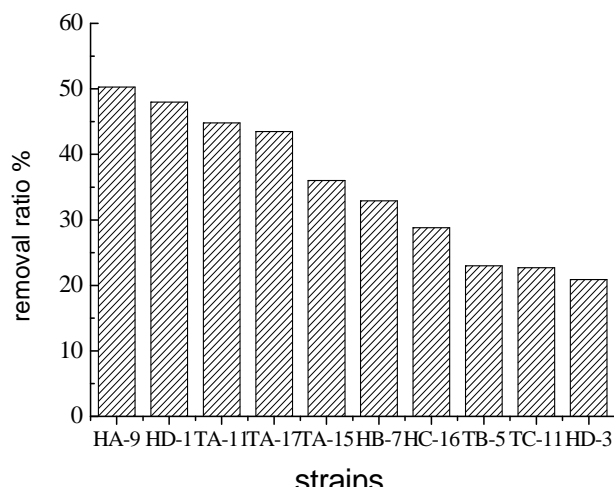
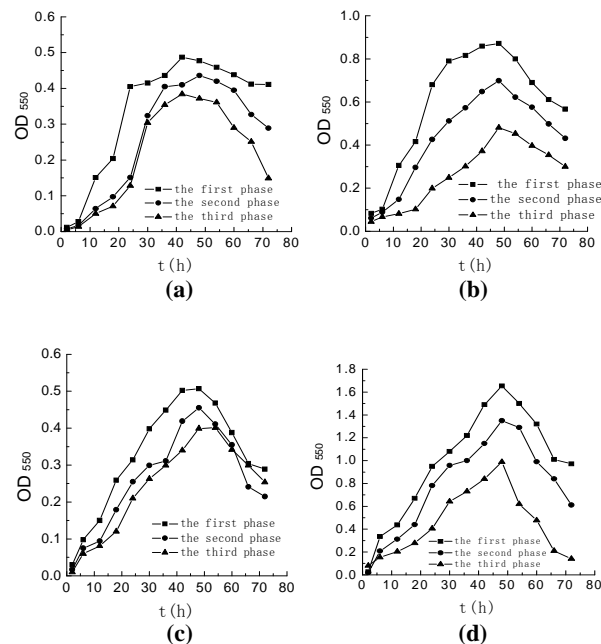
③: The 10 strains of microorganism which can degrade the oil were listed in the table above.

3.1.2. Secondary Screening of Strains

The secondary screening standard of the strains is the removal ability of COD_{Cr}.

We inoculated the single strain to the oil containing wastewater with the pH value 7.0~7.2 and rotation speed 140r/min in 30°C. After 72 hours' cultivation, COD_{Cr} was determined. We performed the same experiment 3 times and the average result was shown in Figure 1.

In Figure 1, HA-9 has the highest COD_{Cr} removal ratio of 50.3%, the next is the strain named HD-1 48%, and then TA-11, TA-17, with the removal ratio of 44.8%

**Figure 1. Variation of degradation ratios of pure strain.****Figure 2. Result of high oil domesticating.**
(a)—TA-11; (b)—TA-17; (c)—HD-1; (d)—HA-9

and 43.8% respectively. Consequently, the four strains named HA-9、HD-1、TA-17 and TA-11 are chosen to domesticate in the following experiment.

3.2. Taming of Stains

4 strains selected were domesticated, of which the result is shown in Figure 2.

In Figure 2, the value of the optical density OD_{550} reflects the number of bacteria in suspension, thereby reflecting the propagation of growth of microorganisms. According to the growth tendency, the number of bacteria reaches to the highest value within about 48h with the extension of time, while the trend becomes slow after 48h. It indicates that strains have a good capacity for diesel degradation within a certain period of time, and can survive in high oil concentration.

3.2.1. Morphological Characteristics and Growth Curve of Strains

In beef extract peptone solid medium, TA-11 was yellow, transparent, smooth in surface, round uplift for the colony, and regular around. Cells were short rod-shaped, positive in gram stain when they were observed in the microscope.

In beef extract peptone solid medium, TA-17 was pink, opaque, smooth in surface, of round colonies, smaller, and regular around. Observed in the microscope, cells were spherical, positive in gram stain.

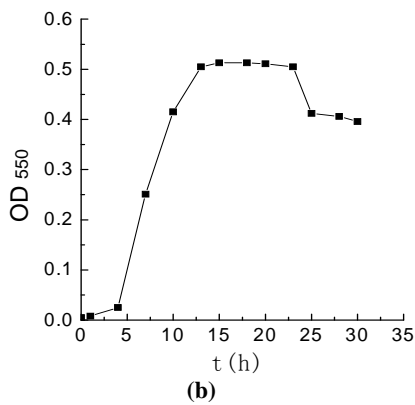
In beef extract peptone solid medium, HD-1 was pink, opaque, smooth in surface, of round colonies, regular of the edge. Observed in the microscope, cells were rod-shaped, positive in gram stain.

In beef extract peptone solid medium, HA-9 yellow, deep color in center, opaque, of round colonies, regular around. Observed in the microscope, cells were rod-shaped, positive in gram stain.

The morphology characteristics and growth curves of different strains are shown in Figure 3.



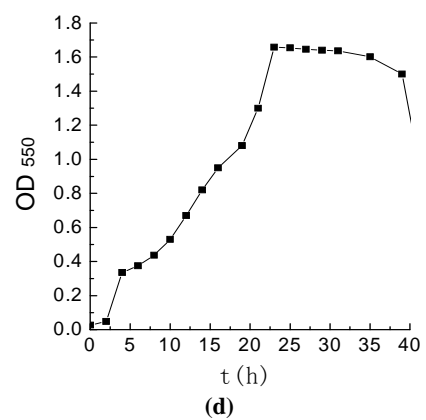
(a)



(b)



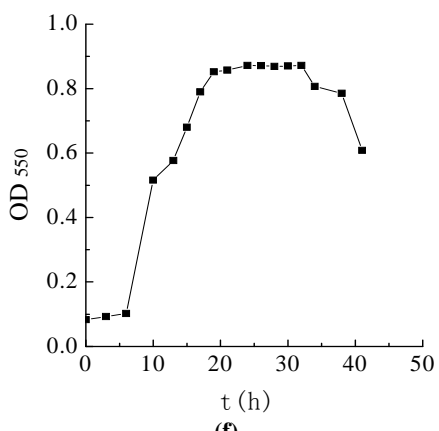
(c)



(d)



(e)



(f)

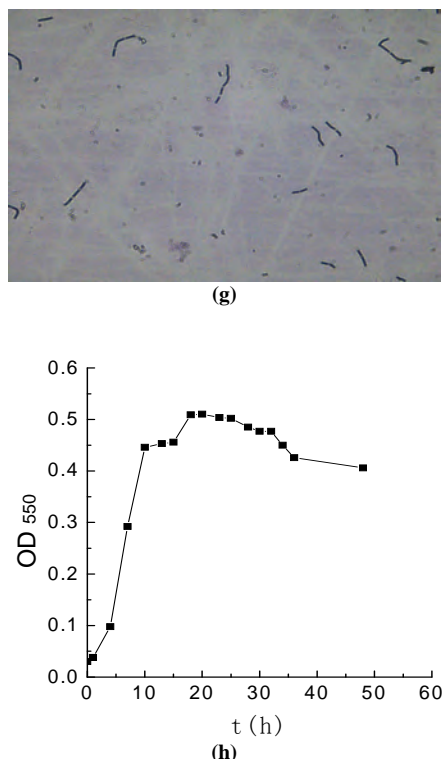


Figure 3. Micro photos and growth curves of microorganism.
(a),(b)—TA-11; (c),(d)—TA-17; (e),(f)—HD-1; (g),(h)—HA-9

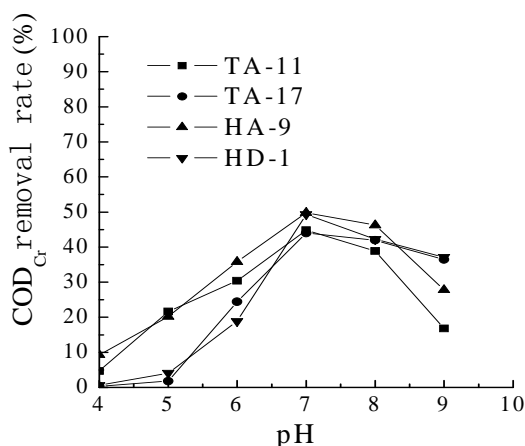


Figure 4. Influence of pH on COD_{Cr} removal.

3.3. The Influence of Environmental Factor on COD_{Cr} Removal Effect

3.3.1. The Influence of Original pH Value on COD_{Cr} Removal Effect

pH value has a great influence on living activity of microorganism. It mainly changes electric charge on the cell's membrane, thereby affecting microorganism's absorbability of nutrient; affects the enzyme's acting;

transforms the acquirable ability of nutrient and the toxicity of injuring in their living circumstance. All kinds of microorganism have their own and optimal pH value.

In order to investigate the influence of original pH value on COD_{Cr} removal effect, we took bacterium liquid 2ml from each single bacteria, put them into 50ml wastewater of different pH value respectively, cultivated them at 30 °C and rotate speed of shaking bed of 130r/min, and then measured the COD_{Cr} removal ratio after 64h. The result is shown in Figure 4.

The optimal pH value range of four bacteria is 7-8. In this scope, their removal rates are high. When pH<5, the removal efficiencies of COD_{Cr} in the wastewater are very limited. When pH> 8, the removal efficiencies of all kinds of microorganism are obvious declined. The result shows that it is suitable for the four stains of bacteria to survive in a neutral condition, while it is not conducive to microbial growth and the degradation of oil in the condition of too high or too low pH value.

3.3.2. The Influence of Temperature on COD_{Cr} Removal Effect

The principal part of wastewater treatment is kinds of microorganism which have special function. And their growth and propagating have consanguineous connections with the temperature. Microorganisms' growth is complicated biochemical reaction, which requires a certain range of temperature to perform in. The temperature range is wide (-10~95 degree Celsius), but each kind of microorganism can only growth in a definite range of temperature. In the range of the optimal temperature, microorganisms are vigorous physical activity, which conducts high treatment efficiency of the wastewater. And above or below this temperature range, it will injure microbial enzymatic systems, and affect the microorganisms' metabolism and the degradation of organic pollutants.

In order to investigate the influence of temperature on COD_{Cr} removal effect, we took each single bacterium liquid, put them into 50ml wastewater with pH value about 7.0, cultivated them at different temperatures and rotate speed of shaking bed of 130r/min, and measured the COD_{Cr} removal ratio after 64h. The result is shown in Figure 5.

As shown in Figure 5, when the scope of temperature is between 25 to 35 degree Celsius, removal ratios of these four bacterium are high. In conclusion, the optimal degradation temperature is 30 degree Celsius.

3.3.3. The Influence of Inoculation Amount on COD_{Cr} Removal Effect

In order to investigate the influence of inoculation amount on COD_{Cr} removal effect, we took each single bacterium liquid of 1ml, 2.5ml, 5ml, 7.5ml, 10ml, put them

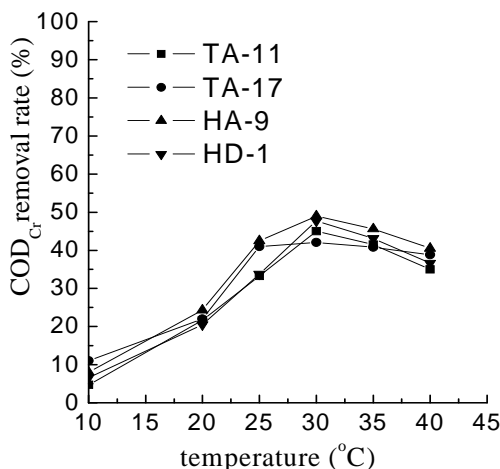


Figure 5. Influence of temperature on COD_{Cr} removal.

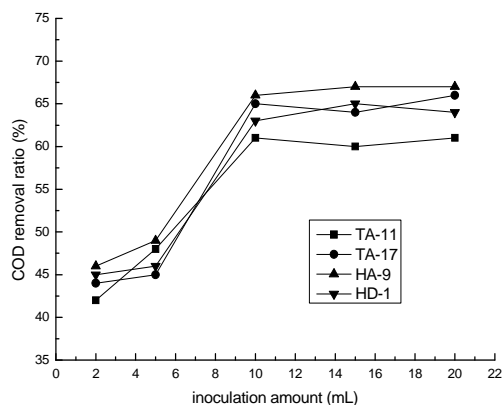


Figure 6. Influence of inoculation amount on COD_{Cr} removal.

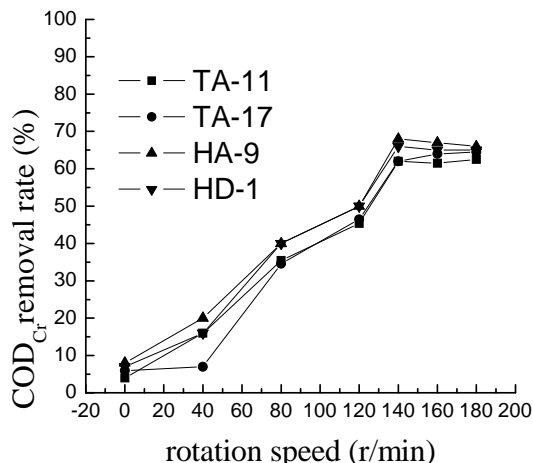


Figure 7. Influence of shaking rate on COD_{Cr} removal.

into 50ml wastewater with pH value at about 7.0, cultivated for 64h at 30°C and rotate speed of shaking bed of 130r/min, and then measured the COD_{Cr} removal ratio. The result is shown in Figure 6.

It can be seen that the less of inoculation amount, the higher concentration of residual COD_{Cr}. When the inoculation amounts are 2% and 5% respectively, the removal ratios of the 4 strains are less than 50%. And when the amount is over 10%, the influence on removal ratio is not obvious. Considering the economic benefit, 10% inoculation amount is optimal.

3.3.4. The Influence of Aeration Intensity on COD_{Cr} Removal Effect

The speed of shaking bed is used to represent aeration intensity in this experiment. We have investigate the influence of aeration intensity on COD_{Cr} removal effect at the range of 0~180 r/min.

We chose each single bacterium liquid, put them into 50ml wastewater with pH value about 7.0, in the 30 degree Celsius temperature conditions, cultivated them at the speed of 0, 40, 80, 120, 140, 160 and 180 r/min respectively for 64h. At last, we contrasted the COD_{Cr} removal ratios in the wastewater of different bacterium liquids at different speeds. The result is shown in Figure 7.

As the result shown in Figure 5, with the increase of speed, COD_{Cr} removal ratios in the oil containing wastewater are in upward trend. When the speed is at 140r/min, the COD_{Cr} removal ratios are the highest, especially the removal ratio of HA-9 can be 68%.

3.3.5. The Influence of Mix-Bacterium on COD_{Cr} Removal Effect

We took 5ml bacterium liquid of each bacterium, put all of them into 50mL wastewater with pH value about 7.0 in the 30 degree Celsius temperature conditions, cultivated them for 64h at the speed of 140r/min. At last, we measured COD_{Cr} removal ratios which changed with time, and compared with the equivalent single-strain vaccine. The result is shown in Figure 8. As shown, the removal ratio of the mix of efficiency is higher than that of each single stain.

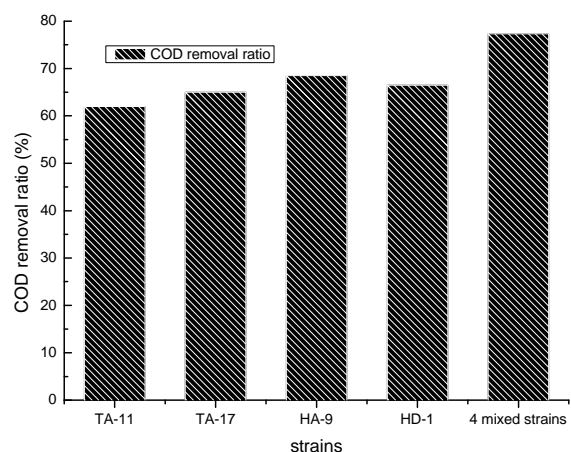


Figure 8. Removal ratio of COD_{Cr} for mixed bacilli.

Table 4. Comparation of the removal ratios of COD_{Cr}.

Strains	TA-11	TA-17	HA-9	HD-1	4 mixed strains
Removal ratio	Add nutriments	74	76	80	78
	No add	60	65	68◎	78

3.3.6. The Influence of Nutriment on COD_{Cr} Removal Effect

It is not only enough organic matters, but also many kinds of well-proportioned nutrient that are required in the growth of microorganism, including C, N, P, S and many microelements such as K, Ca, Mg, Fe and vitamins. Domestic sewage can meet the requirement. As a result, domestic wastewater which was simulated with compounds of 0.4% NH₄NO₃, 0.8% K₂HPO₄, 0.8% KH₂PO₄, 0.1% MgSO₄·H₂O and distilled water with pH value around 7 is added to the oil containing water in this experiment. Their proportional is 1:1, and COD_{Cr} of the mixed wastewater is 850 mg/L. We added 10% of total inoculation amount, and 2.5% of inoculation amount of each single bacterium, into the mixed wastewater, and cultivated them in 30°C, at rotate speed of shaking bed of 140r/min for 64h. Compared with the wastewater which is diluted as twice of the original, we investigated the removal ratio of COD_{Cr} of immobilized bacterium. The result is shown in Table 4.

The result shows that the removal ratios of each strain have increased after 64h. So it is helpful to improve the removal effect if a certain amount of domestic sewage is added into the oil containing wastewater in practical treatment.

4. Conclusions

1) We have separated four objective stains of bacterium which have high efficiencies on removal of oil and COD_{Cr} in the oil containing wastewater from soil polluted by heavy oil and activated sludge biochemical treatment system of an asphalt plant wastewater in Panjin. And they are named in the laboratory: TA-11, TA-17, HA-9 and HD-1. It is observed in the microscope that the four stains of bacterium are gram-positive.

2) The biochemical degradation tests on the oil containing wastewater show that the treatment effects of each stain are best when the pH value is 7.0, the rotation speed 140r/min, the inoculation amount 10% and the

temperature of circumstance 30 degree Celsius. And after 64h's cultivation, the COD_{Cr} removal ratio can reach approximately 68% of single bacterium. The COD_{Cr} removal efficiency of the mix stains is higher than that of any single stain.

3) It is mixing a certain amount of domestic sewage with the oil containing wastewater that will also improve the removal efficiency of COD_{Cr} in practical treatment.

5. References

- [1] S. B. Hou, X. M. Xuan, "Status of research and application of the oily wastewater treatment technology [J]," Shanghai Chemical Industry, Vol. 9, pp. 11–14, 2003.
- [2] T. Berrin, "Microscopic characterization of oil droplets removed by flocs after coagulation of oil-water emulsions [J]," Journal of Environmental Science and Health, Vol. 37, No. 2, pp. 127–138, 2002.
- [3] A. M. A. Omar, "Recovery of residual emulsifiable oil from wastewater by flotation lubrication science [J]," Water Science Technology, Vol. 14, No. 2, pp. 275–284, 2002.
- [4] D. D. Qian, L. J. Xu, and J. W. Shi, "Study on high-strength oil-containing wastewater treatment attached yeasts [J]," Energy Environmental Protection, Vol. 23, No. 1, pp. 41–45, 2009.
- [5] G. Q. Liu, J. W. Shen, and C. K. Gao, "Study on treatment oil wastewater by screening high efficient degradation bacteria of crude oil [J]," Technology of Water Treatment, Vol. 34, No. 10, pp. 26–29, 2008.
- [6] G. Yang, "A Course of microbiology experiment [M]," Science press, pp. 15–25, 2004.
- [7] X. Y. Xu, Y. Zhang, and H. B. Li, "Immobilization process of flavobacterium sp. for bioremediation of contaminated surface water [J]," Journal of Northeastern University: Natural Science, Vol. 8, pp. 783–786, 2005.
- [8] X. Y. Xu, Y. Zhang, and H. B. Li, "Chemical embedding immobilization technique of micrococcus sp. used in contaminated surface water remediation [J]," Journal of Northeastern University: Natural Science, Vol. 1, pp. 1146–1149, 2006.

Call For Papers



IEEE



iCBBE

Environmental Pollution and Public Health (EPPH2010)

Special Track within iCBBE

环境污染与人类健康国际学术会议征文

June 21-23, 2010 Chengdu, China

<http://www.icbbe.org/epph2010/>

The International conference on Environmental Pollution and Public Health (EPPH2010), a special track within iCBBE 2010, will be held from June 21st to 23rd, 2010 in Chengdu, China. You are invited to submit papers in all areas of environmental pollution and related health problems. **As we did in EPPH 2009 and 2008, all papers accepted will be included in IEEE Xplore and cited by Ei Compendex and ISTP.**

Topics

Water Quality and Public Health

- Purification of drinking-water supplies
- Treatment, disposal and discharge of wastewater
- New wastewater treatment technologies
- Methods of monitoring water quality
- Modeling and measuring of water pollution
- New water purification technologies
- Ground water pollution control
- Water resources and quality assessment
- Water resource protection and sustainable use
- Hydrobiology and water pollution
- Other topics related to water pollution

Air Pollution and Public Health

- Effects of air pollution on public health
- Sources of air pollution
- Air pollution monitoring and modeling
- Air pollution prevention and control
- Urban/indoor air pollution and control
- Air quality measurement and management
- Global climate change and air pollution

Other Related Issues

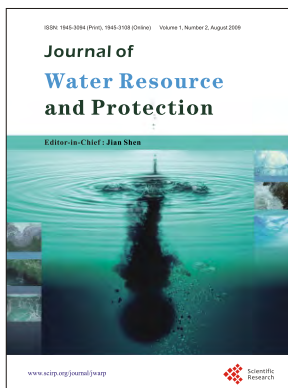
- Chemical pollutants and its effects on health
- Land pollution and its effects on health
- Radiation safety in atomic industry
- Food and drug safety control
- Hazardous materials management
- Solid waste management
- Environmental toxicology
- Risk assessment of contaminated environments
- Ecosystem restoration
- Global climate changes and human health

Important Dates

- ◆ Paper Submission Due: **Oct. 30, 2009**
- ◆ Acceptance Notification: **Dec. 31, 2009**
- ◆ Conference: **Jun. 21-23, 2010**

Contact Information

Website:<http://www.icbbe.org/epph2010/>
E-mail: epph@icbbe.org



Journal of Water Resource and Protection (JWARP)

<http://www.scirp.org/journal/jwarp>

ISSN:1945-3094 (Print), 1945-3108 (Online)

JWARP is an international refereed journal dedicated to the latest advancement of water resource and protection. The goal of this journal is to keep a record of the state-of-the-art research and promote the research work in these fast moving areas.

Editor-in-Chief

Prof. Jian SHEN

College of William and Mary, USA

Editorial Board

Prof. J. Bandyopadhyay
Dr. Antonio Dourado
Prof. Peter Dillon
Dr. Qiuqing Geng
Dr. Jane Heyworth
Dr. C. Samuel Ima
Dr. Valentina Lady-gina
Dr. Dehong Li
Dr. Chih-Heng Liu
Dr. Sitong Liu
Dr. Xiaotong Lu
Dr. Donghua Pan
Dr. Dhundi Raj Pathak
Dr. Van Staden Rudi
Dr. Dipankar Saha
Prof. Matthias Templ
Dr. Dehai Wang
Dr. Yuan Zhao
Dr. Lifeng Zhang
Dr. Chunli Zheng
Prof. Zhiyu Zhong
Dr. Yuan Zhang

Indian Institute of Management Calcutta, India
University of Coimbra, Portugal
Fellow of the Royal Society of Canada(F.R.S.C), Canada
Swedish Institute of Agricultural and Environmental Engineering, Sweden
University of Western Australia, Australia
University of Manitoba, Canada
Russian Academy of Sciences, Russia
Fudan University, China
Feng Chia University, Taiwan, China
Dalian University of Technology, China
Nanjing University, China
Beijing Normal University, China
Osaka Sangyo University, Japan
Griffith University, Australia
Central Ground Water Board, India
Methodology Department of Statistics, Austria
Guangzhou Institute of Geochemistry, China
College of William and Mary, USA
Center for Advanced Water Technology, Singapore
Dalian University of Technology, China
Changjiang Water Resources Commission, China
Chinese Research Academy of Environmental Science, China

Subject Coverage

This journal invites original research and review papers that address the following issues in water resource and protection. Topics of interest include, but are not limited to:

- Water resources and quality assessment
- Rivers, lakes and estuary systems
- Wastewater treatment and sludge biotreatment
- Water purification and water supply
- Water source protection and sustainable use

- Modeling, measuring and prediction of water pollution
- Ground water pollution control
- Reactions and degradation of wastewater contaminants
- Other topics about water pollution

We are also interested in short papers (letters) that clearly address a specific problem, and short survey or position papers that sketch the results or problems on a specific topic. Authors of selected short papers would be invited to write a regular paper on the same topic for future issues of the JWARP.

Notes for Intending Authors

Submitted papers should not have been previously published nor be currently under consideration for publication elsewhere. Paper submission will be handled electronically through the website. All papers are refereed through a peer review process. For more details about the submissions, please access the website.

Website and E-Mail

<http://www.scirp.org/journal/jwarp>

Email: jwarp@scirp.org

TABLE OF CONTENTS

Volume 1 Number 2

August 2009

Long-Term Study of Lake Evaporation and Evaluation of Seven Estimation

Methods: Results from Dickie Lake, South-Central Ontario, Canada

H. X. YAO..... 59

Dechlorination of Trichloroethylene in Groundwater by Nanoscale Bimetallic

Fe/Pd Particles

T. L. LI, S. J. LI, Y. C. LI, Z. H. JIN..... 78

Electrokinetic Phenomena of Modified Polytetrafluoroethylene Membranes in the Oily Sewage from Oil Field

A. G. LIN, Y. H. YAO, G. LIU, G. Z. ZHANG, X. F. LIN..... 84

Plantago Ovata Efficiency in Elimination of Water Turbidity

G. N. BIDHENDI, T. SHAHRIARI, S. SHAHRIARI..... 90

Remove of Phenolic Compounds in Water by Low-Temperature Plasma:

A Review of Current Research

J. F. ZHANG, J. R. CHEN, X. Y. LI..... 99

Water Quality Analysis of the Songhua River Basin using Multivariate Techniques

Y. LI, L. Y. XU, S. LI..... 110

Modeling and Control of pH in Pulp and Paper Wastewater Treatment Process

J. Y. KANG, M. X. WANG, Z. J. XIAO..... 122

Health Risk Assessment on Rural Drinking Water SafetyA Case Study in Rain

City District of Ya'an City of Sichuan Province

F. Q. NI, G. D. LIU, H. Z. REN, S. C. YANG, J. YE, X. Y. LU, M. YANG..... 128

Uncertainty Analysis of Interpolation Methods in Rainfall Spatial DistributionA

Case of Small Catchment in Lyon

T. TAO, B. CHOCAT, S. Q. LIU, K. L. XIN..... 136

Screening and Domestication of High Effective Microorganism Used in Oil

Containing Wastewater Remediation

X. Y. XU, X. CHEN, Y. D. FAN..... 145

